Available online at **www.joac.info**

ISSN: 2278-1862

Journal of Applicable Chemistry

2024, 13 (3): 441-520

(International Peer Reviewed Journal)

New Chemistry News

$^{-}N=C=N^{-}$

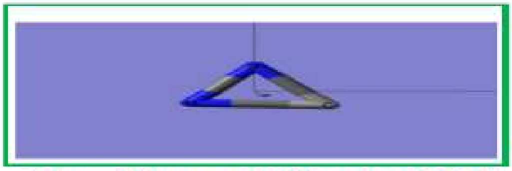

New News of Chem (NNC)

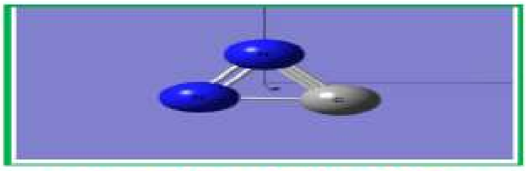

ChemNewsNew (CNN)

...CNN – 62b...*I am* ...

...*Intelligence Augmented Medical...* *Neuro Surgery*

Part 2. Fits (Figure Image Table Script ...)Base

Information Source	sciencedirect.com;	
S. Narasinga Rao M D **Associate Professor,** **Emergency Medicine dept.,** **Andhra Medical College,** **King George Hospital** **Visakhapatnam, A.P., India**	**K. Somasekhara Rao, Ph D** **Dept. of Chemistry,** **Acharya Nagarjuna Univ.,** **Dr. M.R.Appa Rao Campus,** **Nuzvid-521 201, India**	**R. Sambasiva Rao, Ph D** **Dept. of Chemistry,** **Andhra University,** **Visakhapatnam 530 003,** **India**
snrnaveen007@gmail.com (+91 9848136704)	sr_kaza1947@yahoo.com (+91 98 48 94 26 18)	rsr.chem@gmail.com (+91 99 85 86 01 82)

Conspectus: “Intelligence Augmented Medicine (I am)” is the pragmatic tool of state-of-knowledge for human health care. It comprises of hierarchical/ hybrid/fused transient disciplines with an inner core focus on disease confirmation and treatment in this decade and with expected higher level of accuracy for coming generation(s) even in economically deprived countries. A set of typical medical specialisations of concern are Neurology, Surgery, Anaesthesiology, Cardiology, Pulmonology, Gynaecology, Venereology, Urology. Hepatology, Ophthalmology, Dermatology, Oncology etc.

In this series of medical news highlights, the impacts/benefits of current-state-of-art-of evolved AI-and-medical/surgical tools had been described.

The present news item (Graphics-Flyer/Image-Flyer) “Fits.Base. Neuro Surgery” is also a passive information collection for Neuro-surgery. It incorporates numerical data, figures, images, tables, graphs, literary scripts etc. A few studies described deal with Glioma, Cerebrovascular disorders, Spine Surgery, Hematoma and so on. Robotic Machines and Virtual/real/mixed realities brought renaissance in Neurosurgery. The models employed are No-new- U-Net.”, Physics Informed NN, ChatGPT, xAI, ML//CNN-Transformer Models. We had been involved in the active-mode-of-FitsB in the object-oriented-search, picking up knowledge/intelligent bits in the medical (Progress of medical diagnosis,surgery, post-operation health care)/chemical chores.

Keywords: Artificial intelligence (AI); Medical diagnosis, Neurology, Surgery; CNN : [C [Computations; Computer; Chemistry] NN [New News; News New; Neural Nets; Nature News; News of Nature;]]

K(nowledge)Lab
rsr.chem1979

Neuro Surgery

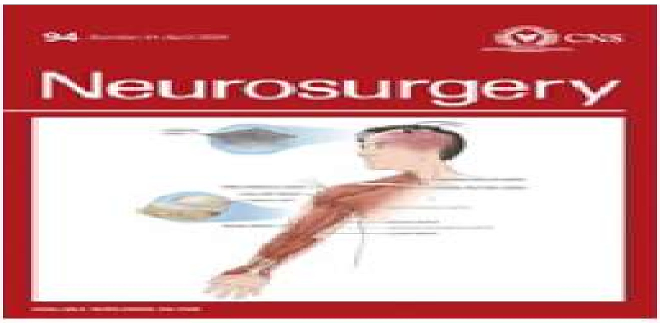

Neural Nets

42

Visual representation of an artificial neural network

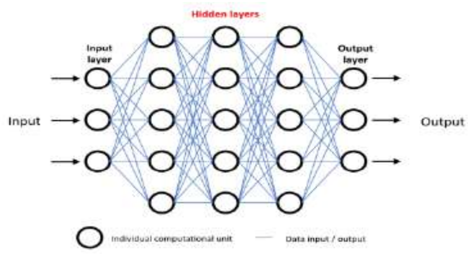

“Black box” solution of a task

- ✓ Number of data inputs are processed through many hidden layers of computational units → output.
- ✓ Ex: inputs may be tumour grade, location, and patient demographics. outputs may be survival

prediction or response to certain therapeutics

- Inability to understand how outputs are generated due to complexity of hidden layers
- Raises concerns regarding trust in deep learning predictive models

11

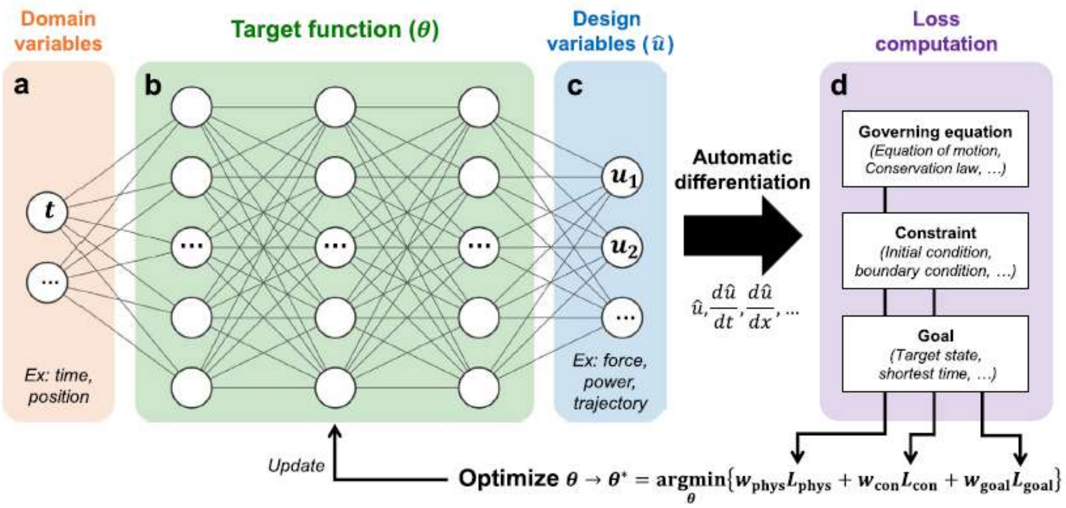

Neural network architecture using physics-informed loss Fn to solve the optimization task.

- ✓ (a) The domain variables (ex. time or position) as neural network inputs. (b) The target function to be optimized (θ), composed of multi-layer perceptrons. (c) The design variables as neural network outputs. (d) The loss functions (physics loss, constraint loss, and goal loss) which are weighted-summed for the final objective function

Physics Informed NN (PINN)

11

PINN

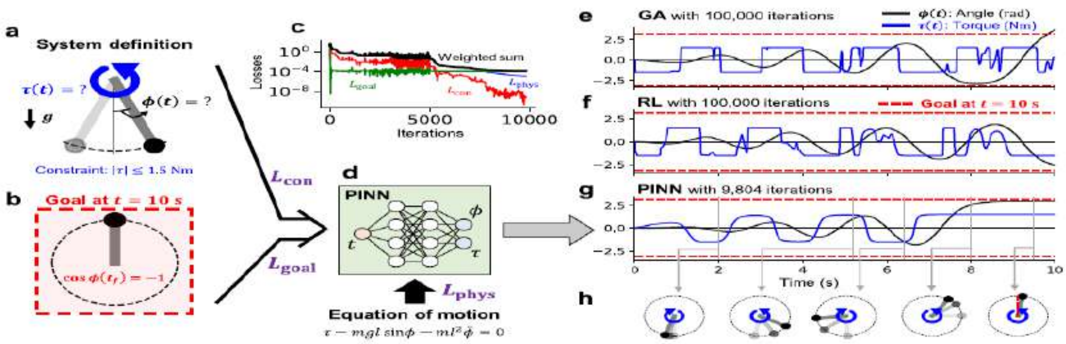

Application for optimizing the torque scenario in swinging up a pendulum.

- ✓ (a) The description of the fixed-axis pendulum, where the design variables are the angle φ and the torque τ as functions of time t.

- (b) The goal state in this optimization task, cos φ = −1 at t = 10 s .
- (c) The history of loss values over iterations.
- (d) The illustration of the neural network incorporating the equation of motion into its objective function. The input is t and the outputs are φ and τ .
- (e) A baseline result of a GA algorithm.
- (f) A baseline result of an RL algorithm using TD3. Both GA and RL produce wiggling torque scenarios.
- (g) The result of PINN, which determines swinging the pendulum back and forth to accumulate its energy to reach the goal.
- (h) Several snapshots of swinging up the pendulum.

11

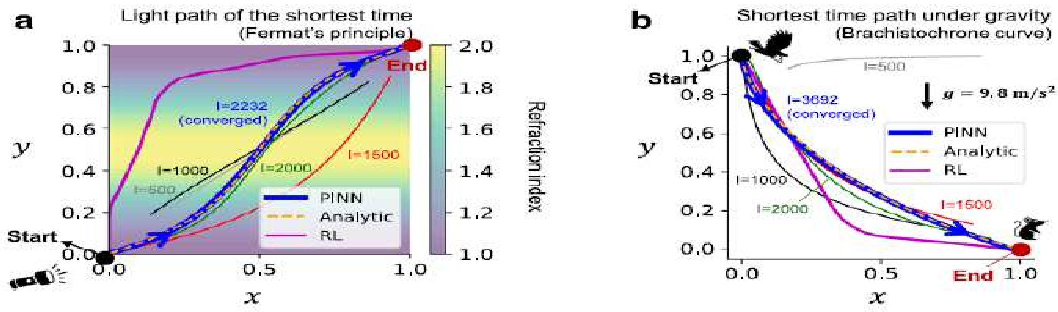

Applications of PI (Physics Informed) --NN for determining the shortest-time path under specific environments.

- (a) Finding the shortest-time path of a light ray within the medium where the refraction index varies along y.
- (b) Finding the shortest-time descent path between two given points under constant gravity.
- In the two figures, the analytic solutions are given in yellow dashed lines and the converged solutions by PINN are shown in blue. For baselines, the results using RL with 105 iterations are shown in magenta lines

Ensemble models in PINN, RL, and GA

11

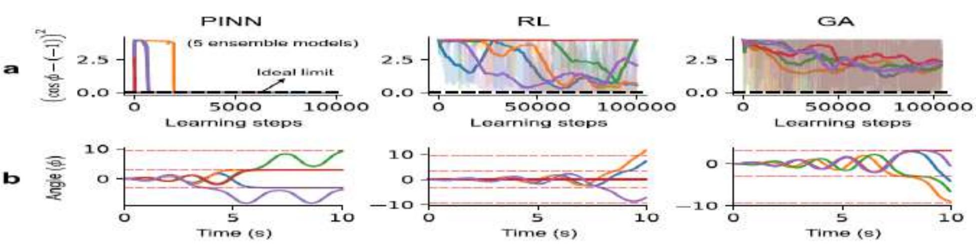

Variation among five ensemble models in PINN, RL, and GA.

- ✓ (a) The learning curve variation. For the RL and GA curves, smoothed lines are shown in solid lines, while the original curves are indicated with transparent colors.
- ✓ (b) The variation of inference results after the training, without exploration noise. The goal states ($\cos\varphi = -1$) are also shown in red dashed lines

Diagnosis of Cerebrovascular disorders with AI/robotics

32

Studies on AI/robotics for the diagnosis of cerebrovascular disorders

Author	Year	Type of study	Title	Time	Sample size	AI/robotics subtype	Key objective	Key findings
Akiyama et al. [41]	2020 (September)	Retrospective review	Deep Learning-Based Approach for the Diagnosis of Moyamoya Disease	2009 to 2016	84	Deep learning algorithm	Moyamoya disease diagnosis	AI analyzing T2-weighted images showed high-accuracy results in distinguishing between atherosclerotic disease and Moyamoya disease at the level of the basal cistern, basal ganglia, and centrum semiovale.
Kordzadeh et al. [33]	2019 (March)	Prospective cohort study	The Role of Artificial Intelligence in the Prediction of Functional Maturation of Arteriovenous Fistula	2012 to 2016	266	Deep learning neural network model	AV fistula maturation prediction	With 10 given patient attributes, AI could predict functional maturation of AV fistula with >80% accuracy ($p < 0.01$).
Lang et al. [35]	2020 (October)	Retrospective review	Evaluation of an Artificial Intelligence-Based 3D-Angiography for Visualization of Cerebral Vasculature	2019	15	Deep learning neural network model	Cerebral angiography optimization	An AI-based 3DA technique based only on a single contrast-enhanced run that functions with approximately half of the radiation required for the conventional subtraction technique shows comparable results to standard 3D DSA with a significant reduction in patient radiation dose.
Silva et al. [26]	2019 (November)	Retrospective cohort study	Machine Learning Models can Detect Aneurysm Rupture and Identify Clinical Features Associated with Rupture	2002 to 2018	615	Machine learning algorithm	Aneurysm rupture detection	The model can accurately classify aneurysm rupture status based on previously established predictors. The model suggests that location is significantly more important than size when estimating rupture risk. The ML techniques show promise in clinical neurosurgical applications.
Faron et al. [27]	2019 (June)	Retrospective review	Performance of a Deep-Learning Neural Network to Detect Intracranial Aneurysms from 3D TOF-MRA Compared to Human Readers	2015 to 2017	85	Deep learning neural network model	IC aneurysm diagnosis	Statistical analysis revealed no significant differences in overall sensitivity between the neural network, reader 1, and reader 2. Human readers detected a significantly higher portion of aneurysms (<3 mm) compared to the neural network in this study. In a clinical setting, neural network algorithms may potentially increase detection rates of cerebral aneurysms.
Zhu et al. [28]	2020 (May)	Retrospective review	Stability Assessment of Intracranial Aneurysms Using Machine Learning Based on Clinical and Morphological Features	2014 to 2018	1897	Machine learning random forests (RF) and support vector machine (SVM) and automated neural network	IC aneurysm diagnosis	ML models displayed better performance than the statistical LR model and PHASES score in intracranial aneurysm stability assessment.

PRISMA
Literature Scrutiny

12

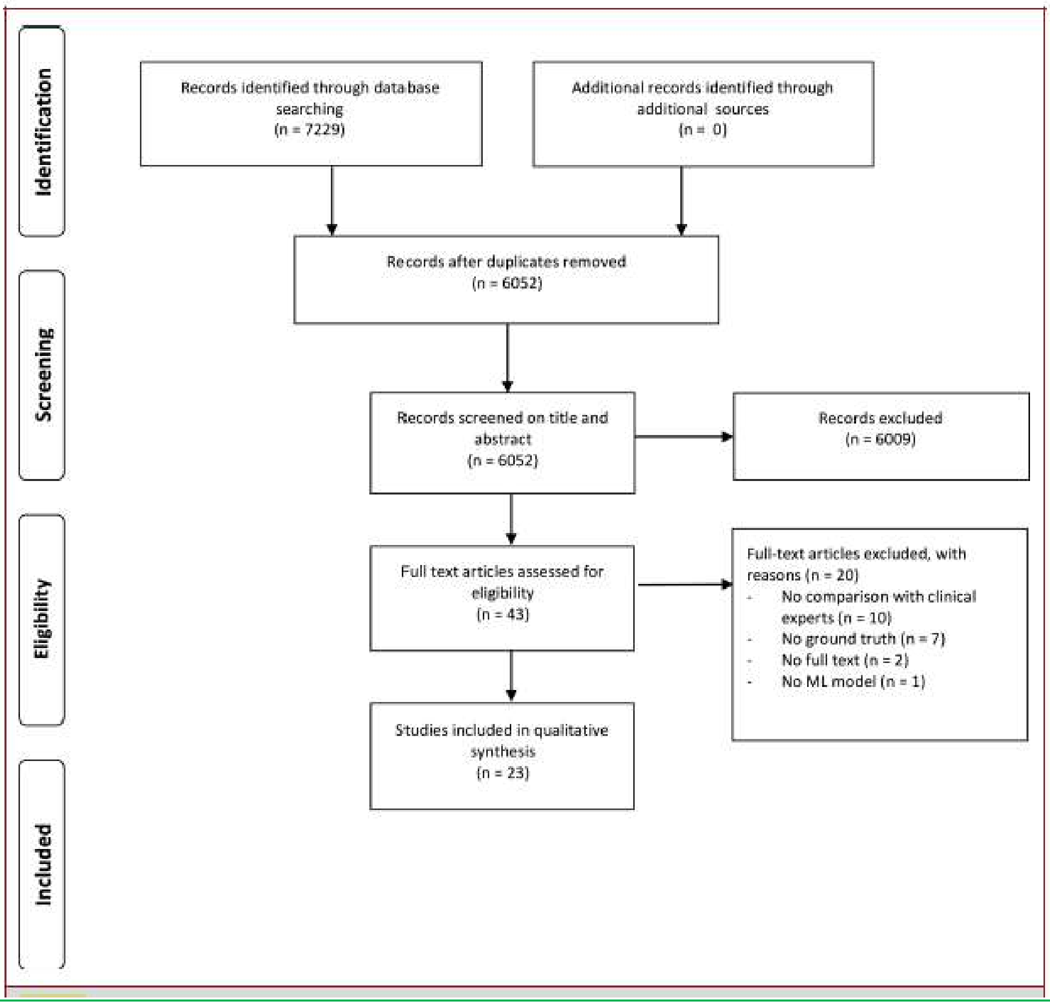

- ✓ PRISMA flow diagram of systematic identification, screening, eligibility, and inclusion.
- ✓ After screening 6052 studies, 23 studies were included in the final analysis.

32

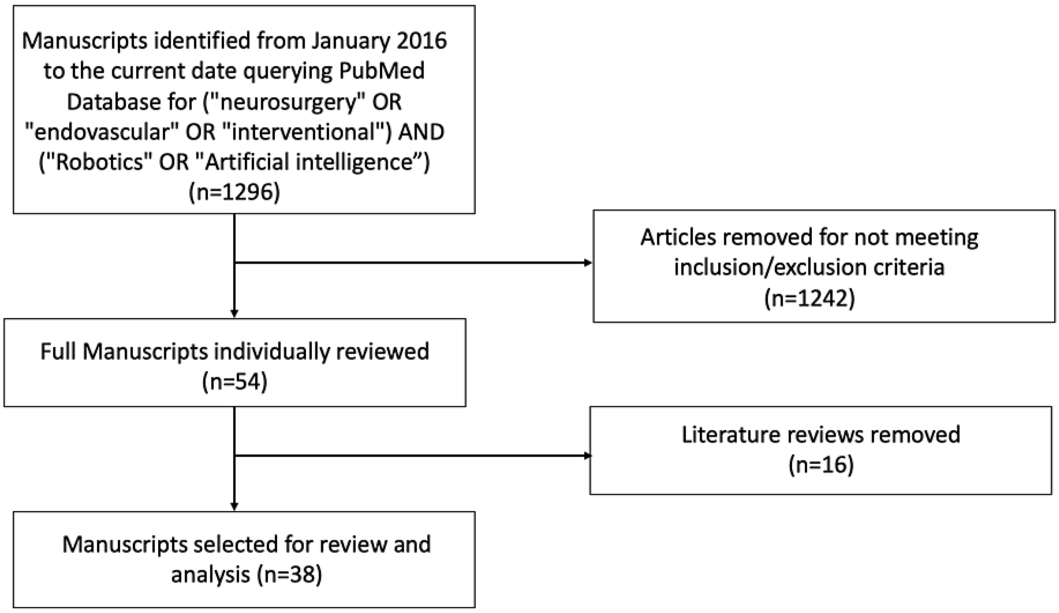

Article selection flowchart.

31

Flowchart diagram of literature search

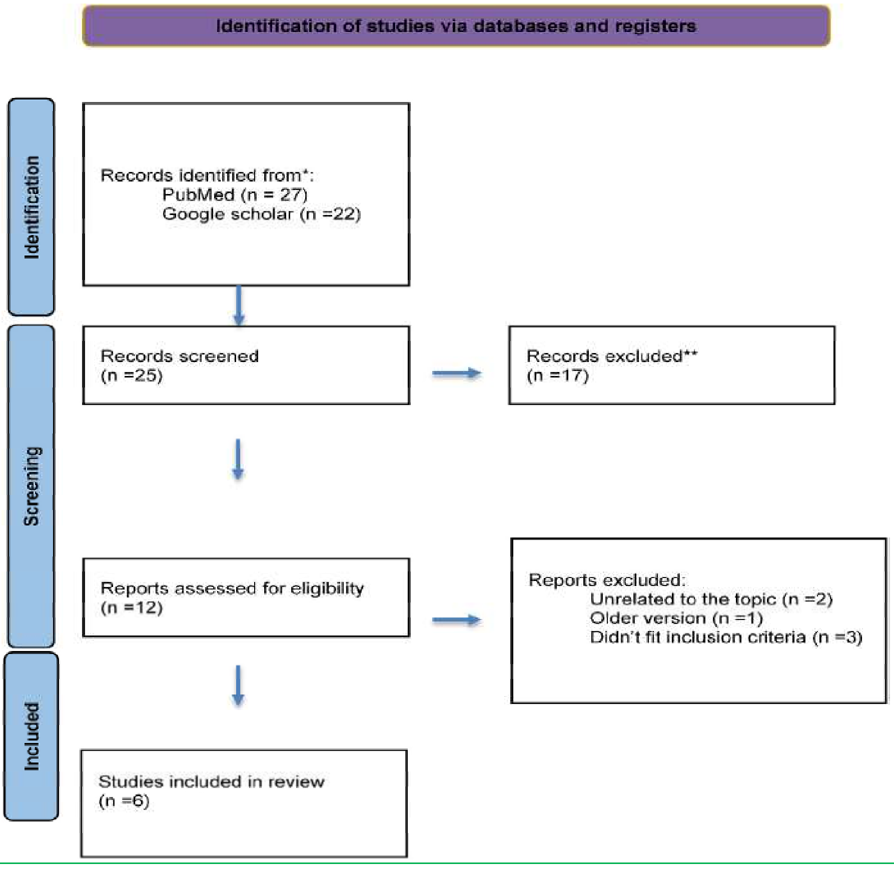

40

Trends in artificial intelligence research in neurosurgery

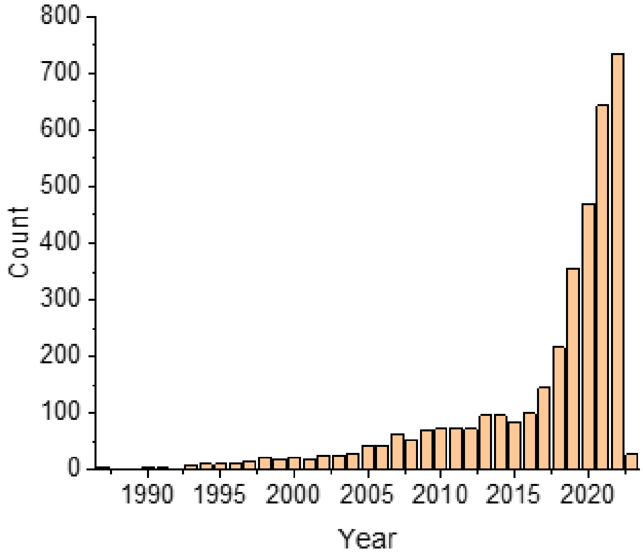

40

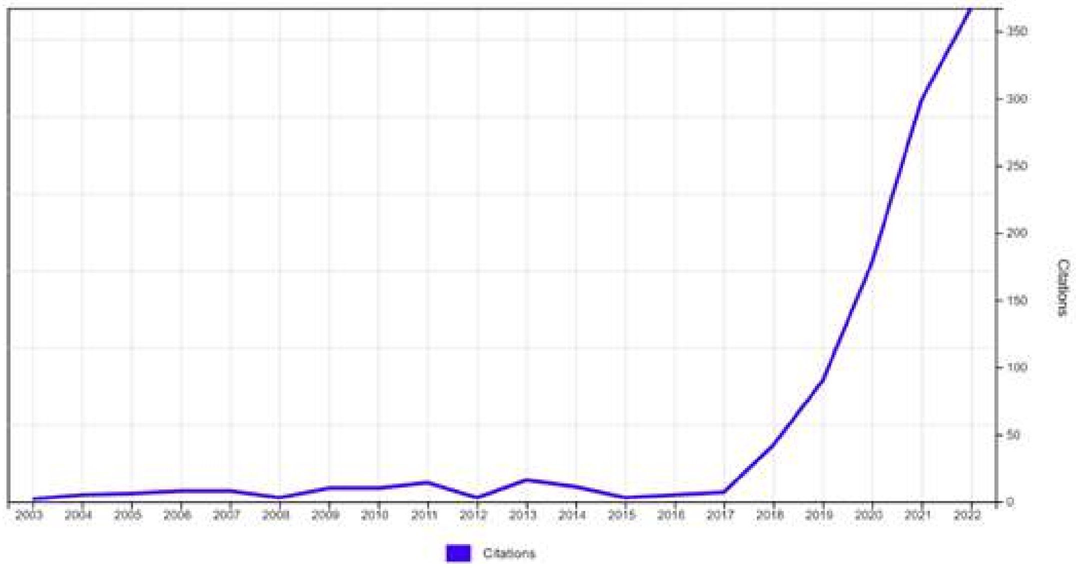

Trends in citations for artificial intelligence in neurosurgery in a year wise manner.

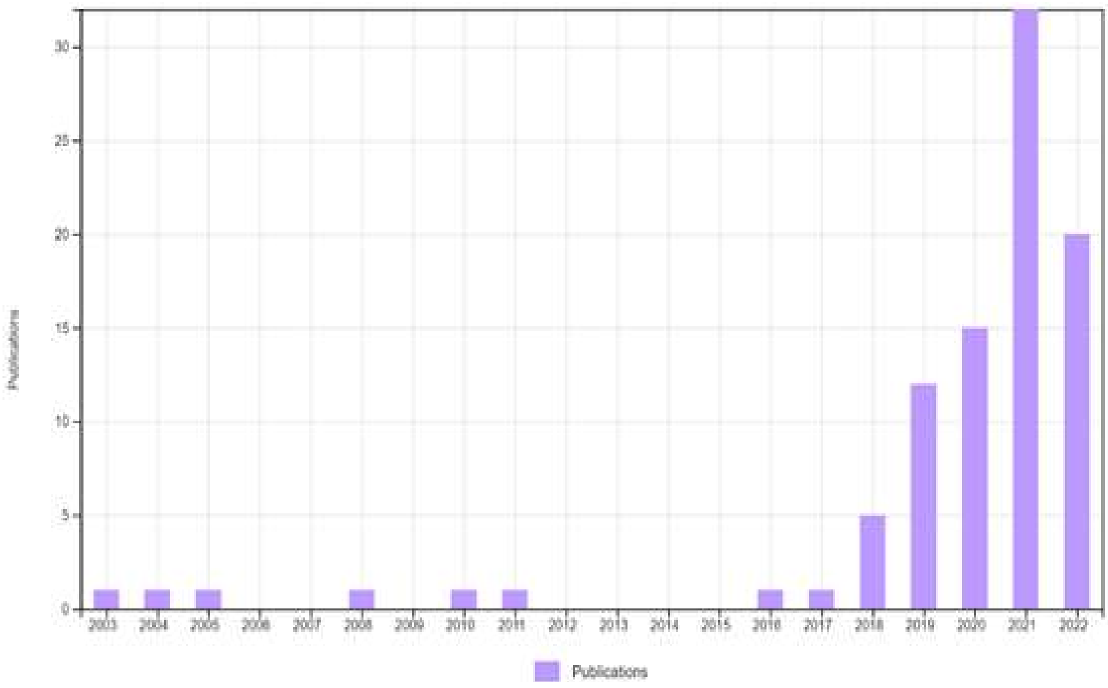

✓ Trends in publications for artificial intelligence in neurosurgery in a year wise manner.

40

Current trends and scope of artificial intelligence in neurosurgery

Neurosurgical areas trends	Salient problems	Pros	Cons
Neurooncology	Diagnostic studies	Large volume of data can be analyzed	High-end computing
Functional Neurosurgery	Prognostic studies	Better than models requiring human assistance	Knowledge of coding and computational sciences
Spine surgery	Prediction tools	Automation reduces clinical burden and increases accuracy	Reliance on reliable data
Vascular neurosurgery	Preoperative decision making		Prone to devastating errors
Neurotrauma	Intraoperative guidance		Not suitable for all problems
	Postoperative		
	Education		
	Research		

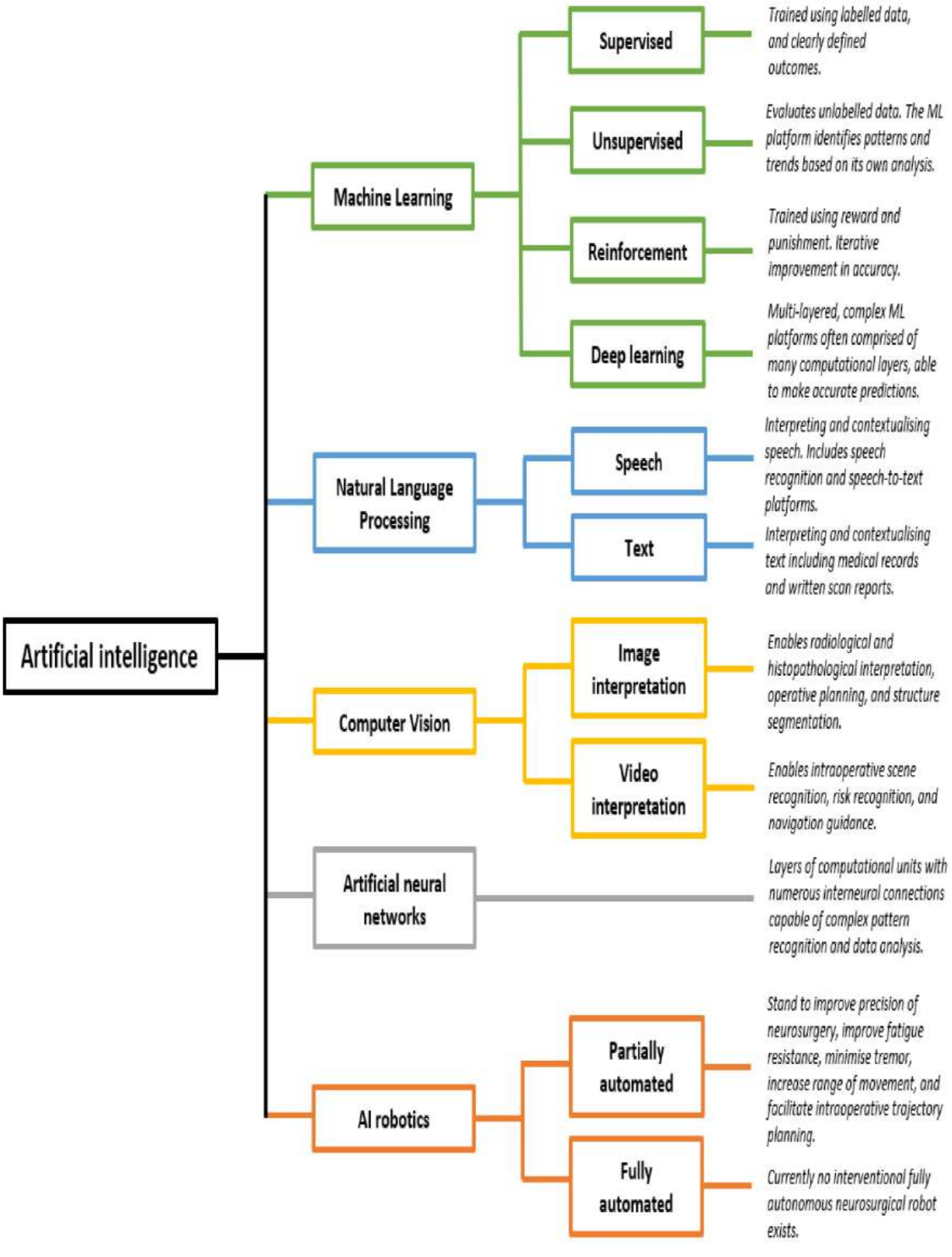

Artificial intelligence and subdomains.

- Clinical applications for brain tumour surgery patients.
- Numerous other subfields of AI exist, a
  - this schematic is not exhaustive

15

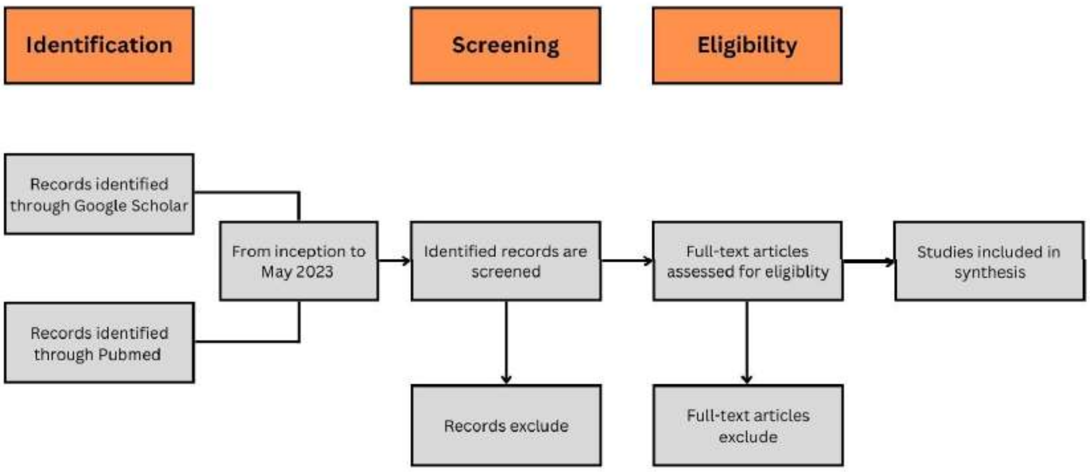

Literature Search Method.

- ✓ PubMed and Google Scholar were searched
- ✓ AI-related keywords: English Language publications
- ✓ Published from inception to May 2023.
- ✓ Observational studies, case–control studies, cohort studies, clinical trials, meta-analyses, reviews, and guidelines

34

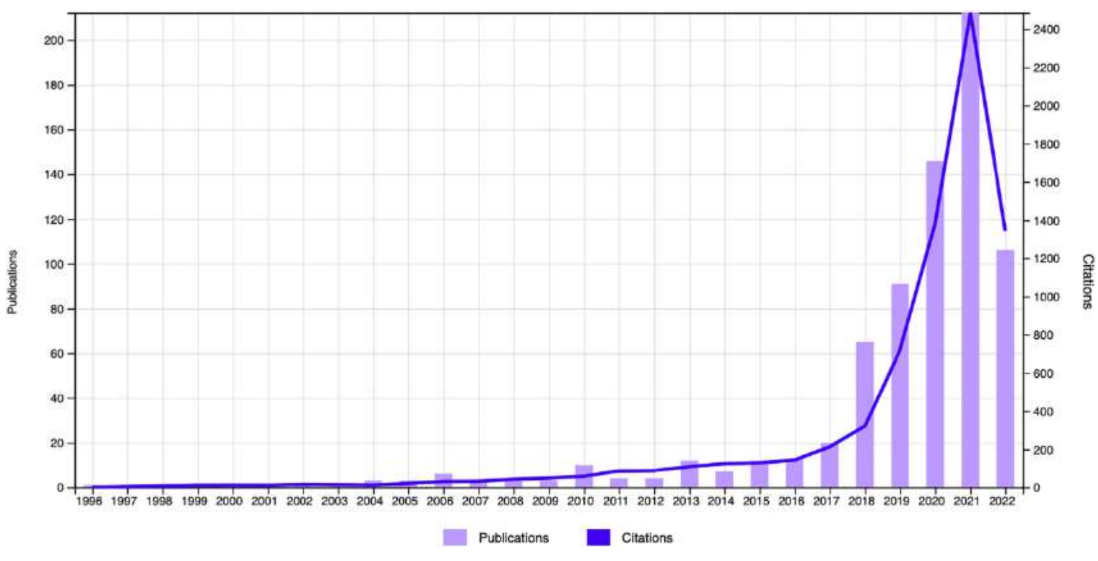

Trends in publications and citations pertaining to the use of AI in neurosurgery, from 1996 to the present date. AI, artificial intelligence.

- ✓ Web of Science electronic database search
- ✓ As of July 2022,

- ✓ Search strategy: [“artificial intelligence” OR
    - “machine learning” OR “deep learning”
    - OR “natural language processing” OR
    - “support vector machine” OR “naïve
    - bayes” OR “Bayesian learning” OR
    - “artificial neural network” OR “random
    - forest” OR “machine intelligence” OR
    - “k-nearest neighbor” OR “decision tree”
    - OR “data mining” OR “fuzzy” OR
    - “computational intelligence” OR
    - “computer reasoning”] AND
    - [“neurosurgeon” OR “neurosurgery” OR
    - “skull base surgery” OR “spine surgery”
    - OR “brain surgery” OR “cerebrovascular
    - surgery” OR “endovascular” OR
    - “neurosurgical”].
- ✓ No limitations with respect to the language
- or year of publication of articles.
- search yielded 731 results which were
- subsequently sorted by citation count.
- ! Top-50 most-cited articles
- ! relevant to the scope of this review were retrieved.

34

The Top-10 Most-Cited AI Articles Pertaining to the Field of Neurosurgery

Rank	Year	Title	Citation Count	Average Citations per Year	First Author	Last Author	Journal (IF)	Country
1	2018	Machine learning and neurosurgical outcome prediction: a systematic review	159	31.00	Senders	Arnaout	World Neurosurgery (2.21)	USA
2	2014	Machine learning for outcome prediction of acute ischemic stroke post intra-arterial therapy	102	11.11	Asadi	Mitchell	PLoS One (3.24)	Australia
3	2018	Natural and artificial intelligence in neurosurgery: a systematic review	101	20.20	Senders	Smith	Neurosurgery (5.315)	USA
4	2009	Atlas-based segmentation of degenerated lumbar intervertebral discs from MR images of the spine	90	6.93	Michopoulou	Todd-Pokropek	IEEE Transactions on Biomedical Engineering (4.538)	England
5	2020	EEG based multi-class seizure type classification using convolutional neural network and transfer learning	94	30.67	Raghu	Kubben	Neural Networks (9.657)	India
6	2018	Examining the ability of artificial neural networks machine learning models to accurately predict complications following posterior lumbar spine fusion	78	14.40	Kim	Cho	Spine (3.241)	USA
7	2020	Artificial intelligence to diagnose ischemic stroke and identify large vessel occlusions: a systematic review	75	24.33	Murray	Hui	Journal of Neurointerventional Surgery (3.572)	USA
8	2020	Classification of brain tumors from MRI images using a convolutional neural network	70	23.33	Badza	Barjaktarovic	Applied Sciences-Basel (2.838)	Serbia
9	2018	Spatio-spectral classification of hyperspectral images for brain cancer detection during surgical operations	68	13.20	Fabelo	Sarmiento	PLoS One (3.24)	Spain
10	2010	Use of an artificial neural network to predict head injury outcome	67	4.92	Rughani	Tranmer	Journal of Neurosurgery (5.403)	USA

34

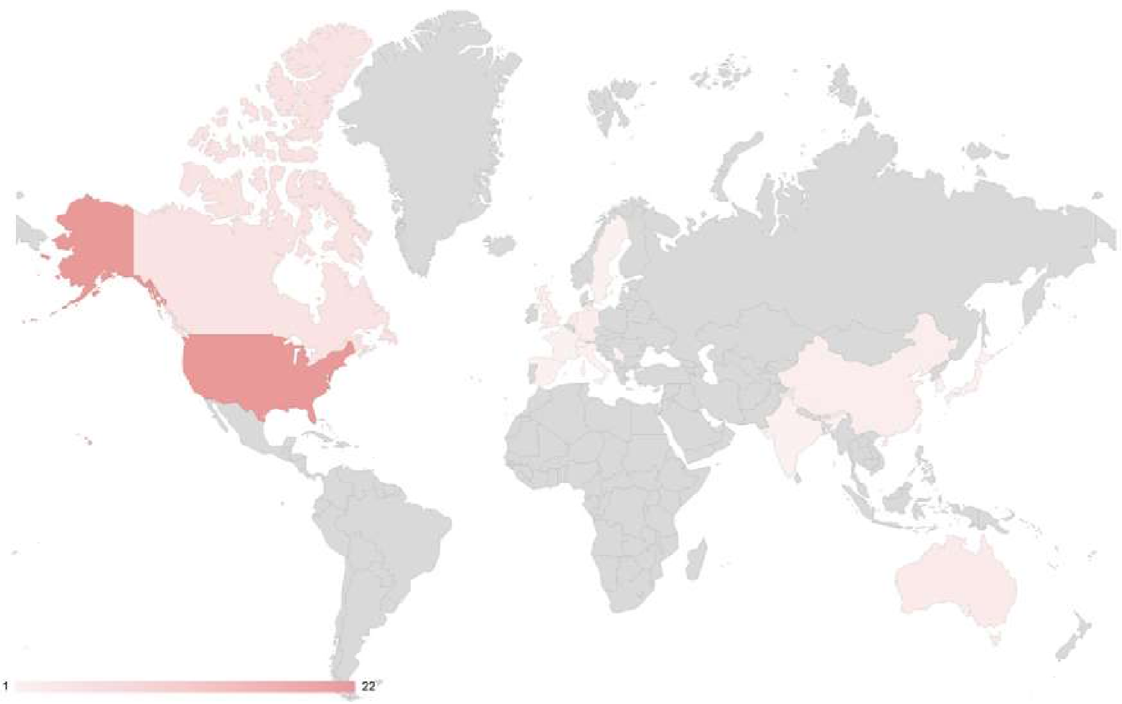

Choropleth map

Relative contribution from different countries to 50 most-cited articles.

34

Areas of Application and

Uses of AI in Neurosurgery

Among the 50 Highest-Cited Articles

Area of Application	Number of Articles	Use of AI	Number of Articles
Spine	13	Prediction model	16
Endovascular	12	Diagnostic and/or imaging aid	14
Neuro-oncology	9	Assisting or enhancing other technologies	8
Trauma	5	Guiding a personalized treatment plan	4
Functional neurosurgery	3	Improvement of surgical technique	3
Education	2	Big data management and analysis	1
Pediatric neurosurgery	1	Non-specific	4
Endoscopic neurosurgery	1		
Non-specific	4		

GOF
ML Models

12

Performance of ML Models and Clinical Experts

First author, year of publication	Output	Input features	Outcome measures	ML models	Clinical experts	P-value
Diagnosis						
Diagnostic tumor classification						
Kitajima, 2009[39]	Differentiate pituitary adenoma, craniopharyngioma, Rathke's Cleft[a]	Age, MRI	AUC	0.990	0.910	NA[d]
Yamashita, 2008[40]	Differentiate brain metastases, glioma grade II-V, malignant lymphoma[a]	Age, history of brain tumor, MRI	AUC	0.95	0.90	NA[d]
Bidiwala, 2004[37]	Differentiate pediatric posterior fossa tumors: medulloblastoma, cerebellar astrocytoma, ependymoma	Age, gender, symptoms, signs, CT, MRI	Sensitivity Specificity PPV	73%-86% 86%-93% 73%-86%	57%-59% 82%-83% 62%-63%	.074[c] .77[c] .17[c]
Arle, 1997[36]	Differentiate pediatric posterior fossa tumors: astrocytoma, PNET, ependymoma/other	Age, gender, MRI, MRS	Accuracy	95%	73%	**<.001[c]**
Tumor grading						
Juntu, 2010[38]	Differentiate between benign and malignant soft-tissue tumors including neural tumors	MRI	Accuracy Sensitivity Specificity AUC	93% 94% 91% 0.92	90% 81% 92% 0.85	.61[c] **.009[c]** 1.00[c] NA[d]
Zhao, 2010[44]	Classify glioma into grade I-IV	Age, MRI	Accuracy overall Accuracy LGG Accuracy HGG Kappa value AUC	82% 82% 85% 0.68 0.870	65% 62% 66% 0.47 0.71	**.001** 09 **.008** NA[d] **.004**
Emblem, 2009[33]	Classify glioma into grade I-IV	MRI	AUC	NA	NA	.56-.97
Abdolmaleki, 1997[54]	Differentiate between low and high-grade astrocytomas[a]	MRI	Accuracy AUC r	89% 0.91 0.87	80% 0.84 0.56	**.003** <.001[c] NA[d]
Christy, 1995[52]	Classify glioma into grade I-IV	MRI	Accuracy	61%	57%	.84[c]

12

Details on Clinical Experts, MLModels, Size Training/Test Set, Validation Method, and Ground Truth

First author, Year of publication	Experts	ML models	Size training set	Validation method	Size test set	Ground truth
Diagnosis						
Diagnostic tumor classification						
Kitajima, 2009[39]	5 general radiologists + 4 neuroradiologists[a]	ANN	43	LOOCV	–	Histological diagnosis
Yamashita, 2008[40]	9 radiologists[a]	ANN	126	LOOCV	–	Histological diagnosis
Bidiwala, 2004[37]	1 neuroradiologist	ANN	33	CV (NOS)	–	Histological diagnosis
Arle, 1997[36]	1 neuroradiologist	ANN	80	5-FCV	–	Histological diagnosis
Tumor grading						
Juntu, 2010[38]	2 radiologists	SVM, ANN, DT(C4.5)	60-100	10-FCV	–	Histological diagnosis
Zhao, 201 0[44]	1 neurosurgeon + 1 neuroradiologist	SVM	106	5-FCV	–	Histological grading
Emblem, 2009[33]	4 neuroradiologists	FCM	–	–	50	Histological grading
Abdolmaleki, 1997[54]	3 neuroradiologists	ANN	43	–	36	Histological grading
Christy, 1995[52]	1 radiologist	ANN, LR	52	–	29	Histological grading
Other applications						
Campillo, 2013[53]	1 neurosurgeon + 1 hospital hygienist physicians	NA	3785	–	1225	Patients identified by expert, NLP or ICD-10 code database
Duun-Henriksen, 2012[51]	1 neurophysiologist	SVM	10	–	10	NA
Tankus, 2009[43]	1 human observer (NOS)	LDA	12	LOOCV	–	Synthetic database with known ground truth
Sinha, 2001[48]	9 pediatric EM attendees + 6 pediatric EM fellows	ANN	382	–	351	CT imaging

22

Evaluation of GOF Metrics and Clinical Outcomes of Artificial Intelligence Models in Neurosurgery Diagnosis and Treatment

Author, Year, Country	Specialty	AI Model Types Used In the Study	Evaluation Metrics and Clinical Outcomes
Merali et al., 2021, Canada [6]	Spinal Neurosurgery	DL (CNN)	Cervical Spinal Cord Compression Detection: Accuracy: 94% Sensitivity: 88% Specificity: 89%
Hallinan et al., 2022, Singapore [7]	Spinal Neurosurgery	DL (CNN)	Spinal Metastases Detection: Internal test sets: Sensitivity: 97.6% Specificity: 93.6% External test sets: Sensitivity: 89.9% Specificity: 98.1%
Doerr et al., 2022, United States [9]	Spinal Neurosurgery	DL (CNN)	Injury Classification Accuracy: 86.8%
Kim et al., 2020, Republic of South Korea [12]	Spinal Neurosurgery	ML (Random forest, XGBoost, Bayesian generalized linear model, decision-making tree model, k-cluster analysis, logistic regression analysis and neural network analysis)	Operation time Accuracy: 97.5% Reoperation occurrence Accuracy: 95.2%
Hopkins et al., 2020, United States [13]	Spinal Neurosurgery	ML (DNN)	Prediction of Postoperative SSI Accuracy: 78.7%
De la Garza Ramos et al., 2022, United States [14]	Spinal Neurosurgery	ML (ANN)	Prediction of Perioperative Blood Transfusion: Accuracy: 77%

AI +{Surgery [neuro]}

15

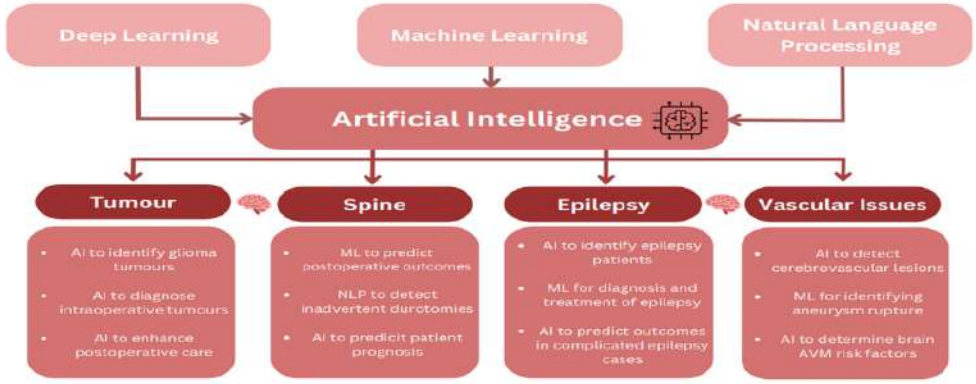

AI in neurosurgery

22

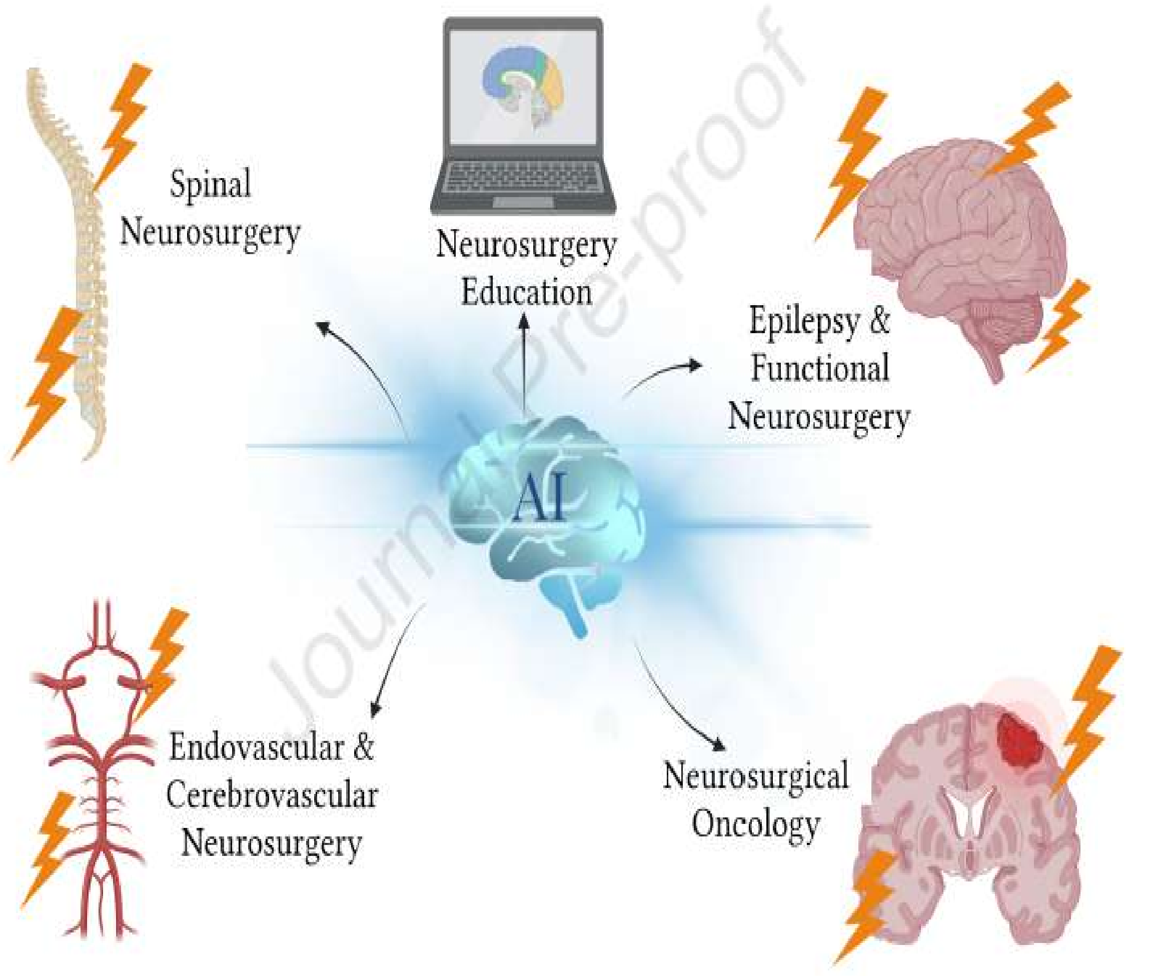

AI + Neuro Diseases

22

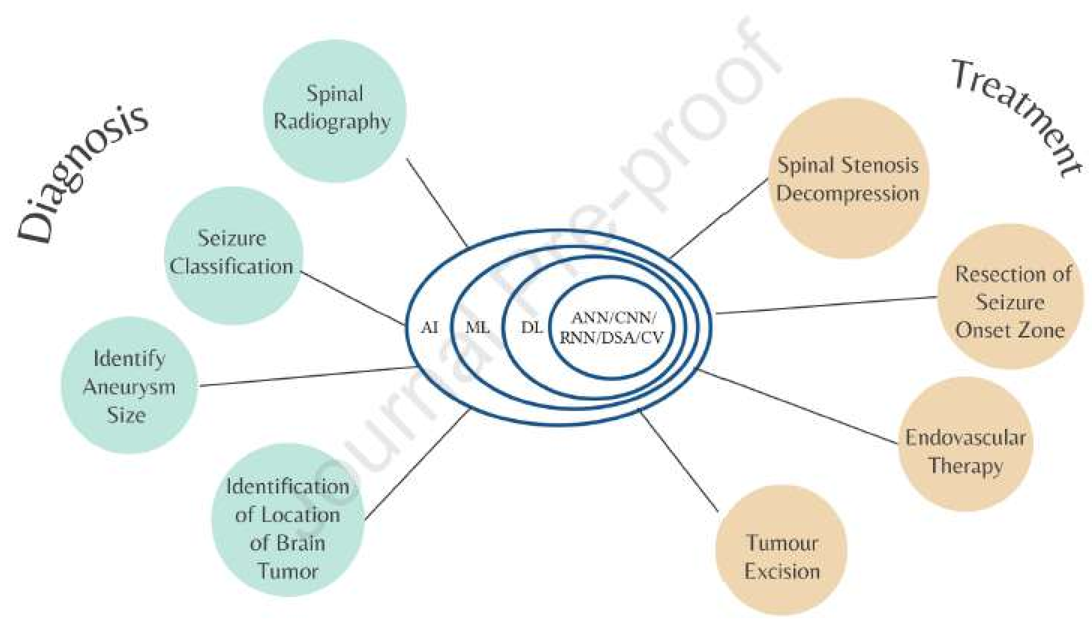

35

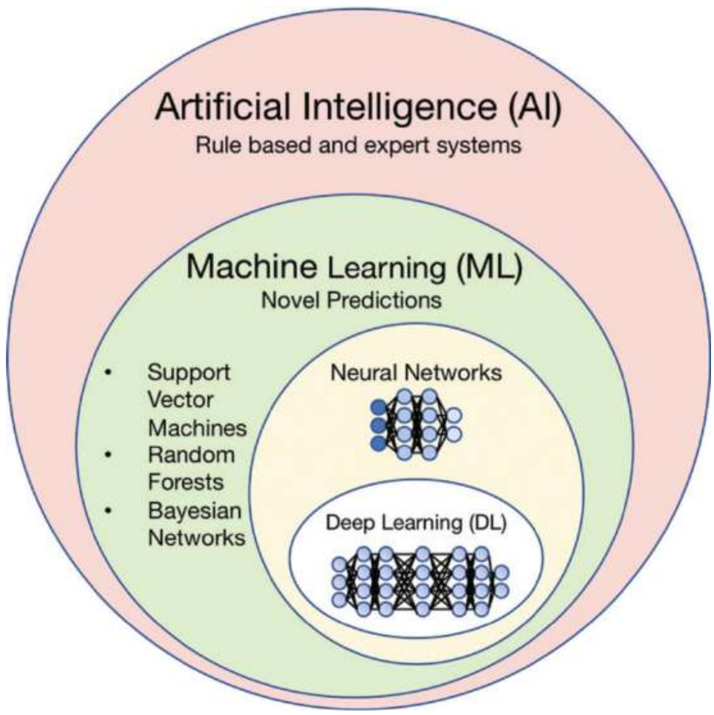

Artificial intelligence Components and their nested relationships

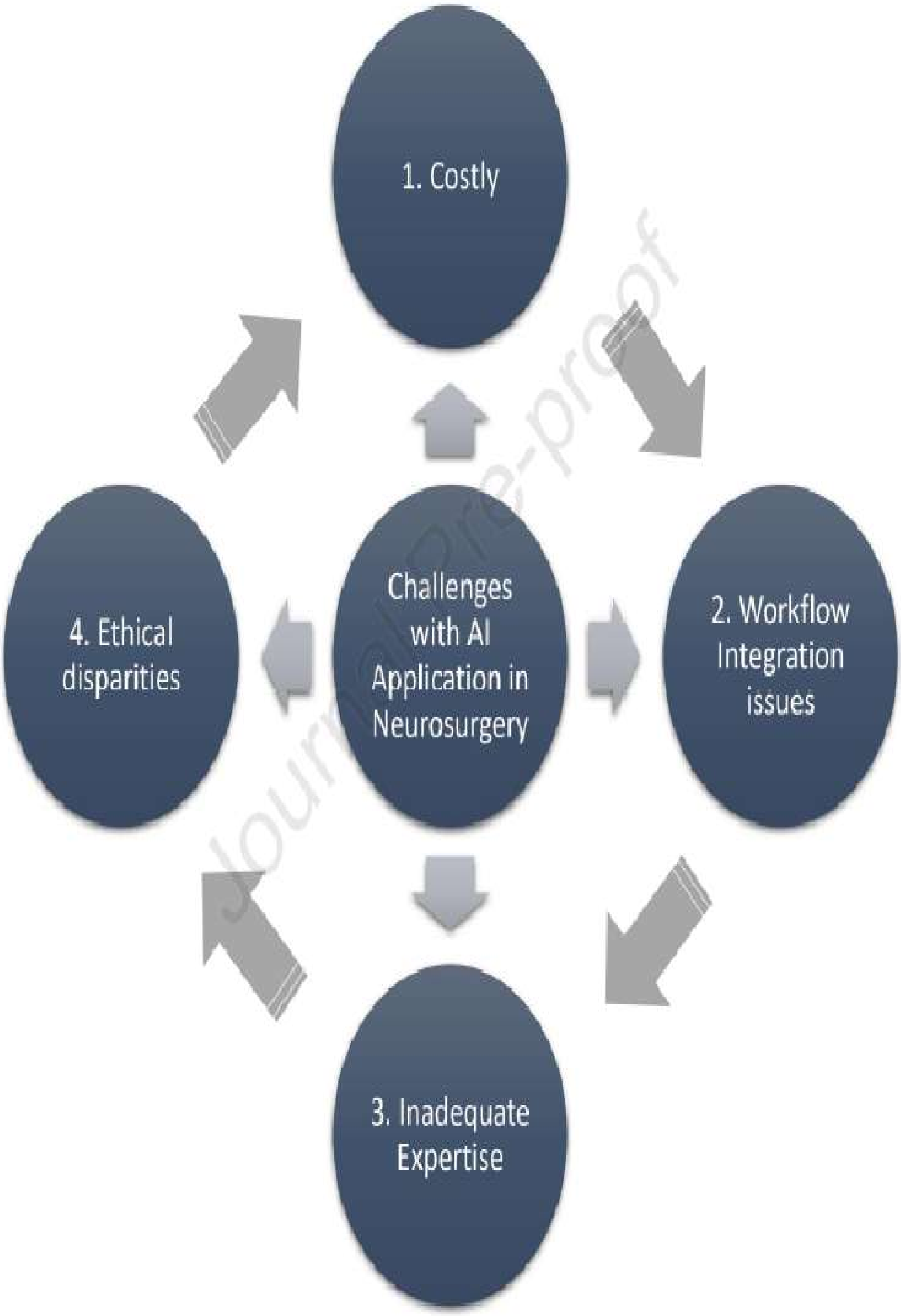
1. Costly
Challenges with AI Application in Neurosurgery
2. Workflow Integration issues
3. Inadequate Expertise
4. Ethical disparities

Future of
AI + Sun {:SUrgery [Neuro]}

15

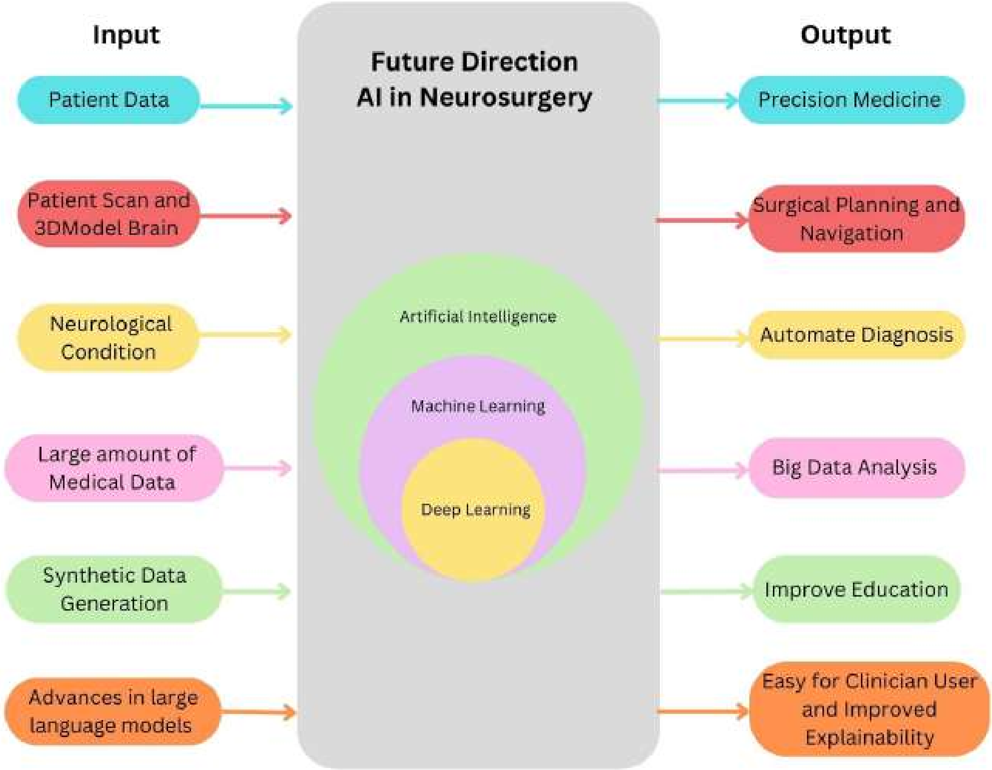

Future direction AI in neurosurgery

ChatGPT (AI) Is Ready to DoChemistry and NeuroScience/Surgery

18

The AI Behind ChatGPT Is Ready to DoChemistry

23

7T MRI

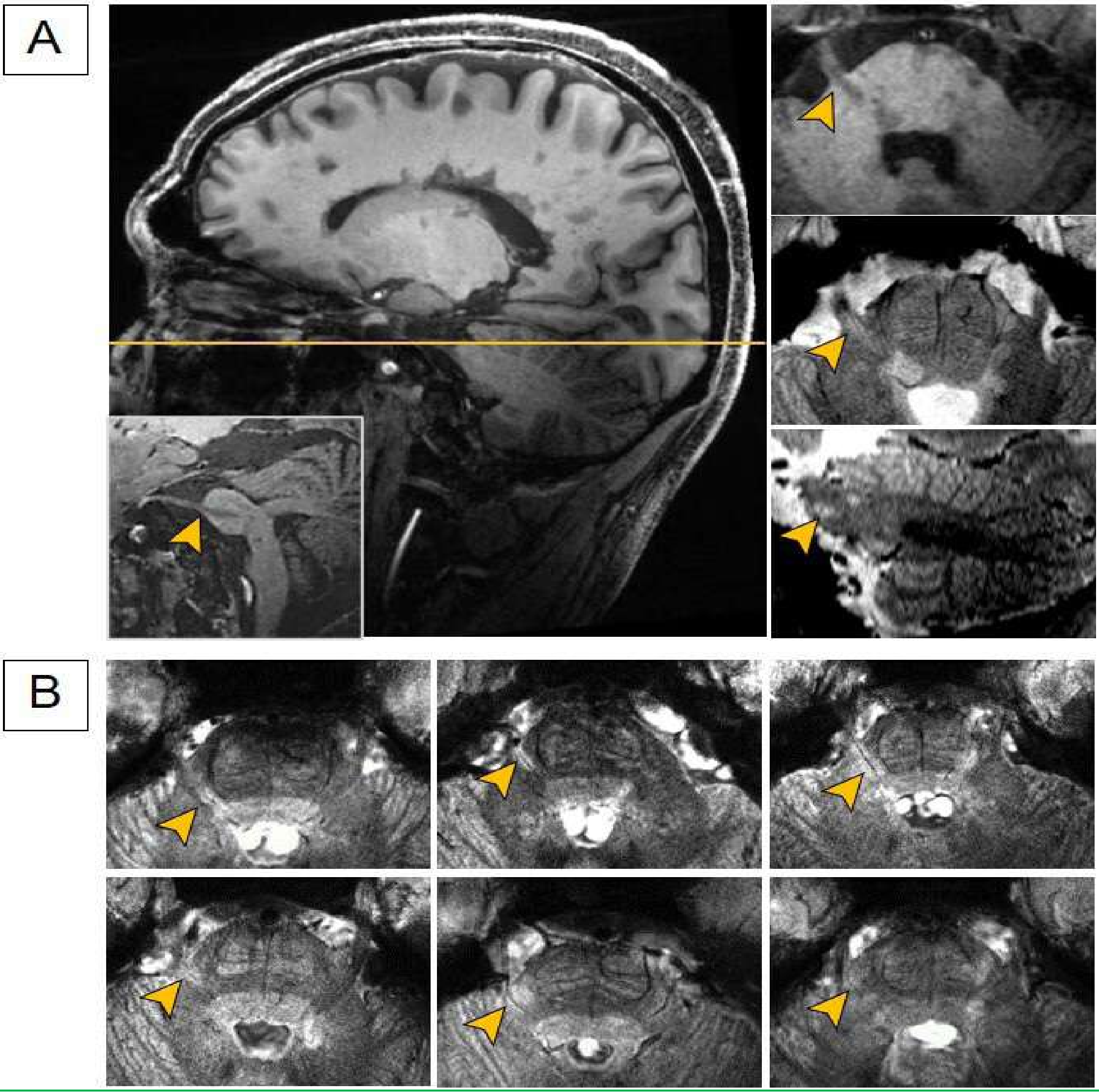

Central vein sign (CVS) in trigeminal lesions of multiple sclerosis on 7T MRI.

- ✓ (A) Representative image of trigeminal lesions and CVS (arrowheads) in patient 10. Sagittal (left panel) and axial (upper, right panel) T1 MPRAGE reveal lesions of the trigeminal root entry zone (REZ) (arrowheads). The dark vein can be visualised in axial and sagittal T2*-weighted image (arrowheads in middle and lower of right panel).
- ✓ (B) FLAIR* axial images of patients 3, 5, 6, 7, 13 and 15 demonstrate a dark vein located centrally in the majority of the trigeminal lesion (arrowheads), especially in REZ. MPRAGE, magnetisation-prepared rapid acquisition gradient echoes.

23

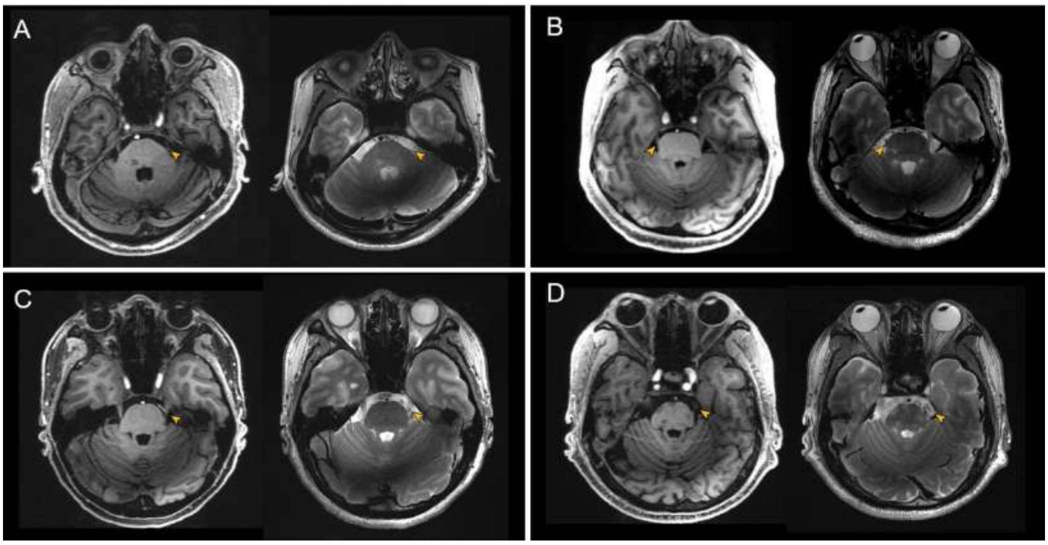

7T MPRAGE-MRA

- ✓ T2-weighted image on the axial plane demonstrate neurovascular compression in patients 1, 4, 9 and 10.
- ✓ The arrowhead indicates the vessels touching the trigeminal nerve.
- MPRAGE-MRA: magnetisation-prepared rapid acquisition gradient echoes-magnetic resonance angiography.

35

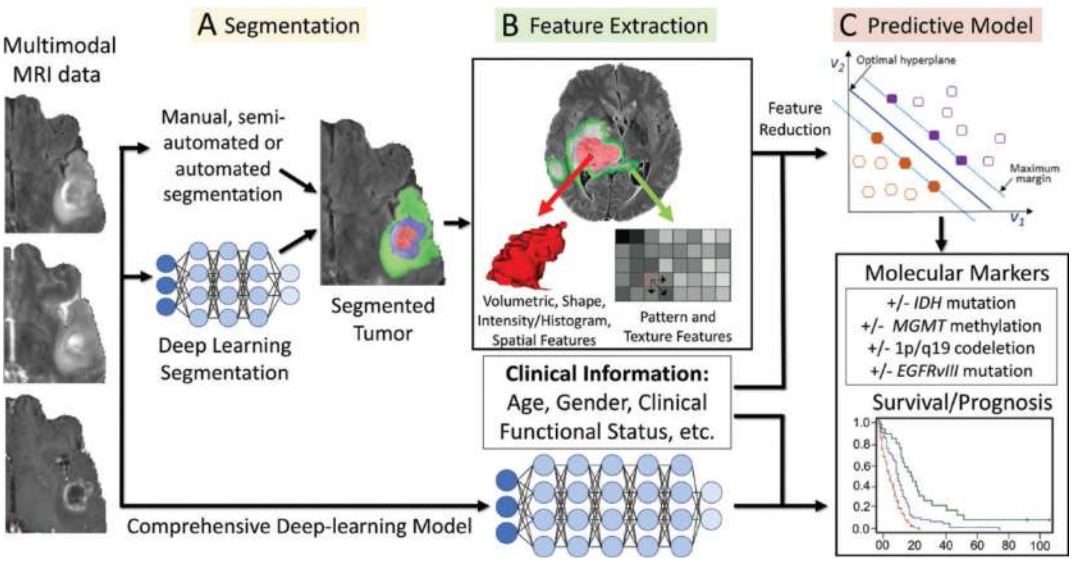

Workflow of radiomics in neuro-oncology.

- ✓ A, After preprocessing steps, multimodal MR images are segmented by using automated or manual methods.
- ✓ B, This is followed by feature extraction with use of a variety of different techniques.
- ✓ C, Machine learning methods are then trained on the features to generate models of underlying molecular markers and predict survival.

- ✓ Deep learning models can be used for performing each of the described steps individually or in a more comprehensive fashion (bottom pathway of figure).
- ✓ EGFRvIII = epidermal growth factor receptor variable III,
- ✓ IDH = isocitrate dehydrogenase,
- ✓ MGMT = O6-methylguanine-DNA-methyltransferase

23

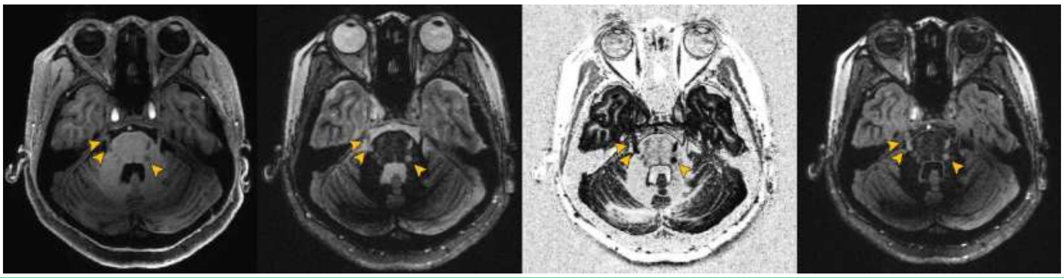

Representative image of trigeminal involvement in FLAWS.

- ✓ The arrowhead illustrated the cisternal trigeminal nerve, root entry zone (REZ) and nuclear zone (patient 15).
- ✓ From left to right are INV2, INV1, UNI and FLAWS images from the FLAWS-MP2RAGE
- ✓ sequence.
- ✓ FLAWS-MP2RAGE, fluid and white matter suppression based on the magnetisation-prepared 2 rapid acquisition gradient echoes

23

Table 1 Clinical and trigeminal nerve involvement characteristics

Num	Age, y	Diagnosis	Disease duration, y	EDSS	Disease-modifying treatment*	Location†	CVS (Y/N)	Facial sensory symptom	Trigeminal neuralgia (Y/N)
Patient 1	20s	RRMS	1	2	Siponimod	R: a, c L: a	N	N	N
Patient 2	20s	RRMS	1	3	Ofatumumab	R: a, c L: a, c	N	N	N
Patient 3	30s	RRMS	2	1	Siponimod	R: c L: c	R: Y L: N	N	N
Patient 4	30s	RRMS	0.3	1	Dimethyl fumarate	R: a	N	Maxillary	N
Patient 5	50s	RRMS	5	2.5	NA	R: a, b	Y	N	N
Patient 6	30s	RRMS	5	2	Dimethyl fumarate	R: a, c L: a	R: Y L: N	N	N
Patient 7	30s	RRMS	5.5	1	Ofatumumab	R: a	Y	N	N
Patient 8	20s	RRMS	2.5	2	Teriflunomide	R: a, c L: a, c	R: N L: N	N	N
Patient 9	30s	RRMS	2	0	Siponimod	L: a	N	Maxillary	N
Patient 10	30s	RRMS	11	2	NA	R: a, b, c L: a	R: Y L: Y	N	N
Patient 11	30s	RRMS	6	2	Teriflunomide	R: a L: a	N	Maxillary, mandibular	N
Patient 12	20s	RRMS	2.25	1	NA	L: a, c	L: N	N	N
Patient 13	20s	RRMS	2	4.5	NA	R: a L: a, b, c	R: Y L: Y	Maxillary	Y
Patient 14	20s	RRMS	4.5	7	Siponimod	R: a, b, c L: a	N	N	N
Patient 15	30s	RRMS	2	6	Siponimod	R: a, b, c L: a, c	R: Y L: Y	N	N

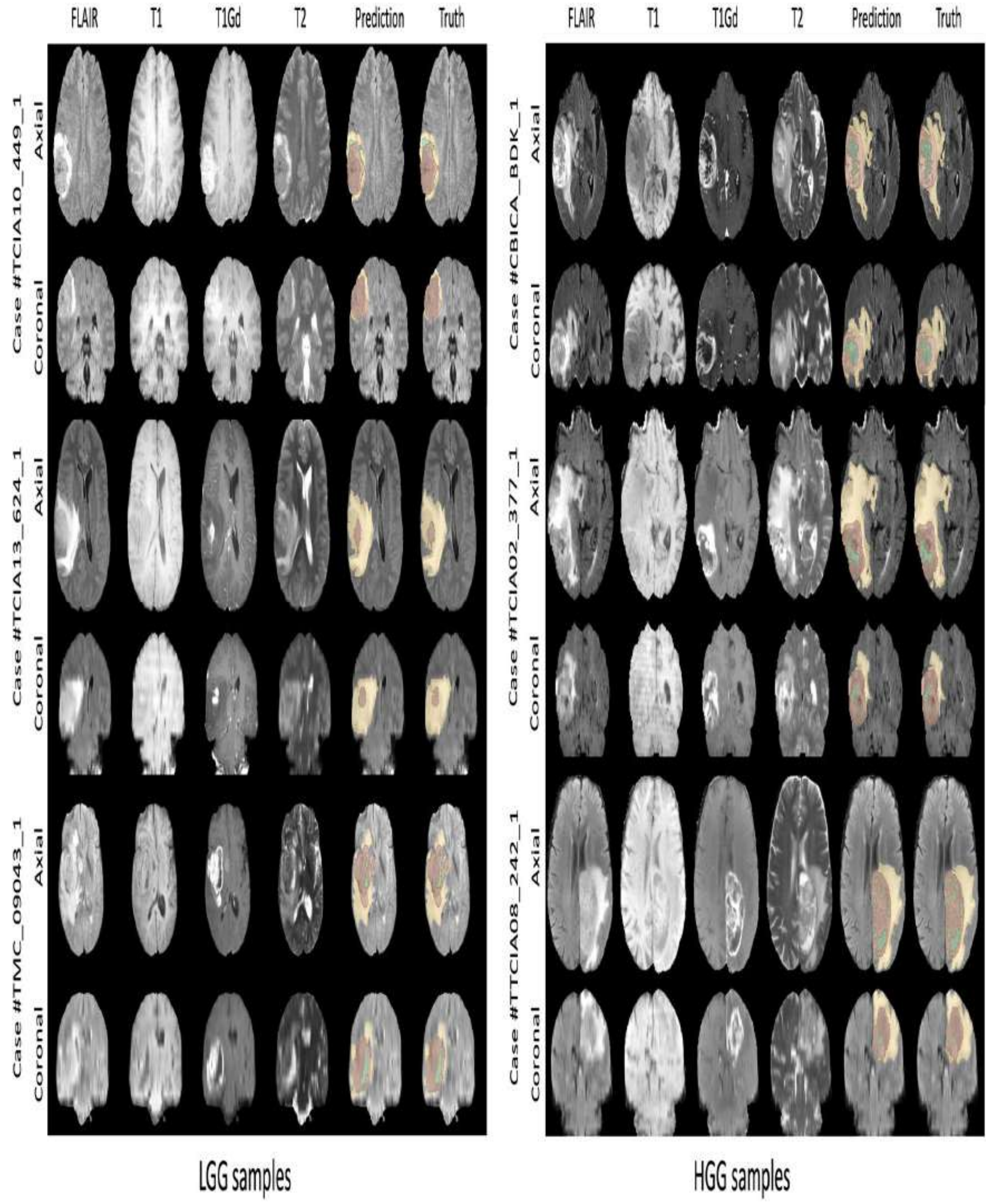

Visual segmentation results of TransXAI on Axial and Coronal views

- ✓ Predictions for three BraTS 2019 Challenge LGG samples (left) and HGG samples (right).
- ✓ Tumor regions are color-coded, with the ET shown in green, the TC including both green and red regions, and the WT representing all the segmentation classes.

Glioma

Landscape of diffuse gliomas

35

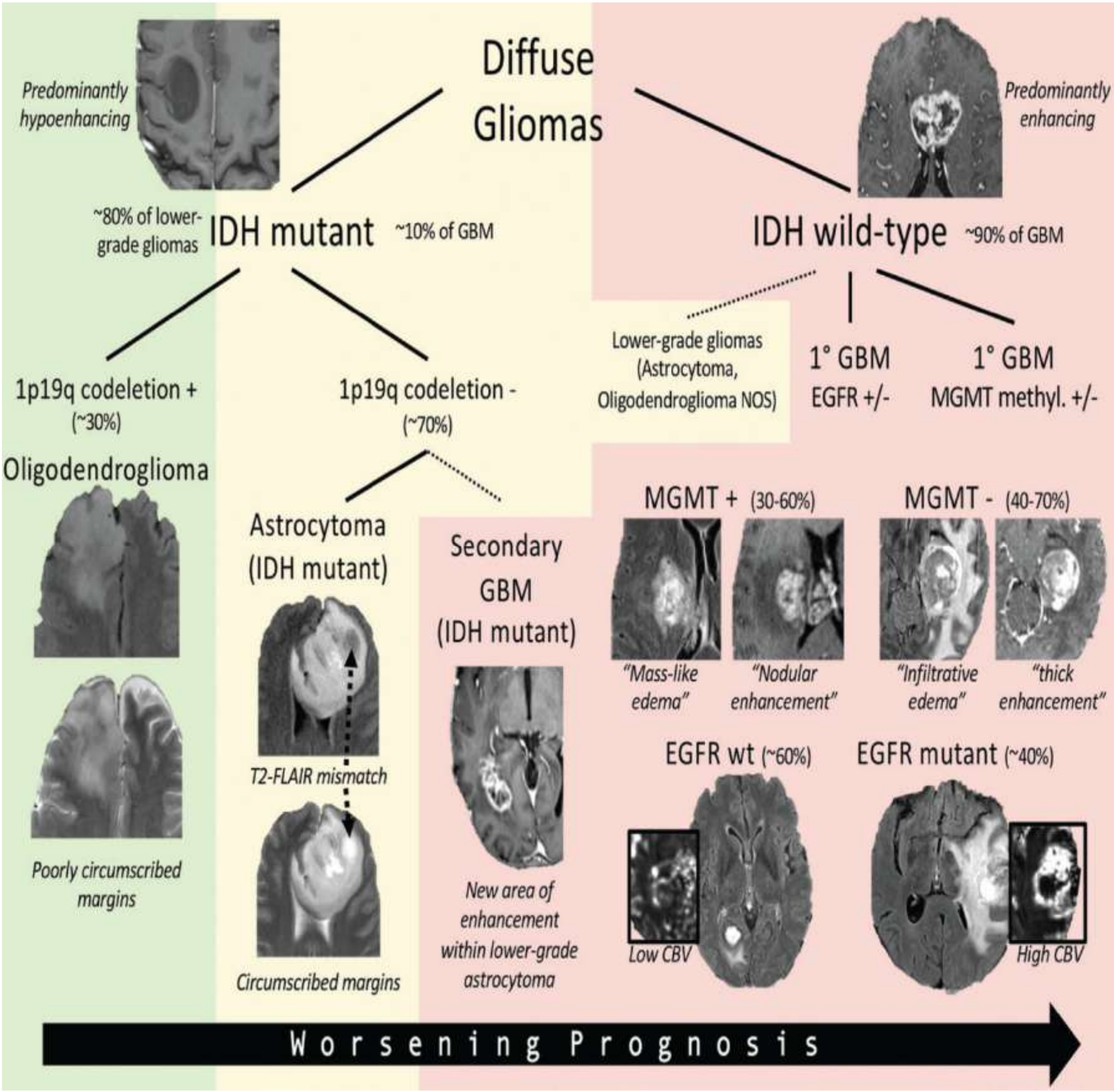

Genomic and radiogenomic landscape of diffuse gliomas

24

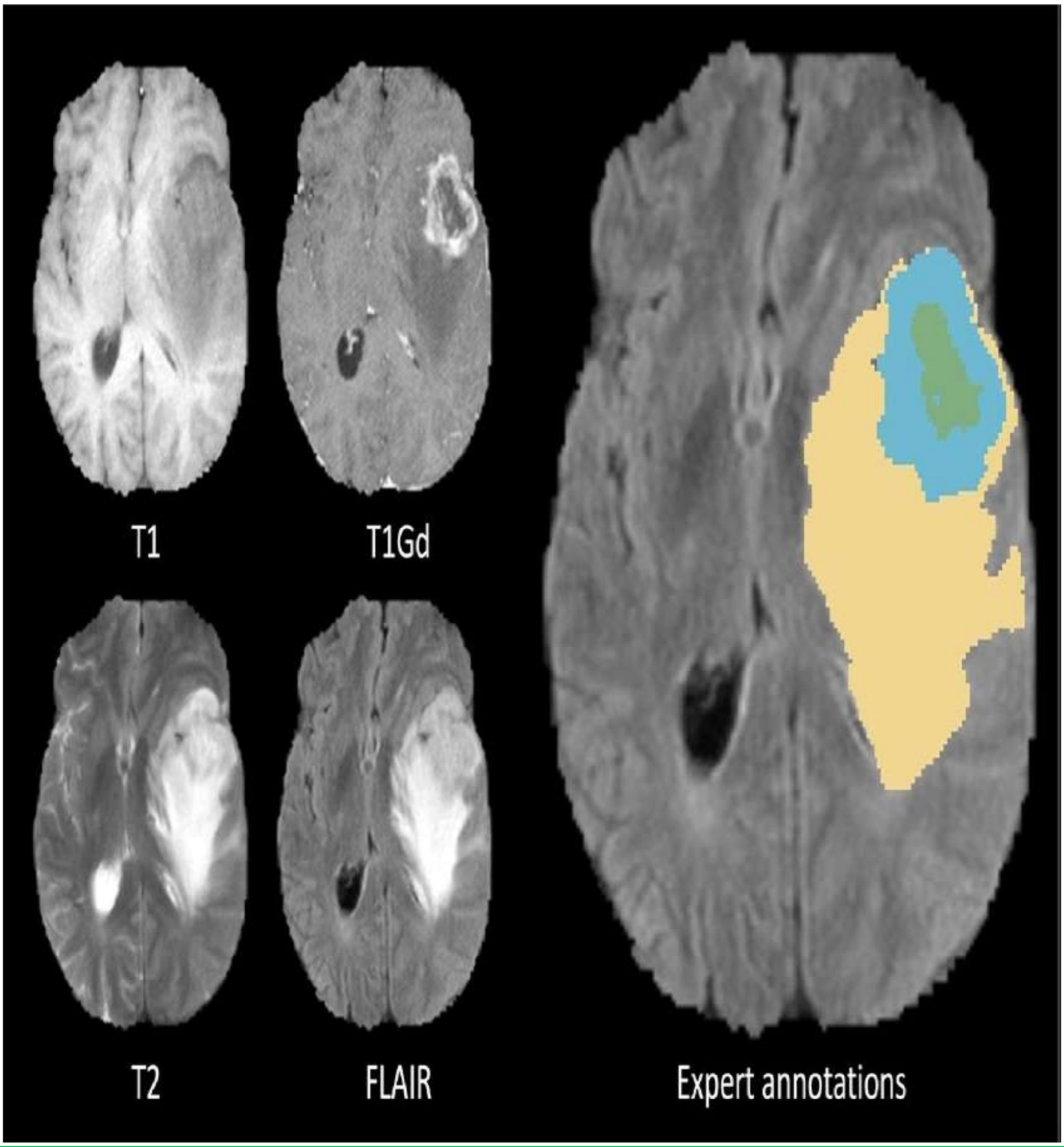

Glioma sub-regions in a sample scan from the BraTS 2019challenge database. Image patches show the different modalities of T1, T1Gd, T2, FLAIR, and annotated expert-labeled tumor segmentation. Ground
truth segmentation is provided for the enhancing tumor (blue) surrounding the non-enhancing necrotic tumor
core (green) visible in T1Gd, and (b) the peritumoral Edema (yellow) visible in the FLAIR, respectively.

MRI +
xAI

24

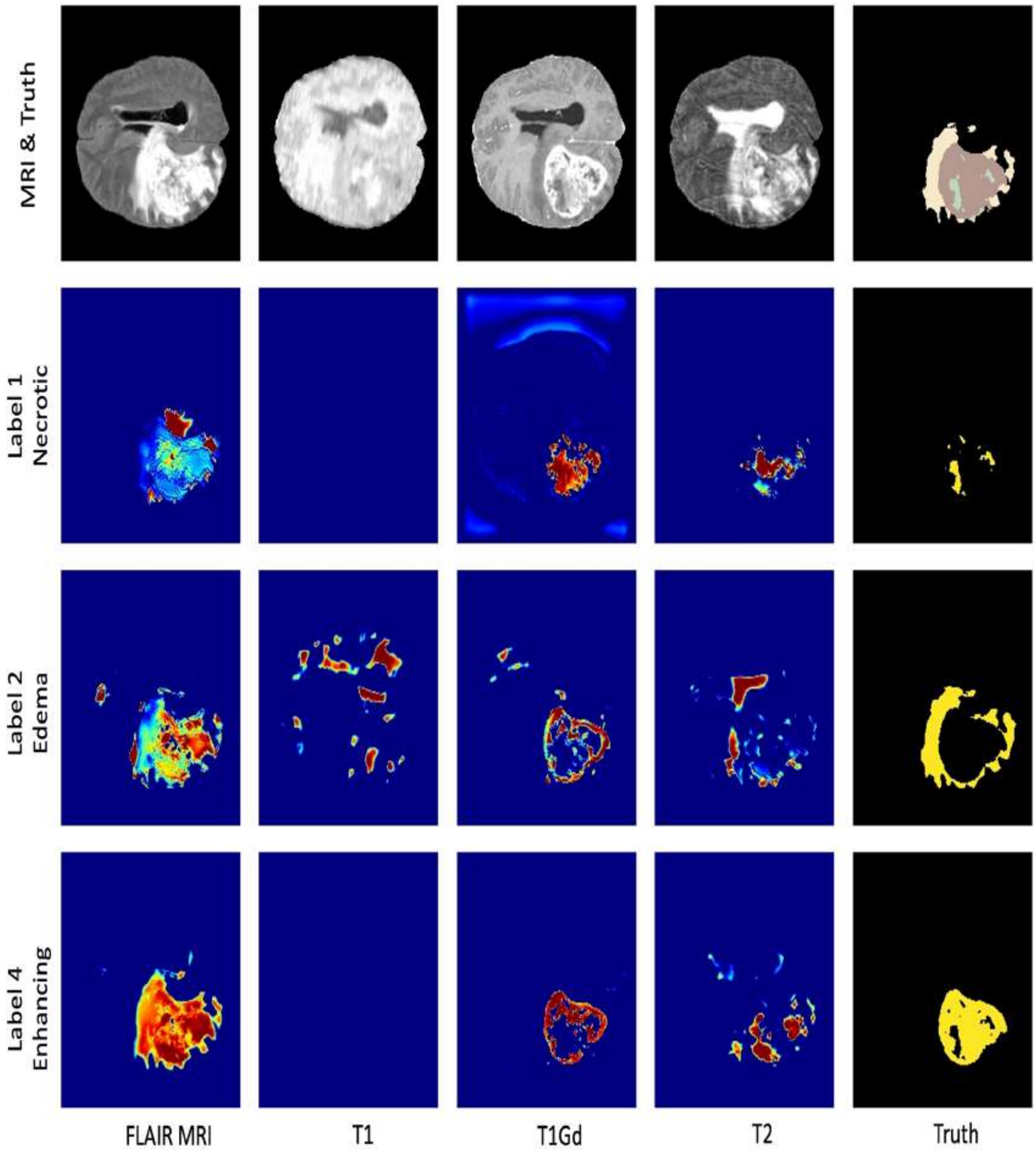

Impact of MRI input modality in the detection of different tumor labels.

- ✓ The first row shows the input MRI sequences and the ground truth annotations.
- ✓ The following rows correspond to label 1 (the necrotic tumor core),
- ✓ label 2 (the peritumoral edema), and label 4 (the enhancing tumor).
- In the saliency maps, warmer regions represent a high score for the specified label detection

24

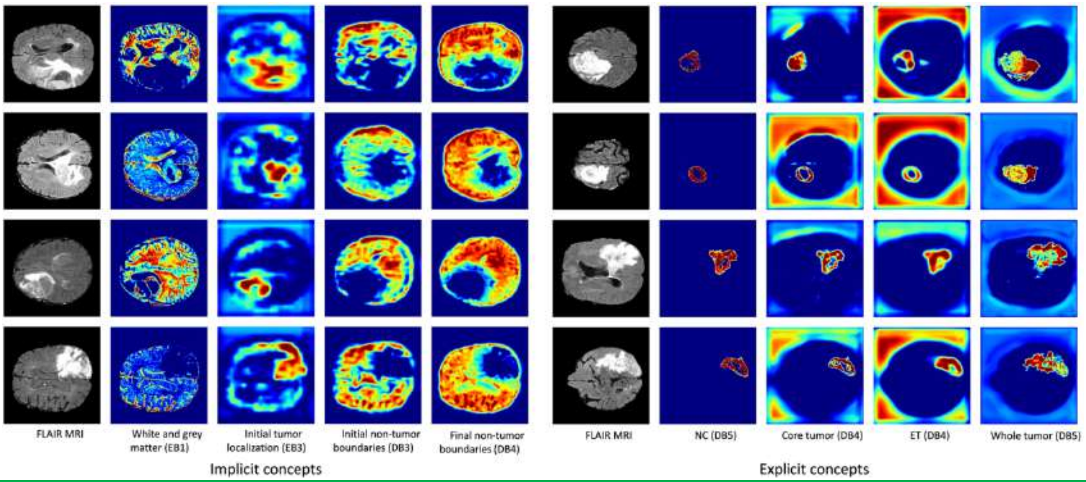

Saliency maps for implicit concepts (left) and explicit concepts (right) learned by individual filters of the CNN model.

- ✓ It is interesting to note that there are no labels for implicit concepts in the training dataset.
- ✓ Warmer regions represent a high score for the specified concept in the prediction map.
- ✓ Note that EB and DB denote the encoder and decoder block layers, individually.

24

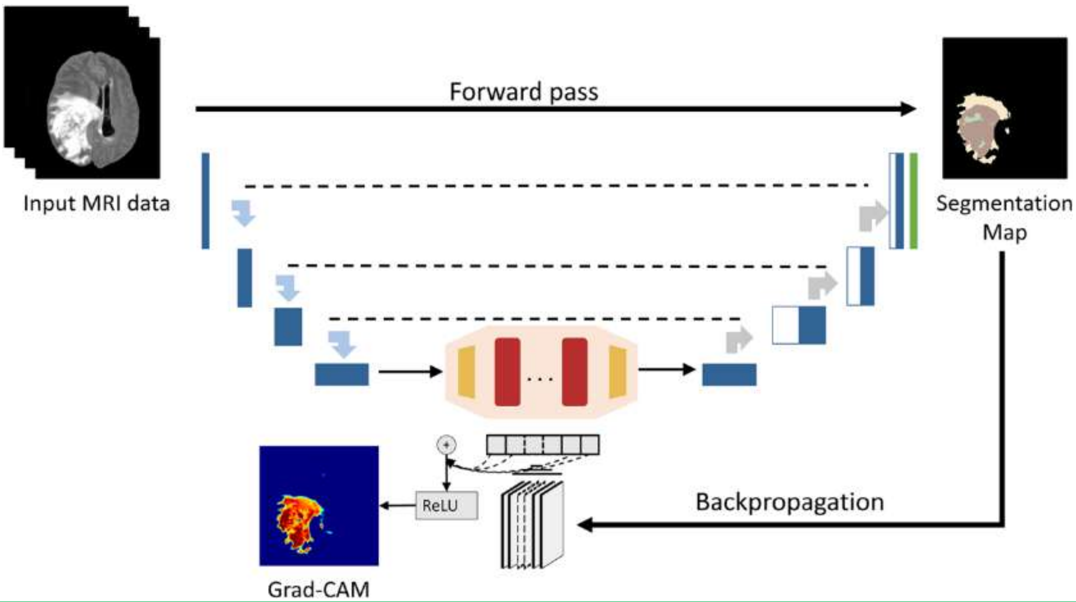

Applying grad-CAM to a sample glioma segmentation CNN model

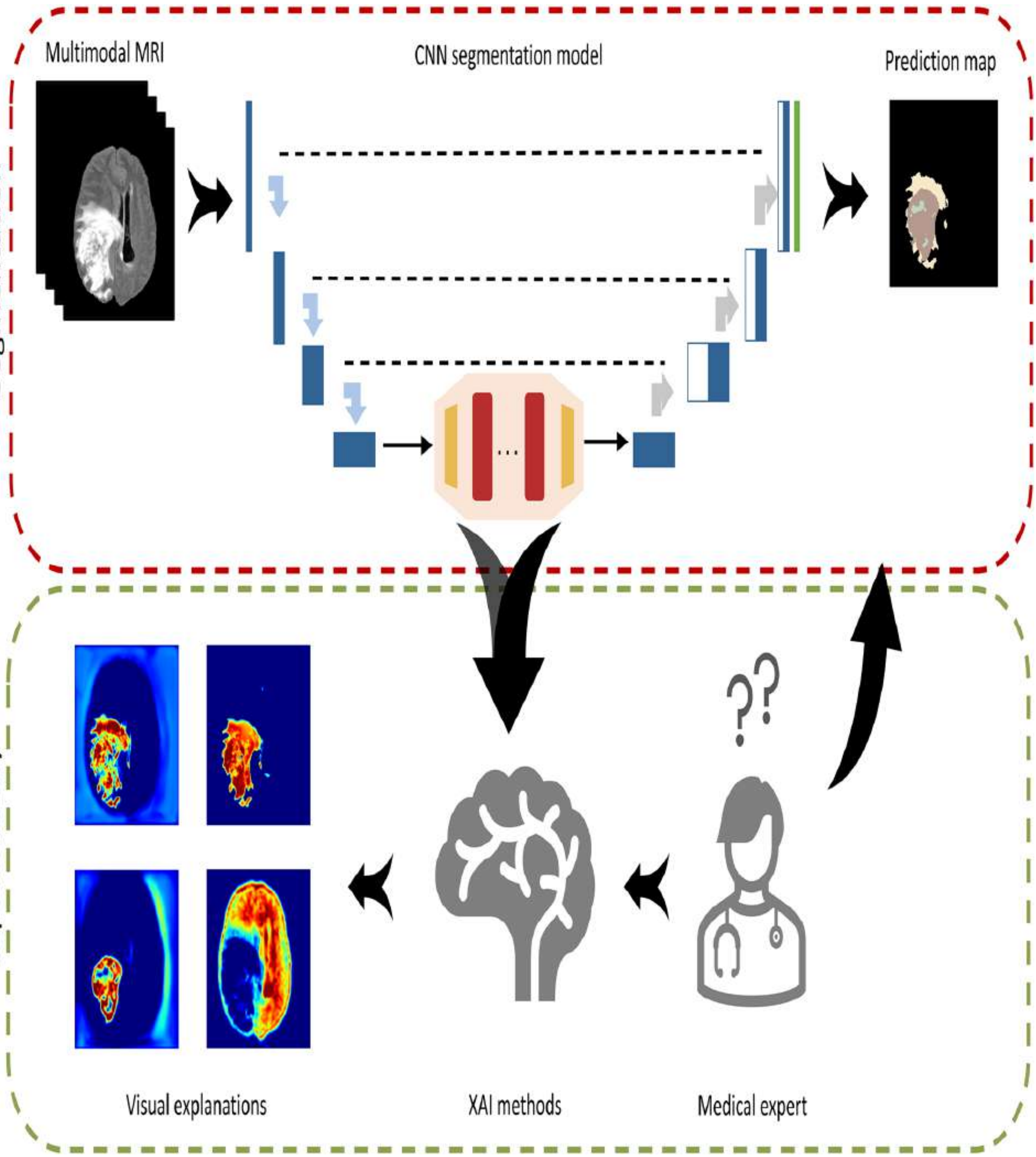

Overall proposed TransXAI pipeline for visual justification of glioma segmentation in brain MRI using a hybrid CNN-Transformer architecture

CNN-Transformer brain segmentation network from mpMRI

24

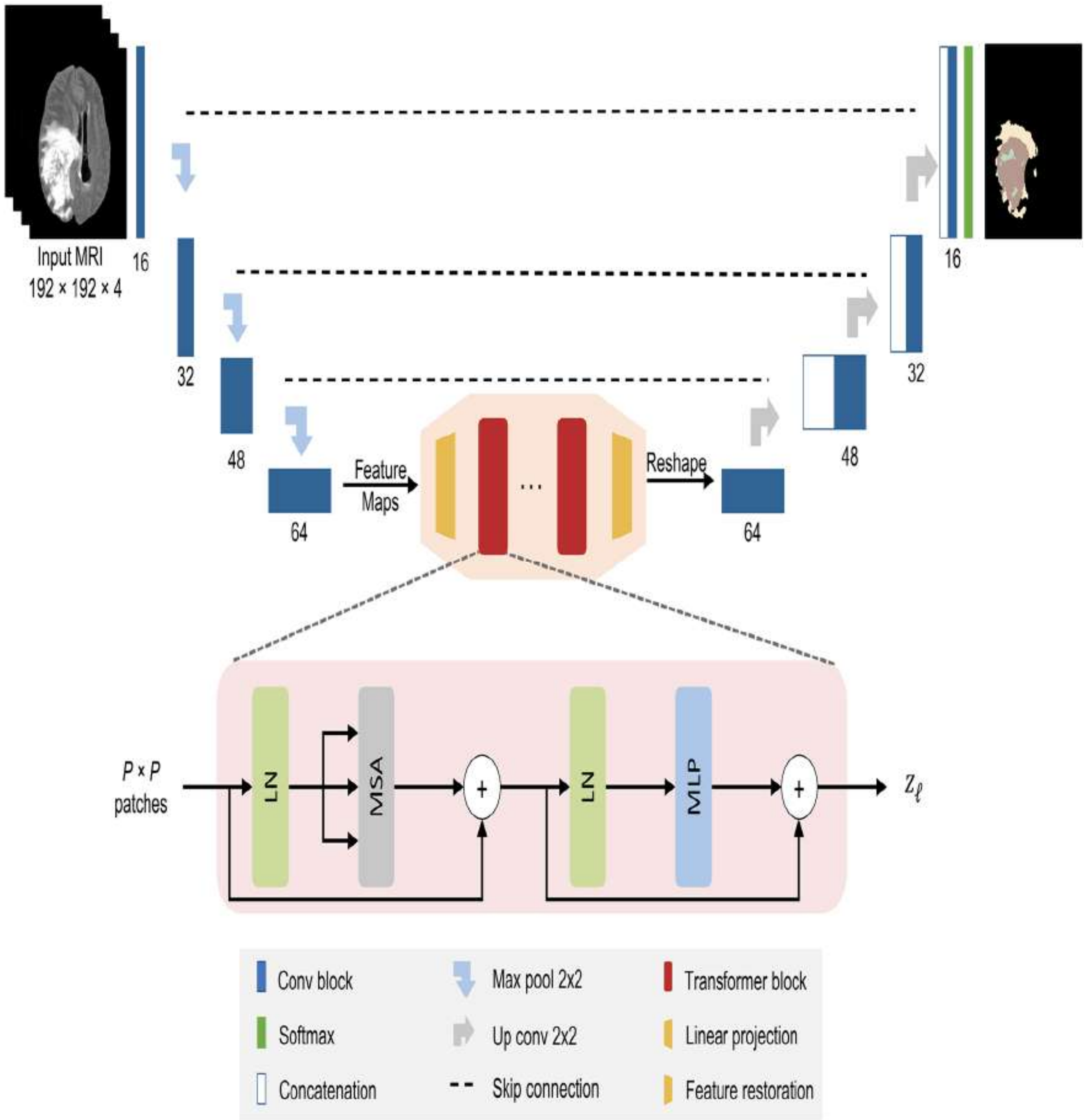

The architecture of the hybrid CNN-Transformer brain segmentation network from mpMRI volumes.

- Input : 2D multimodal MRI of T1, T1Gd, T2, and FLAIR with a patch spatial resolution of 192 × 192 × 4.
- CNN: Has 8 convolution neural blocks (blue boxes),
- each consisting of two successive convolutional layers 3 × 3,
- BN layer; ReLU activation

Exoscope-Assisted Spine Surgery

25

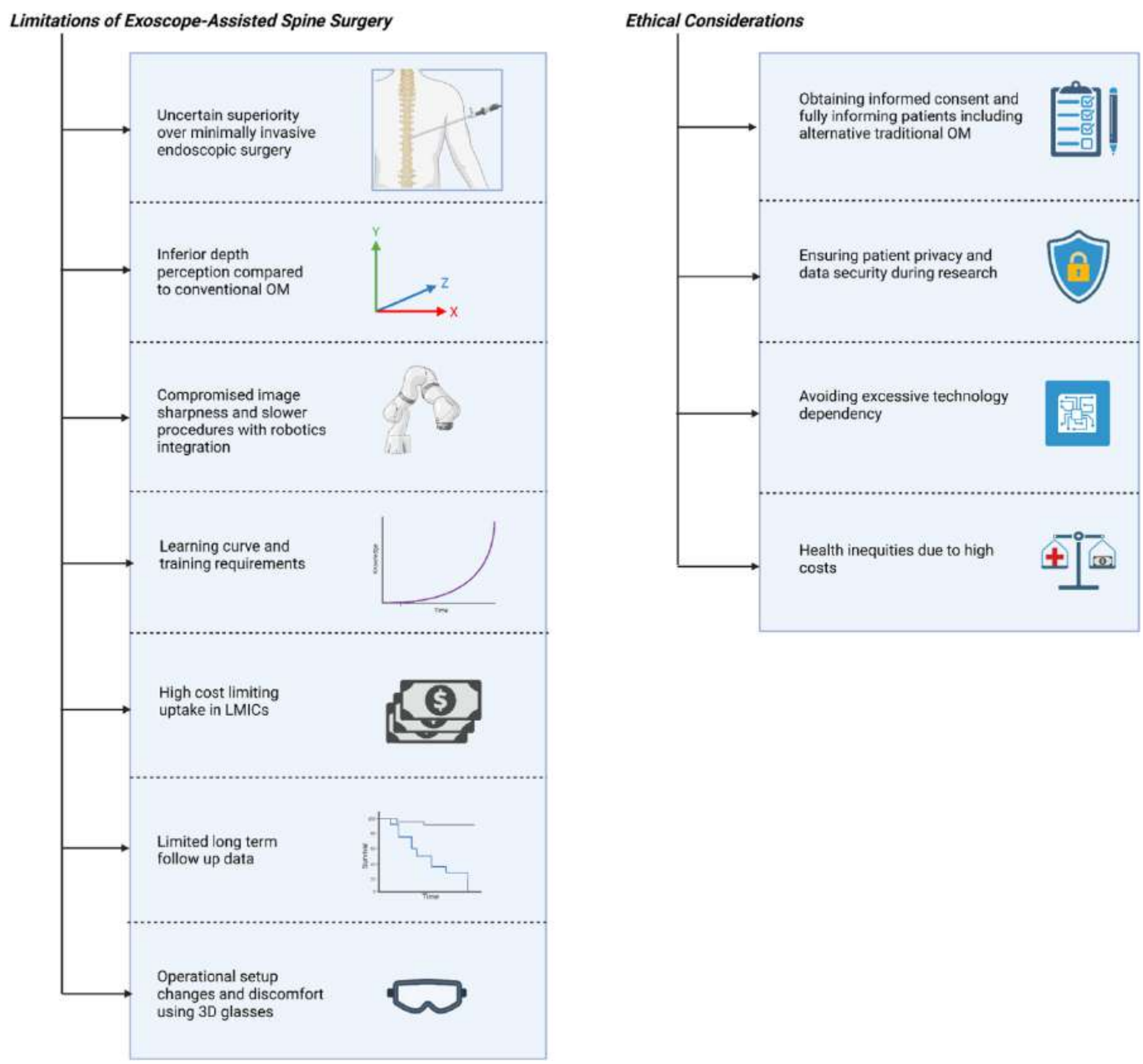

Limitations and ethical challenges in exoscope-assisted spine surgery

Future Prospects with exoscope-Assisted Spine Surgery

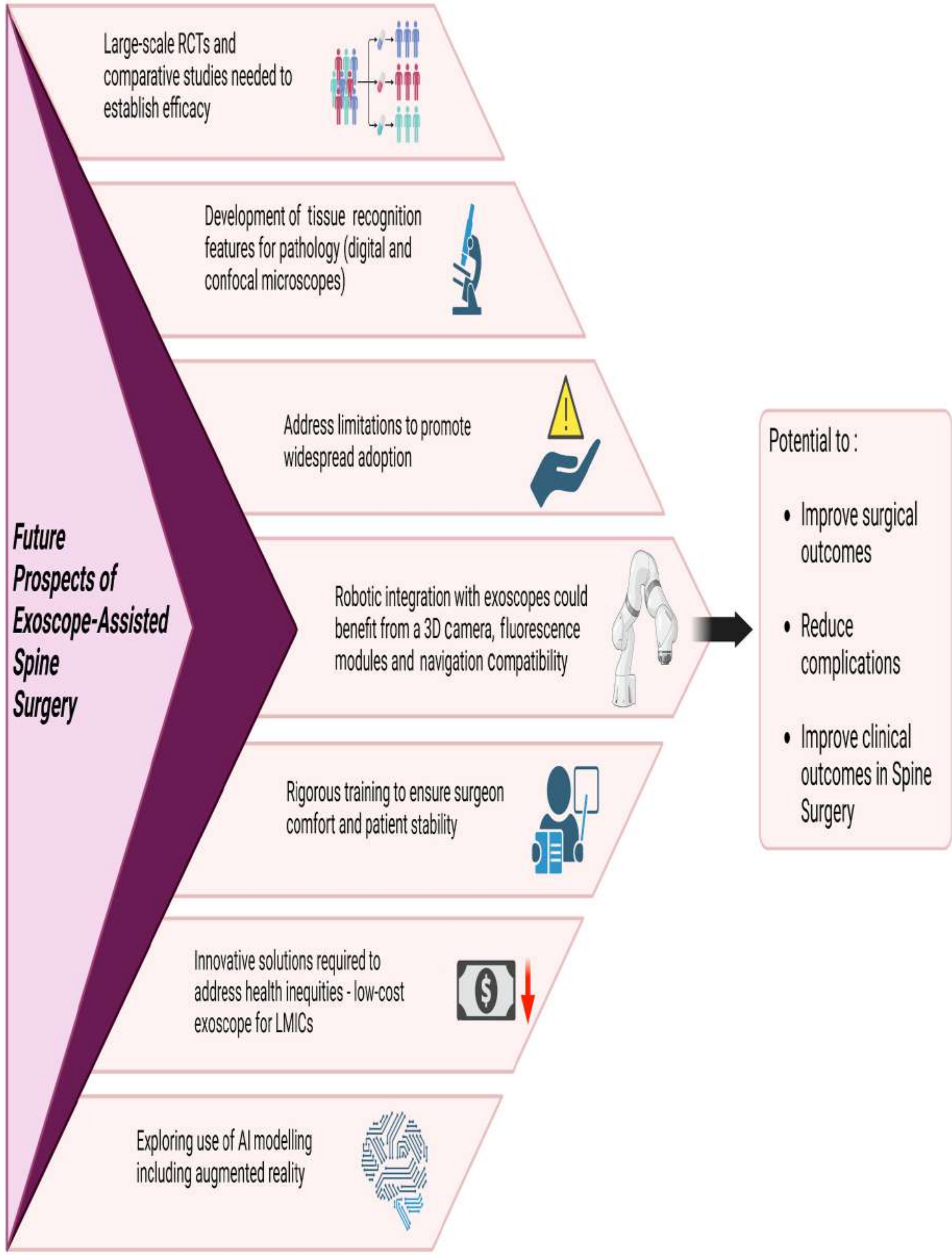
Future Prospects of Exoscope-Assisted Spine Surgery
Large-scale RCTs and comparative studies needed to establish efficacy
Development of tissue recognition features for pathology (digital and confocal microscopes)
Address limitations to promote widespread adoption
Robotic integration with exoscopes could benefit from a 3D camera, fluorescence modules and navigation compatibility
Rigorous training to ensure surgeon comfort and patient stability
Innovative solutions required to address health inequities - low-cost exoscope for LMICs
Exploring use of AI modelling including augmented reality
Potential to :
Improve surgical outcomes
Reduce complications
Improve clinical outcomes in Spine Surgery

Nn_U-Net
“No new U-Net.”

26

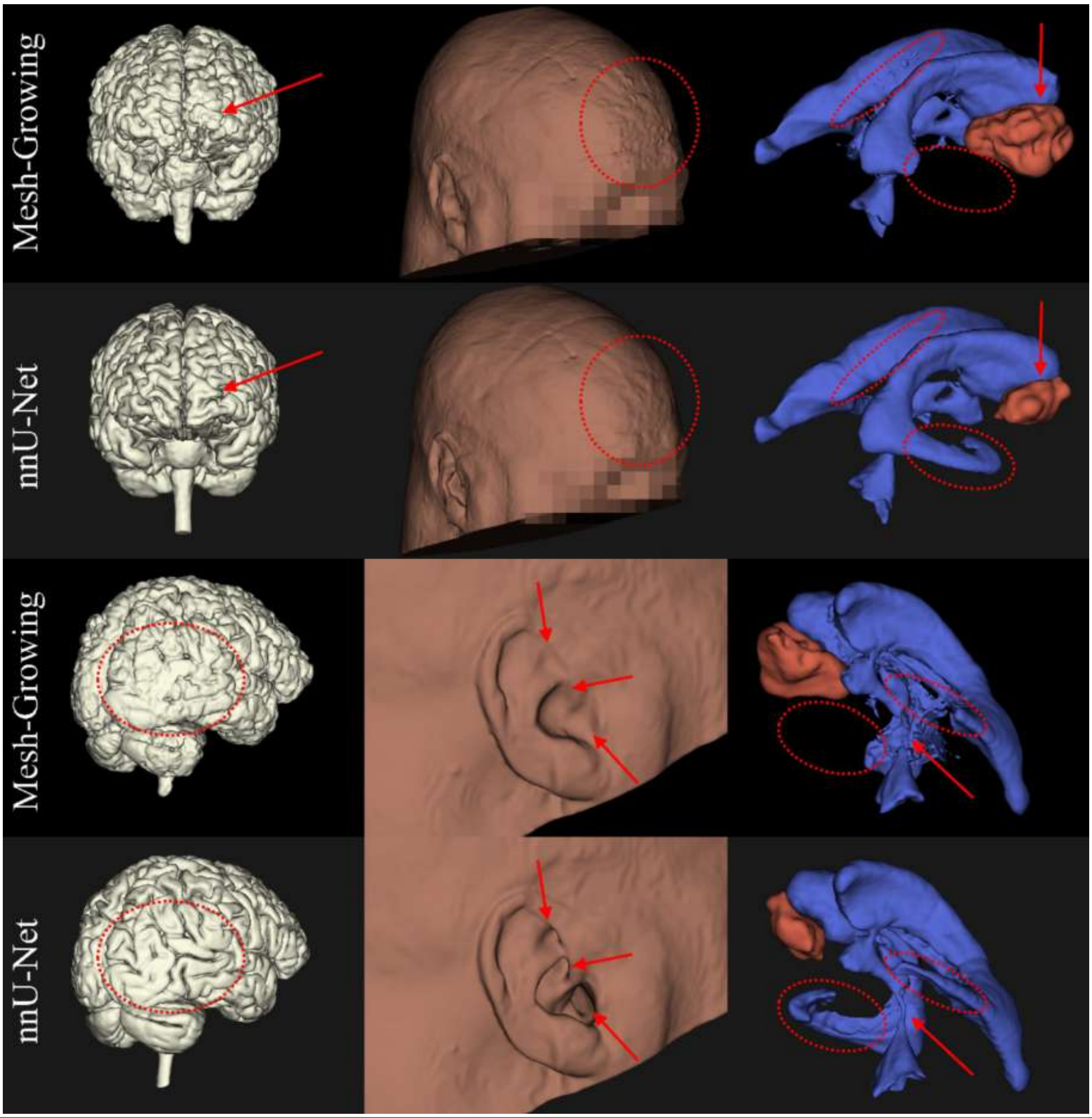

3D comparisons of segmentations generated by our nnU-Net models and Mesh Growing Algorithm (MGA) (denoted row-wise in the margins).

- ✓ These visualize brain (left column, white),
- ✓ Skin (middlecolumn, brown),
- ✓ Ttumor (red, right column) and ventricles (blue, right column).
- ✓ The annotations in red indicate the same region in each segmentation with a notable difference in quality.
- ✓ The MGAoversegmented the tumor in this particular patient

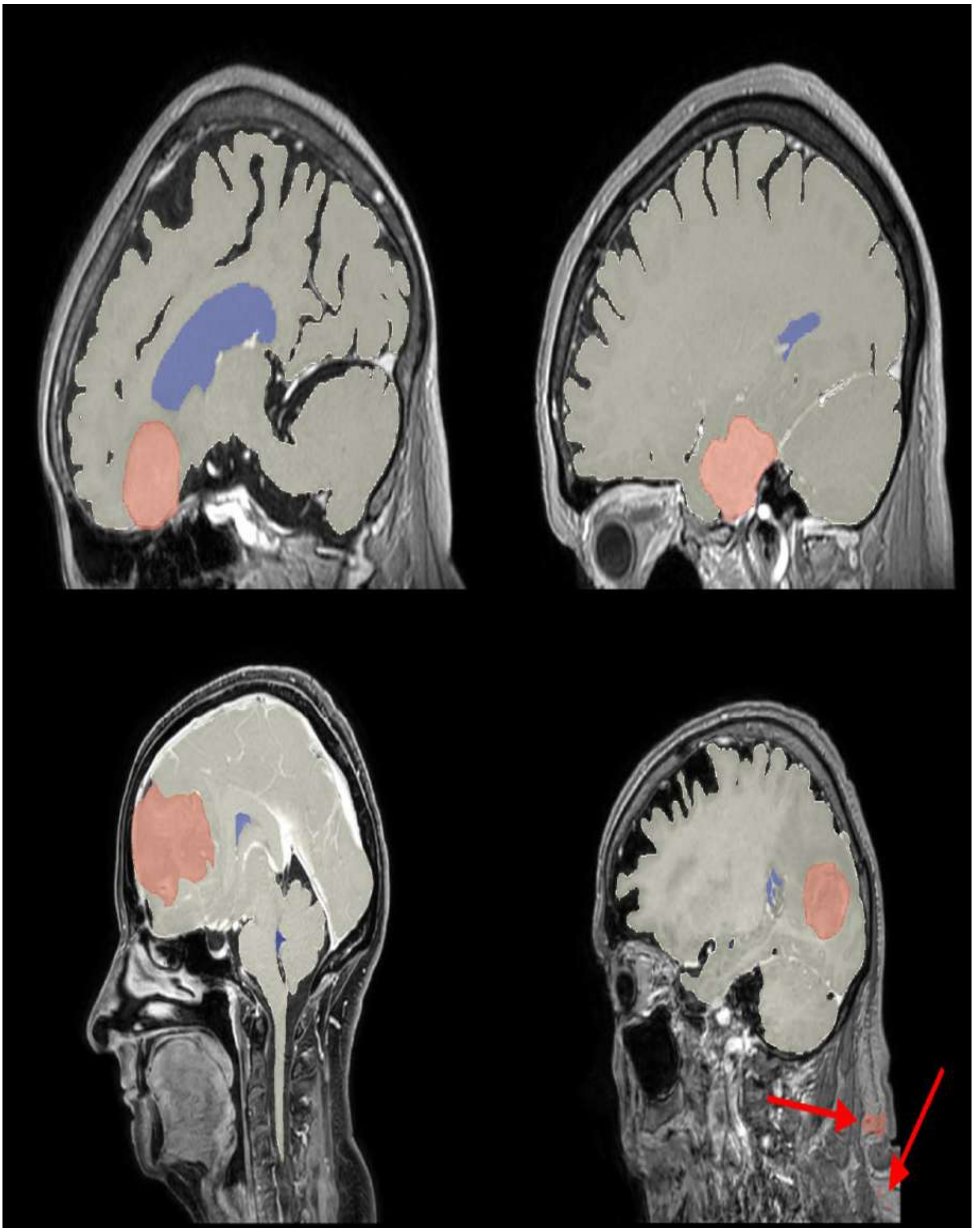

Example sagittal slices from our test set

- Indicates difference in craniocaudal FOV, with the
    - Automatic brain (white), tumor (red) and ventricle (blue) segmentations overlaid.
    - Each slice is positioned to display the bulk of the tumor.

- The top row are examples from Center A,
- Bottom row are examples from Center B.
- Red arrows are used to indicate false positives in the tumor segmentation

26

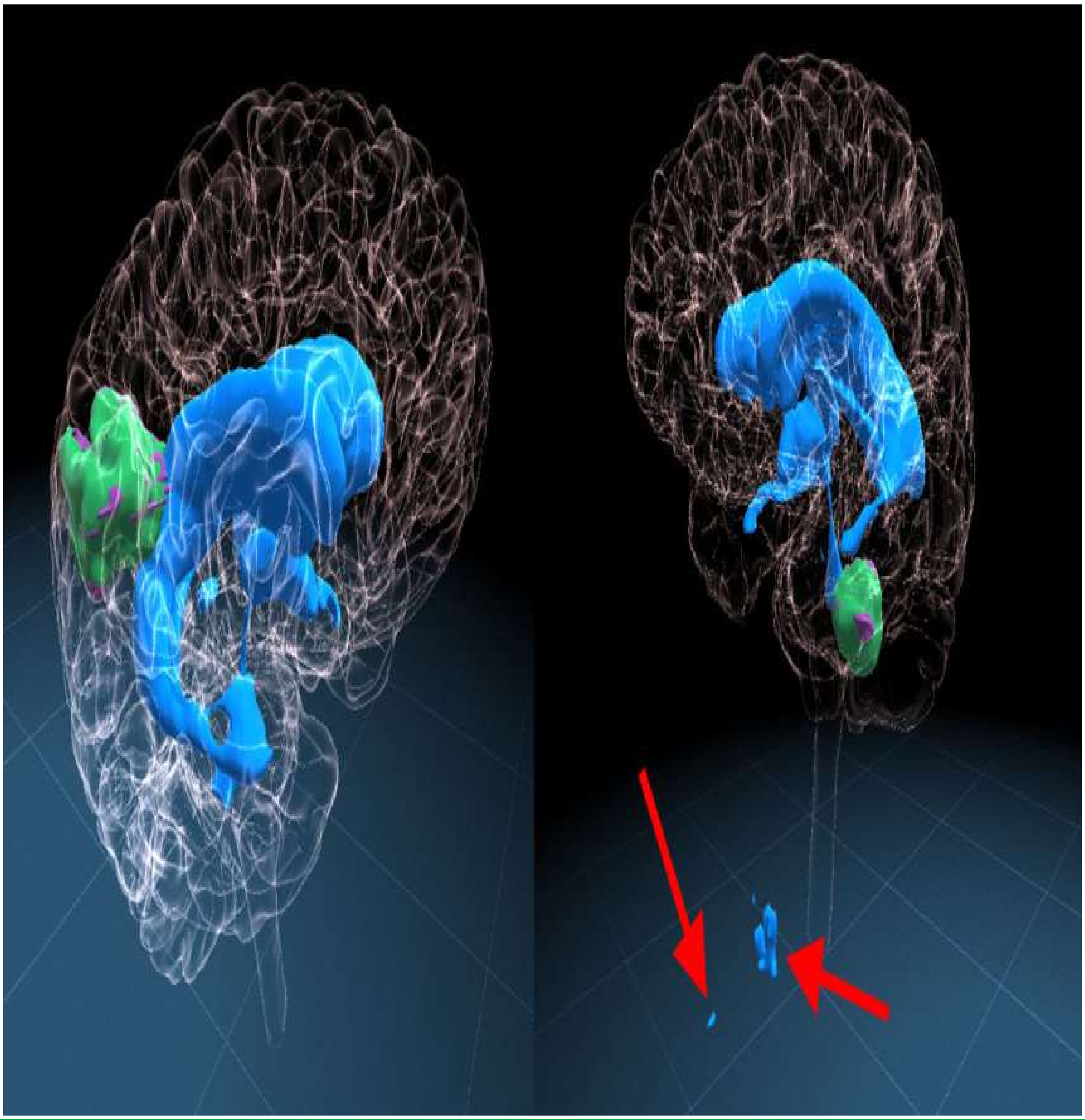

Typical example segmentations on two different patients

- ✓ (left: Center A, right: Center B) generated by our nnU-Net models.
- ✓ Brain segmentation is made transparent,
  - to allow visualization of the underlying anatomy.
- ✓ Ventricle segmentations are blue
- ✓ Tumor segmentation is green
- ✓ Ground truth for the tumor is purple
- ✓ Red arrows indicate false positive segmentations

boxplot showing performance of the MGA and nnU-Netmodels side by side

26

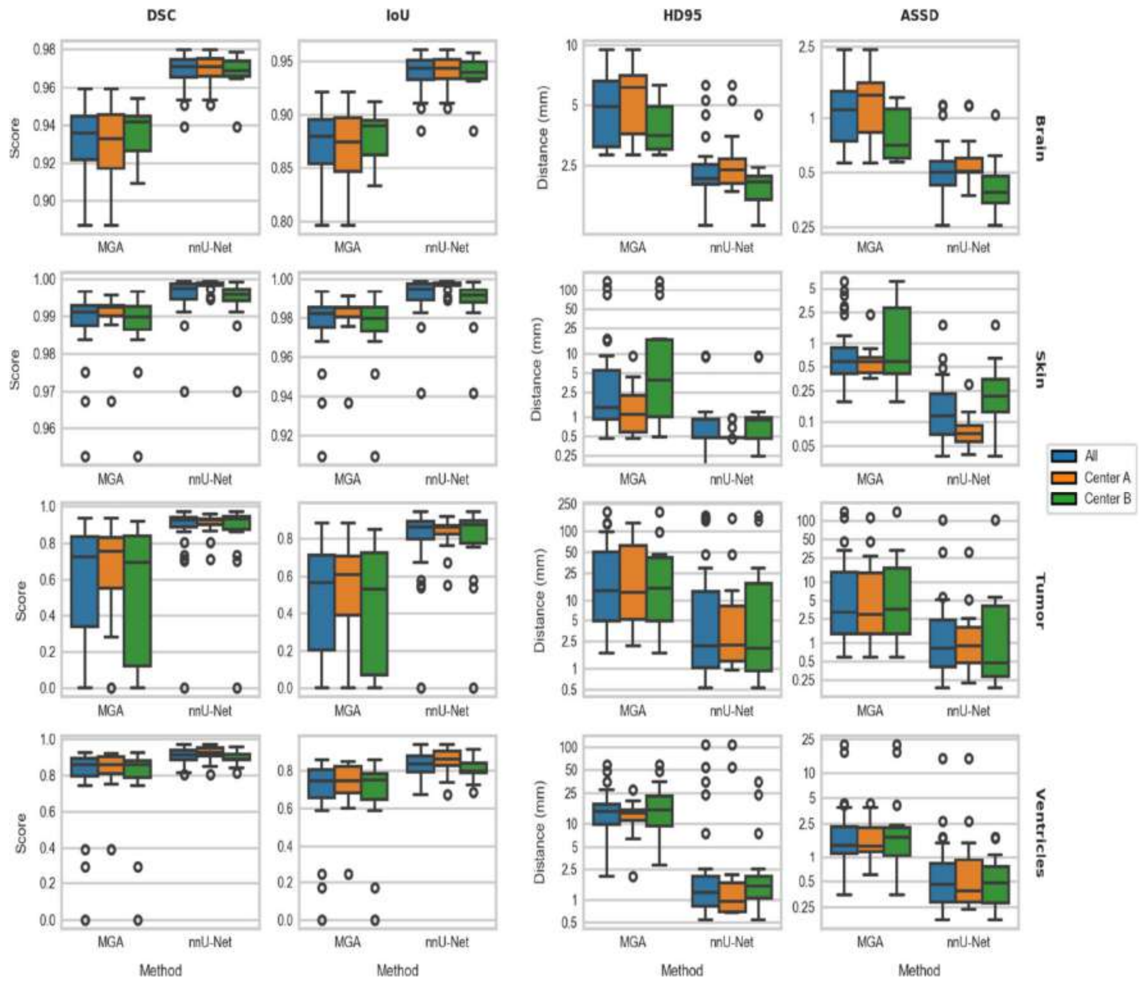

A boxplot showing performance of the MGA and our nnU-Net models side by side.

- ✓ Various anatomical structures are displayed in each row of plots, used metrics are displayed in the columns.
- ✓ Note that the y-axes are independent to maximize visibility, and the HD95 and ASSD plots have a logarithmic y-axis

Telecommunications' room of Neurosurgery Research

27

Telecommunications room of the Neurosurgery Research

- ✓ Department at Barrow Neurological Institute.
- ✓ Servers with high storage capacity receive high-resolution video recordings from the 11 operatingrooms.

AI + neurosurgery system

28

A high-level overview of the proposed AI for neurosurgery system

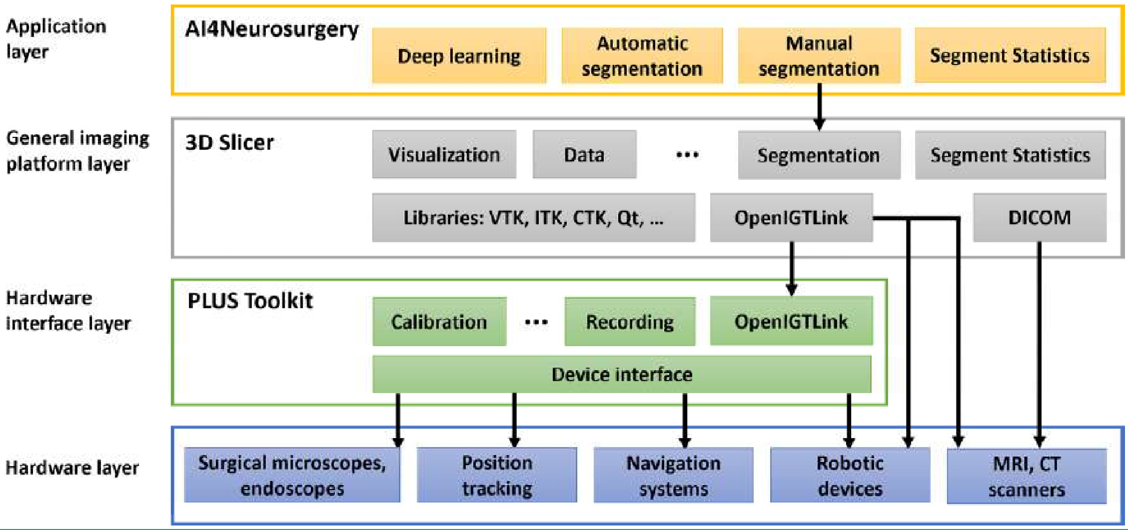

- ✓ Top layer contains the proposed AI4Neurosurgery modules that
- ✓ integrates AI, specifically deep learning, into the medical imaging software

28

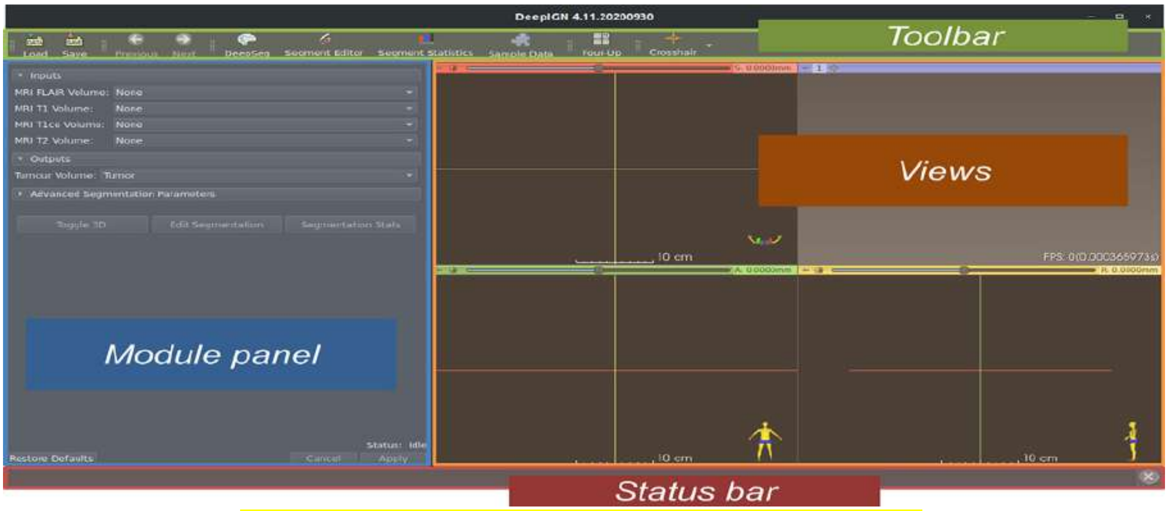

Main user interface of the AI4Neurosurgery application

28

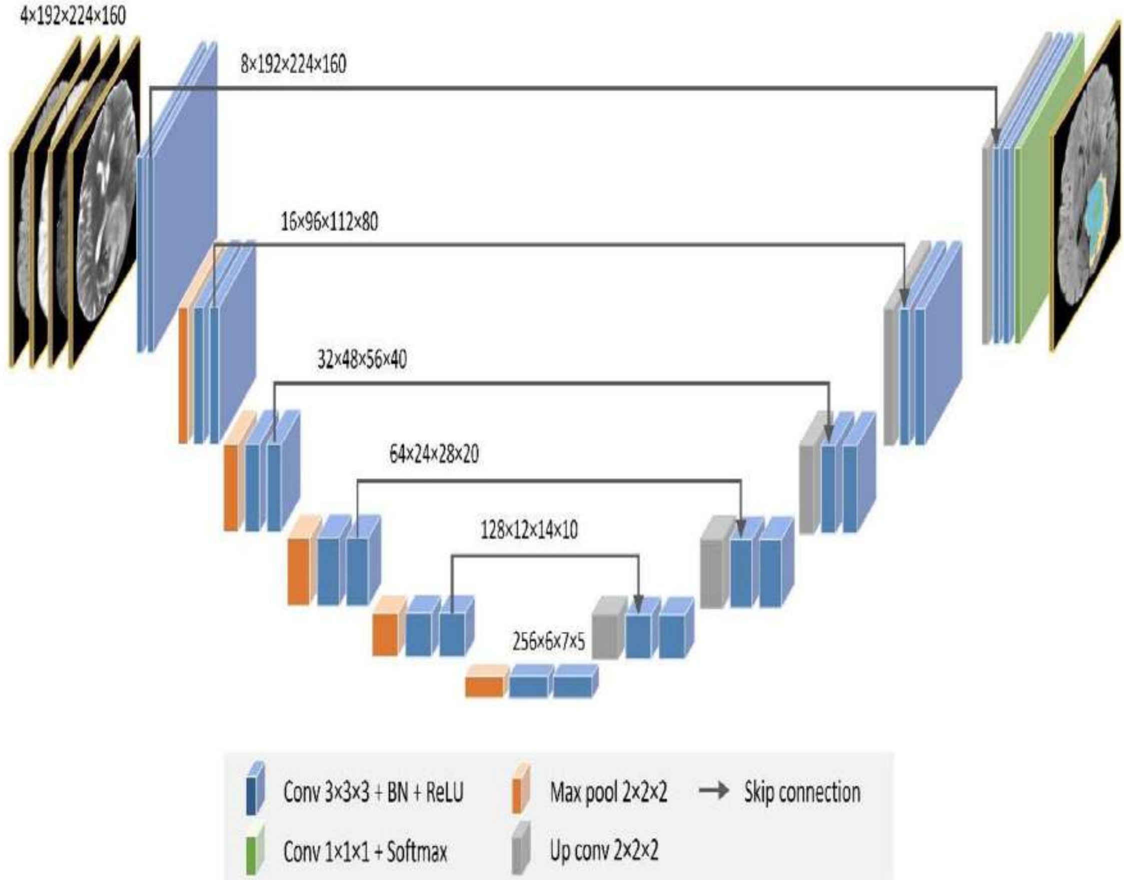

The architecture of the enhanced 3D brain segmentation network (3D DeepSeg) for brain tumor segmentation from mpMRI volumes.

- ✓ Input is a 3D multimodal MRI of

- T1, T1Gd, T2, and FLAIR with a
- patch spatial resolution of 192 × 224 × 160.

✓ The CNN network has 24 convolution neural blocks (blue boxes),

  - four downsampling blocks (orange boxes),
  - four upsampling blocks (grey boxes), and

✓ final softmax output layer (green box).

28

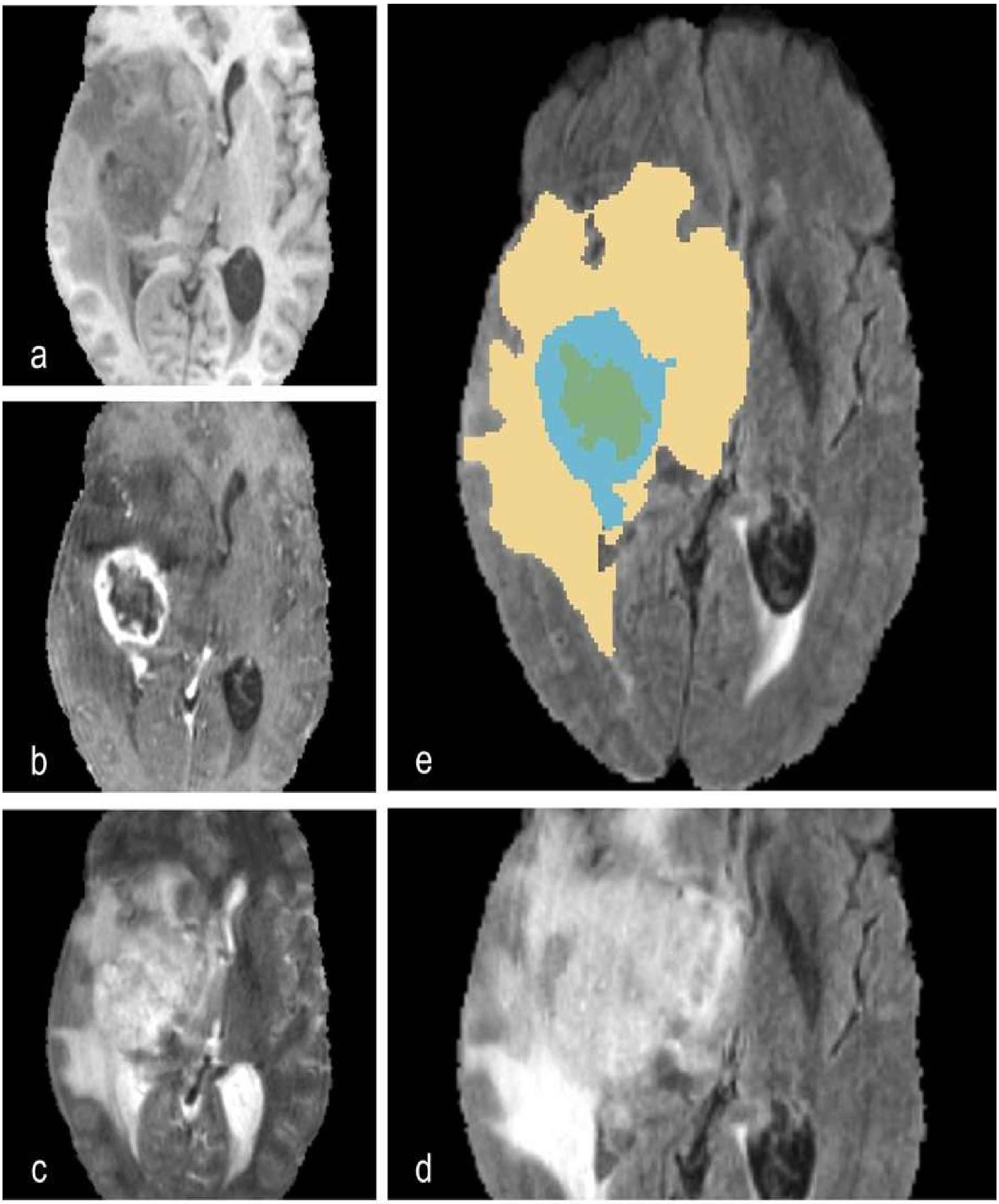

Sample multimodal MRI sequences
from the BraTS 2022 database showing brain tumor pathologies.

- ✓ Shown anti-clockwise from the top left: (a) T1W, (b) T1Gd, (c) T2W, (d) FLAIR, and (e) ground truth.
- ✓ Green, yellow, and blue indicate necrosis, edema, and non-enhancing tumor, respectively.

28

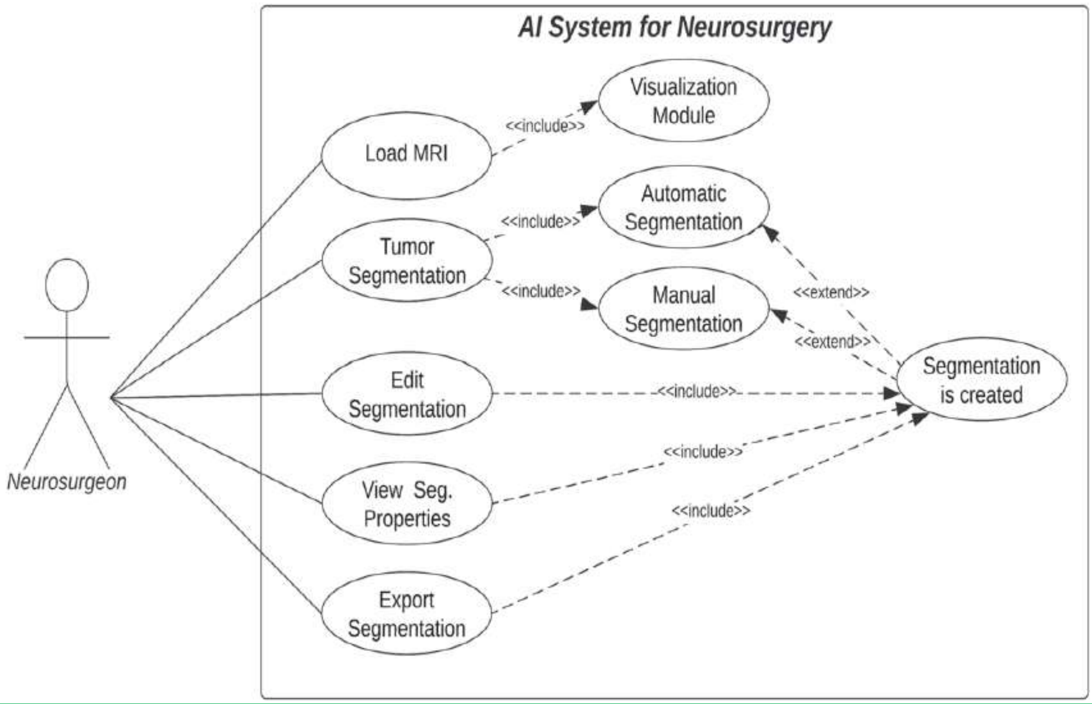

Use case diagram of
proposed AI-for-Neurosurgery application
to evaluate the system's
usability and functionality
in a pre-clinical setting

AI+Neurosurgey system for glioma

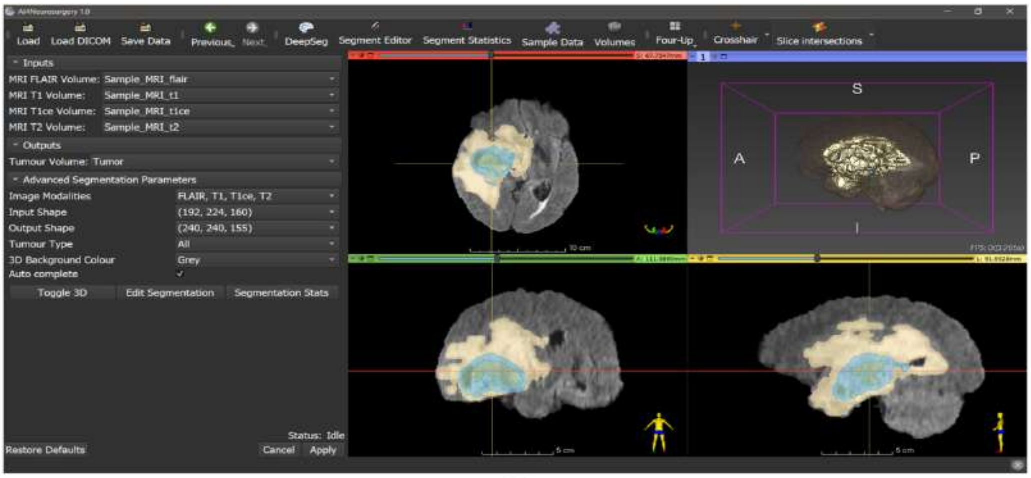

(a)

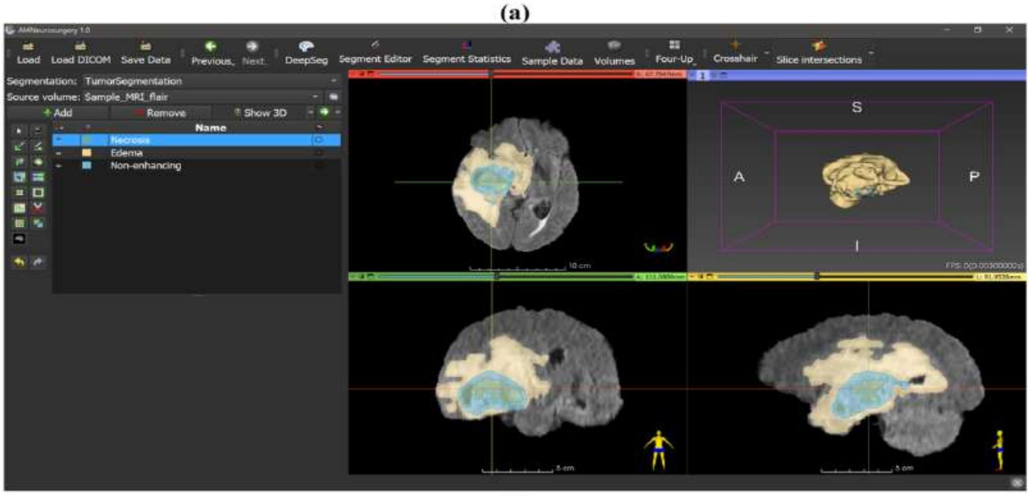

(b)

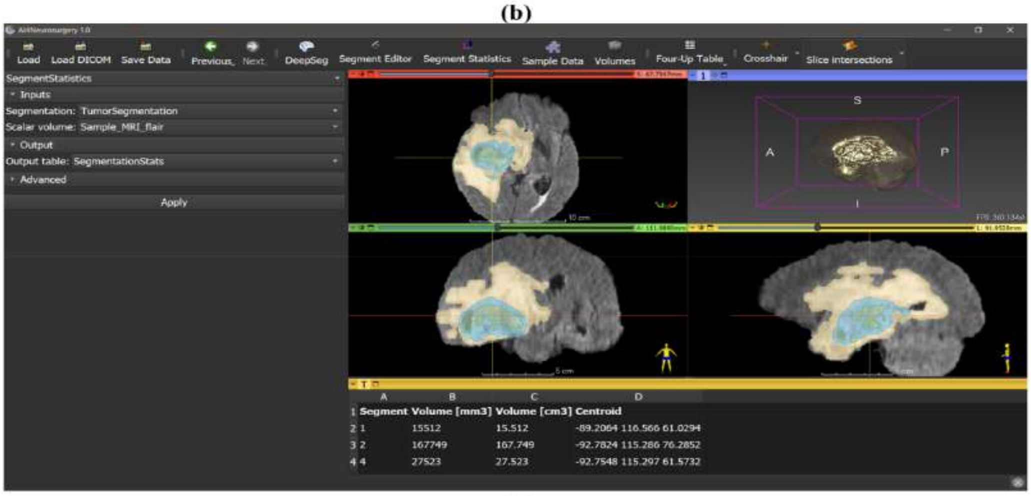

(c)

An example use case scenario for evaluating the proposed AI4Neurosurgey system in high-grade brain glioma surgery.

- ✓ (a) The DeepSeg module, responsible for automatic brain tumor segmentation using deep learning.
- ✓ (b) The Segment Editor module is responsible for creating and
- ✓ editing segmentations using manual and semi-automatic tools, enabling neurosurgeons to

modify and adjust the segmentation results as necessary.

✓ (c) The Segment Statistics module computes intensity and geometric properties for each segment

28

Assessment of the usability via SUS, statements are summed for presentation, rating 1 (=strongly disagree) to 5 (=strongly agree).

Statements\rating	1	2	3	4	5
1. Use frequently	☐	☐	☒	☐	☐
2. Unnecessarily complex	☐	☒	☐	☐	☐
3. Easy to use	☐	☐	☐	☒	☐
4. Support needed	☐	☒	☐	☐	☐
5. Functions well integrated	☐	☐	☐	☒	☐
6. Inconsistency	☐	☒	☐	☐	☐
7. Quick to learn	☐	☐	☐	☐	☒
8. Cumbersome to use	☐	☐	☒	☐	☐
9. Confident using	☐	☐	☐	☒	☐
10. Difficult to learn	☒	☐	☐	☐	☐

AI ; Software; GOF (Accuracy)

31

Latest advances in artificial intelligence methods and softwares along with their respective accuracy matrices.

Study	Aim	Study Type	AI method and software	Accuracy matrices	N
(Rava et al, 2021)[25]	To evaluate an application's capacity to detect and locate LVOs in AIS patients.	Retro prospective	CTA	Accuracy = 81% Sensitivity = 73% Specificity = 90%	303
(Adhya et al, 2021)[26]	Utilize emerging approaches for diagnosis of anterior circulation artery blockages by assessing relative vascular densities.	Prospective	RAPID-CTA	Sensitivity = 80% PPV = 87%	310
(Morey et al, 2021)[27]	To reduce time-to-treatment and improving clinical outcomes.	Retrospective	Viz.ai LVO	Sensitivity = 82% Specificity = 94%	55
(Meng et al, 2022)[28]	Use deep learning pipeline to detect large vascular occlusion (LVO) and predict functional outcomes based on CTA images to optimize LVO patient care.	Retrospective	Inception-V1 I3D	Sensitivity = 89% Specificity = 66% Accuracy = 96%	8650
(Matsoukas et al, 2022)[29]	Evaluate the precision of AI software in a multihospital stroke network.	Prospective	Viz LVO	Sensitivity = 91.1% Specificity = 93.8% Accuracy = 91.2%	1822
(Bathla et al, 2022)[30]	LVO identification at the level of the picture to speed patient triage for mechanical thrombectomy.	Retrospective	4D-CTA/CT perfusion (CTP) images using neural network (NN) models	Sensitivity = 86.5% Specificity = 89.5% Accuracy = 85.5%	306

Hematoma volume

33

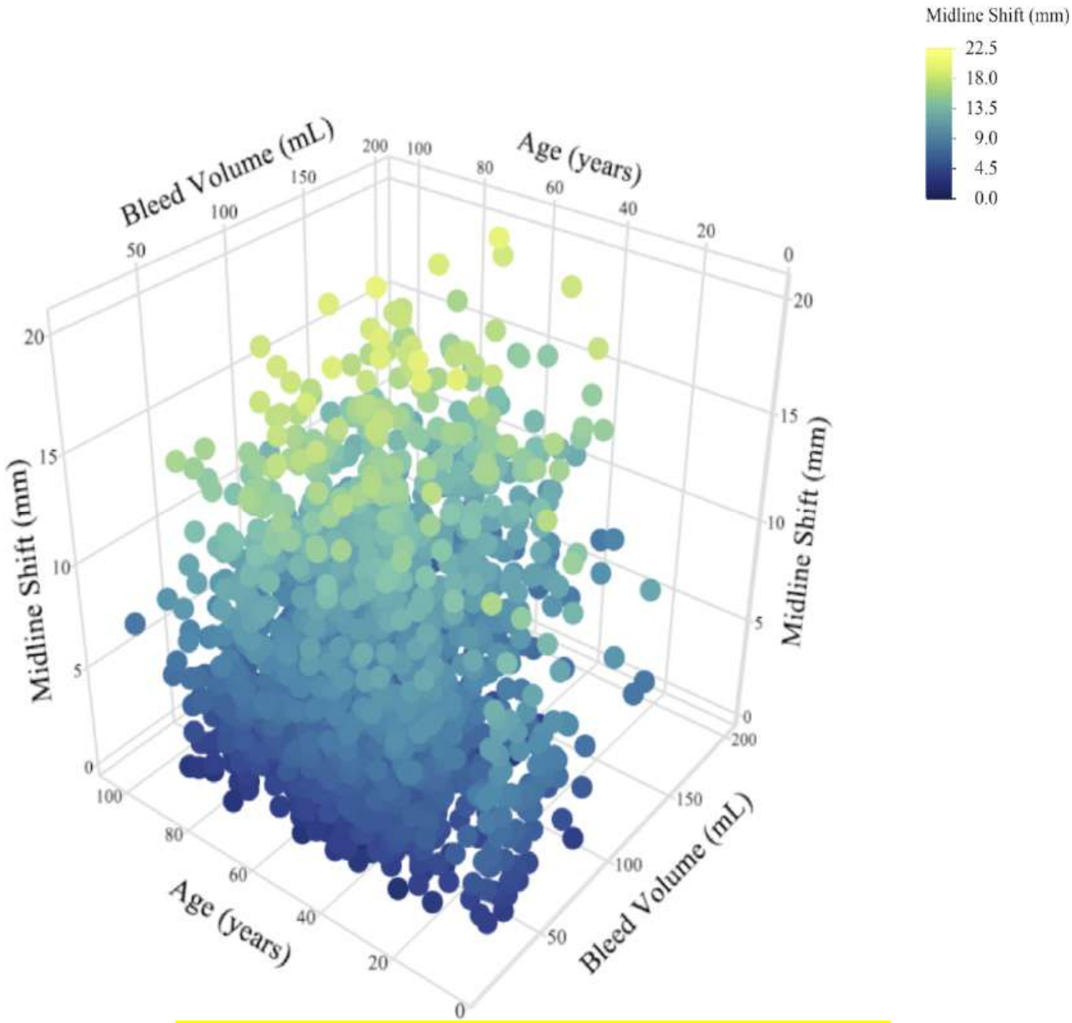

3D Scatterplot of age, hematoma volume, and midline shift

Gradient : represents distribution of midline shift

33

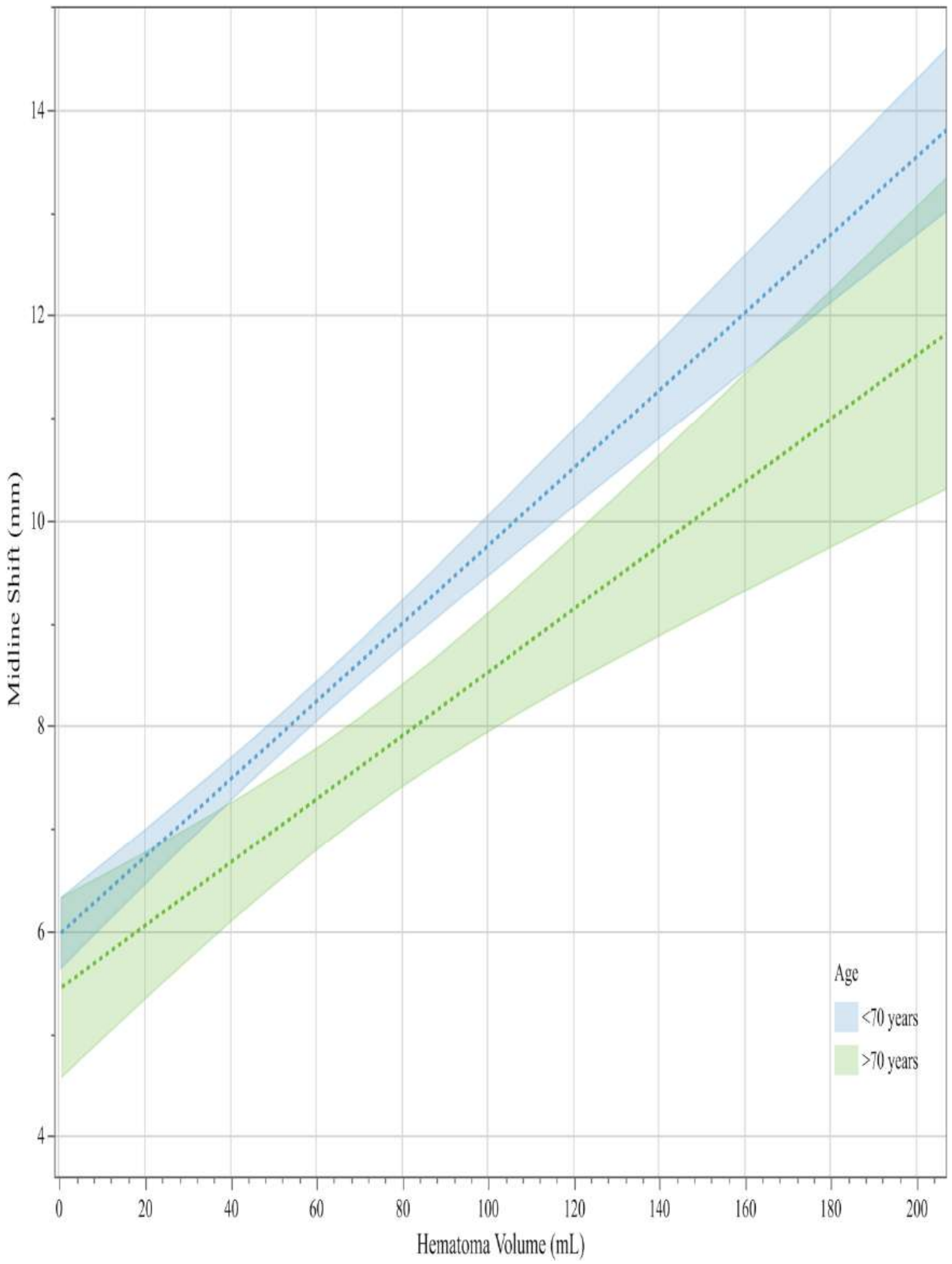

Average midline shift (mm) with 95% confidence interval

- ✓ Regressed over hematoma volume (ml)
    - o For older patients (>70 years) and younger patients (≤70 years

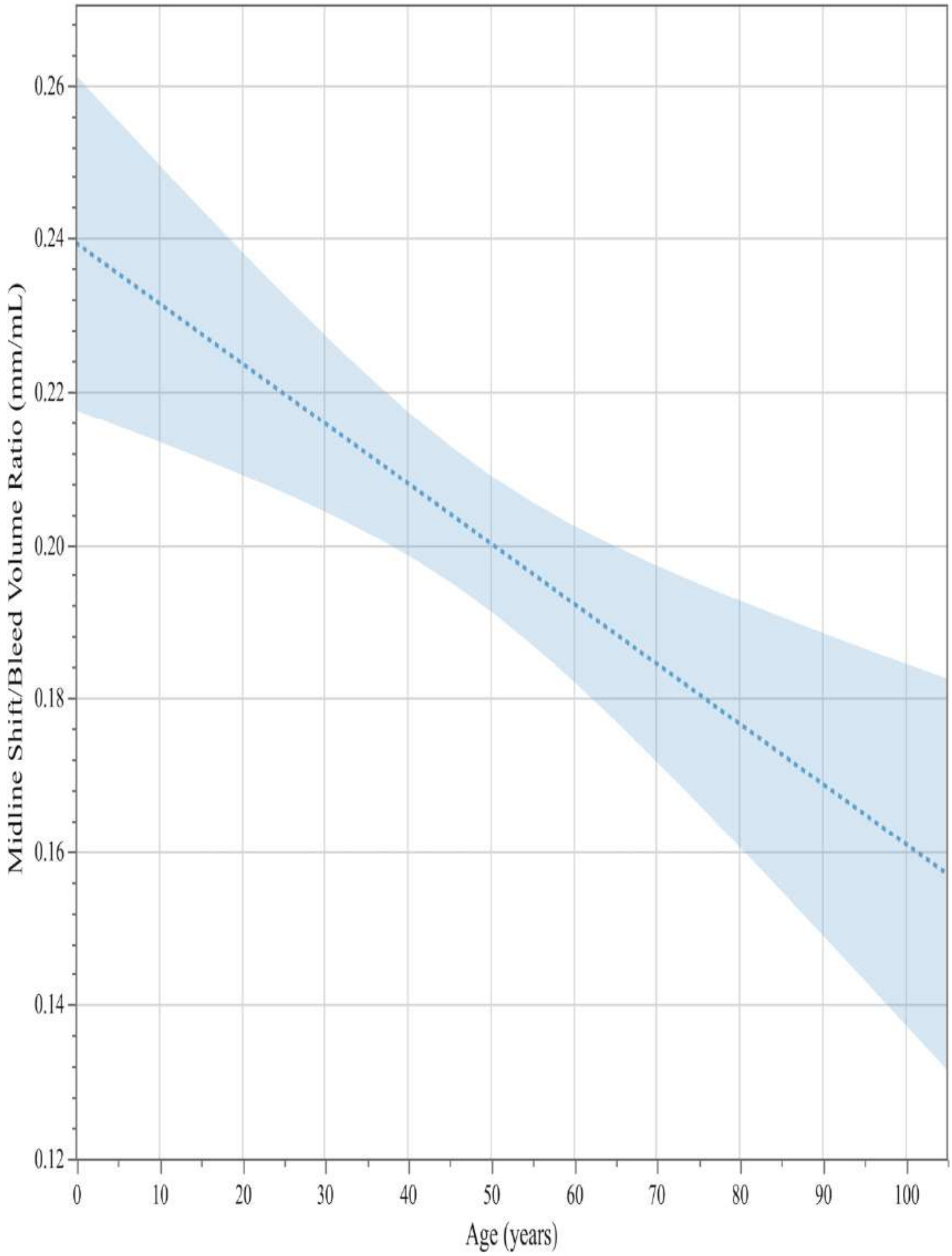

Average ratio of midline shift divided by hematoma volume (mm/mL)

- ✓ With 95% confidence interval regressed over age (years)

33

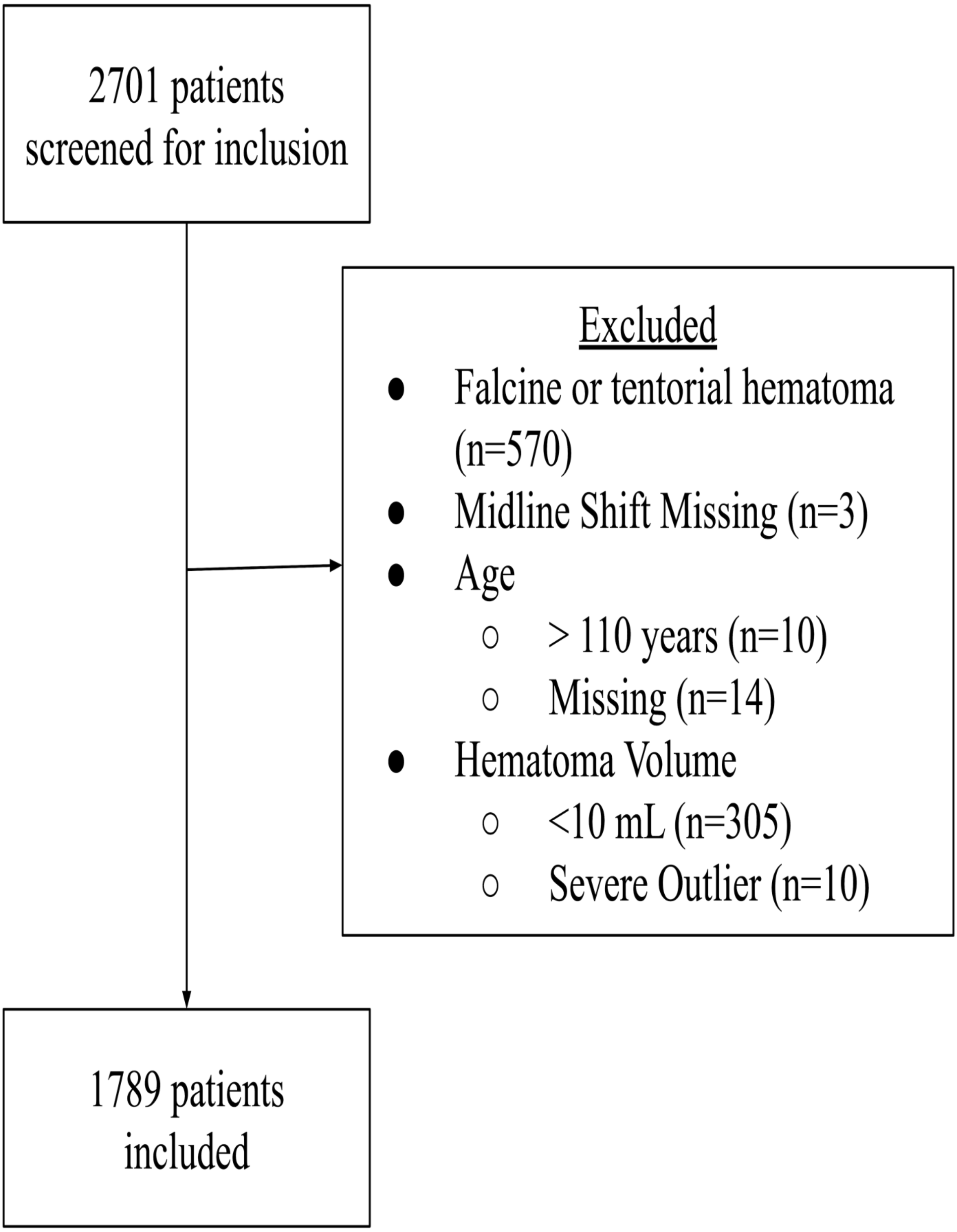

Flowchart of patients meeting inclusion for volumetric analysis

Neuro-oncologic imaging

35

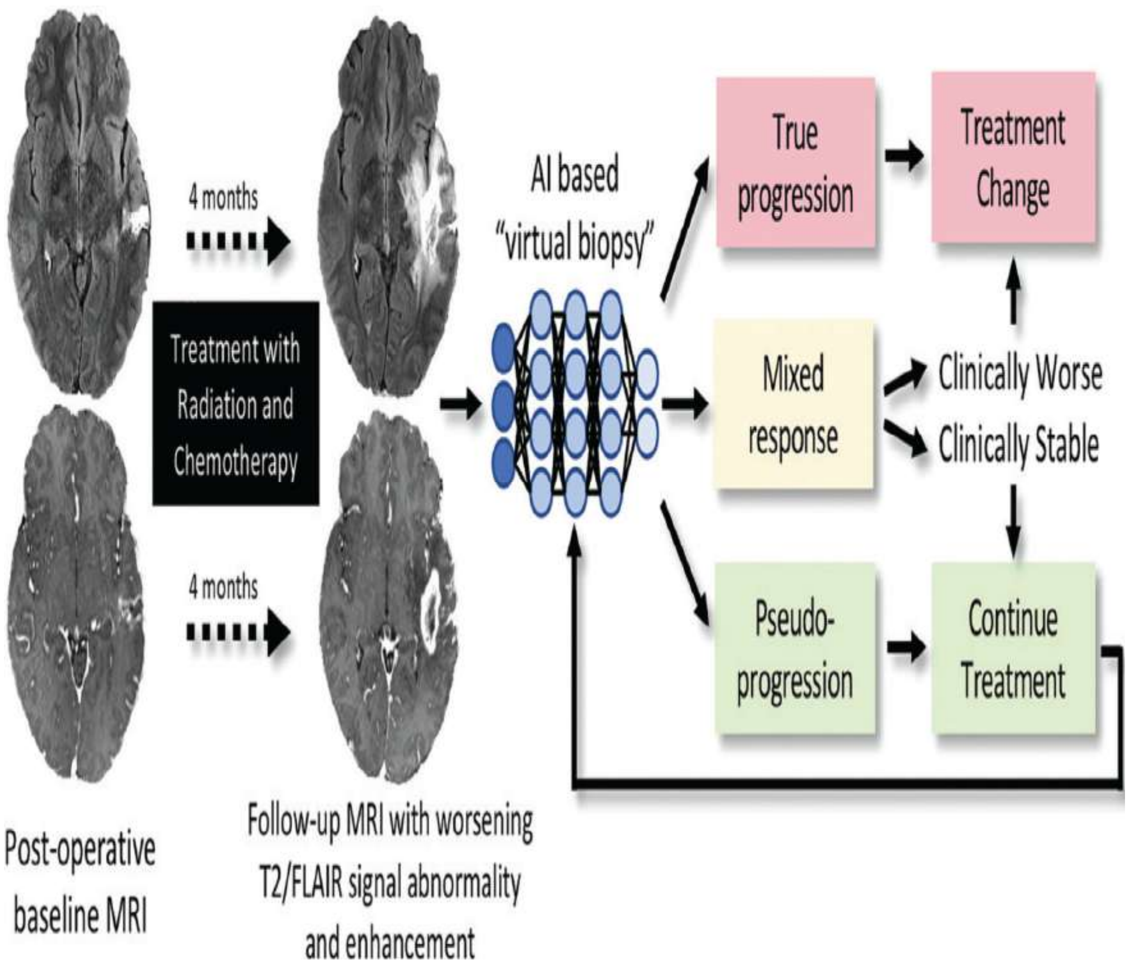

Treatment response in neuro-oncologic imaging

- ✓ After standard-of-care treatment with combined radiation therapy and chemotherapy, increasing T2–fluid-attenuated inversion recovery (FLAIR) signal intensity abnormality and new and/or increasing size of enhancing lesions are often seen
- ✓ Artificial intelligence (AI)–based "virtual biopsy" could assist in distinguishing underlying biology and segregating treatment response into three possible categories: true progression (>75% recurrent and/or residual glioma at pathologic examination), mixed response (25%–75% recurrent and/or residual glioma at pathologic examination), and pseudoprogression (>75% treatment-related changes)
- ✓ Categories dictate distinct therapeutic approaches
- ✓ In this example, the new enhancing lesion was found to represent 100% treatment-related changes at pathologic examination, with few atypical cells

Predictive maps of tumor infiltration

35

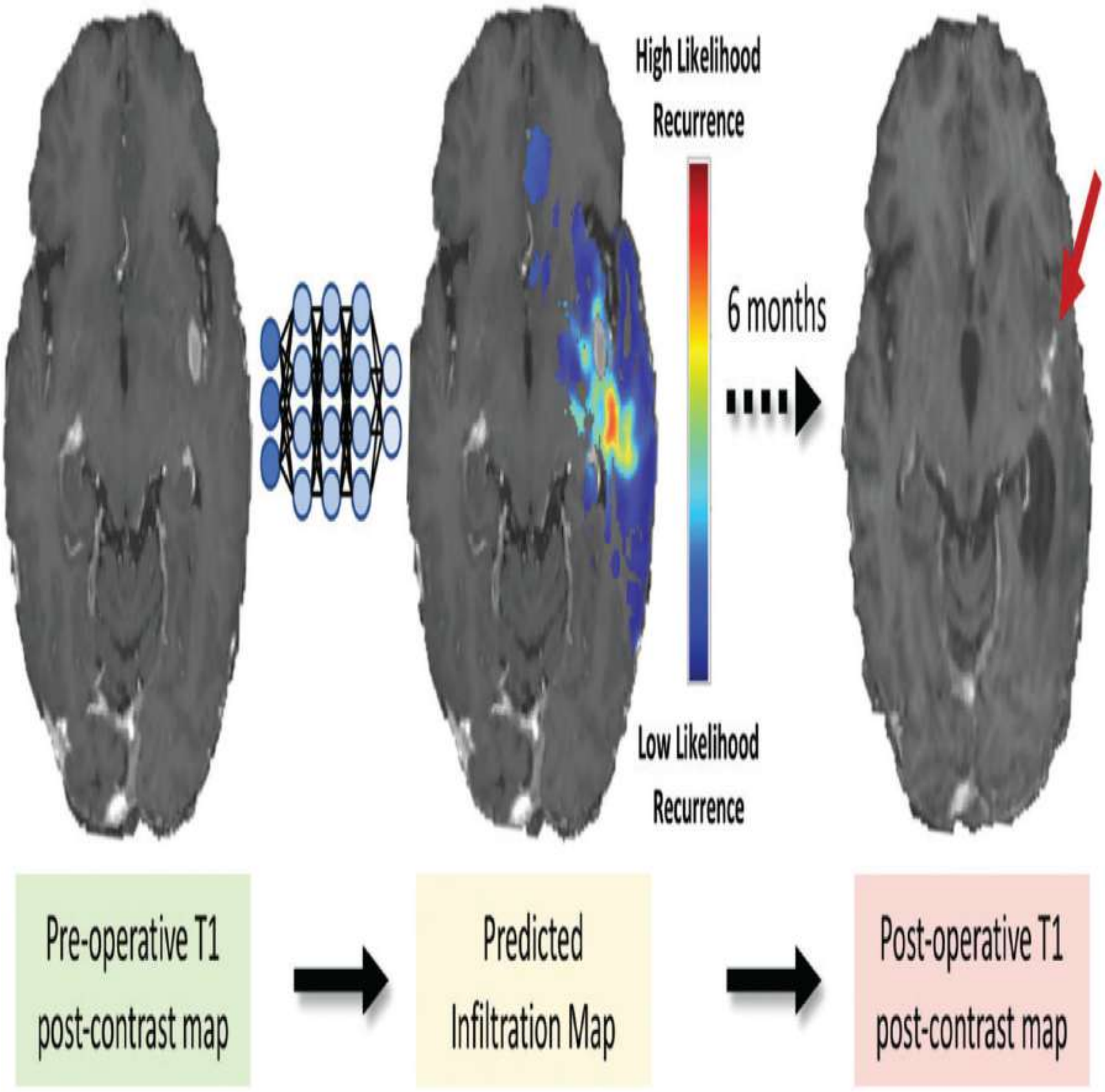

Predictive maps of tumor infiltration

- ✓ Multimodal pre-operative conventional and advanced MRI data
- ✓ Analyzed with support vector machines to generate an estimated infiltration map
  - o overlaid on postcontrast T1-weighted image (red areas signify higher risk)
- ✓ Postcontrast T1-weighted MR image obtained
  - o at 6-month follow-up (right) demonstrates area of recurrence near site of highest predicted infiltration (arrow)

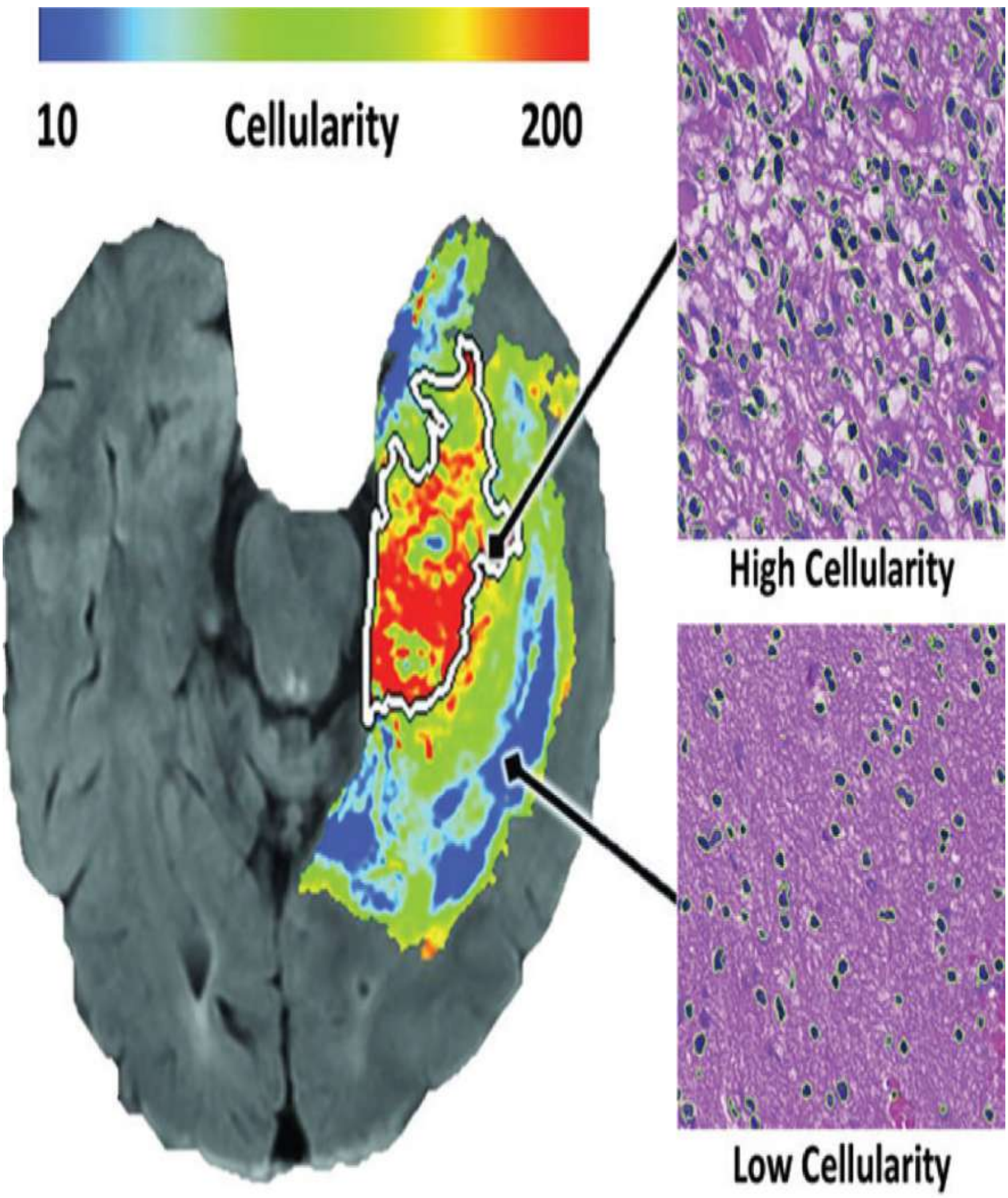

Predicted tumor cellularity map

- ✓ **Left**, voxelwise linear regression model was applied to multimodal preoperative MRI trained on automated cell counts of biopsies localized to different regions on MR image and
  - o used to generate a map of predicted cellularity (red areas signify more cells)
- ✓ **Right**, photomicrographs of biopsy specimens from regions of tumor with high and low cellularity (hematoxylin-eosin stain; original magnification, ×400) (Reprinted, with permission)

42

Barriers and solutions for integration of AI into brain tumour surgery

Barrier	Proposed solution
Requirement of large datasets to train existing ML programs	• Creation of international databases as repositories for training data for brain tumours. • Collaboration between neurosurgical oncology units. • Synthetic multi-parametric MRI image generation.
Selection bias of training data	• Ensure a wide range of demographics used to train ML programs. • Use of international databases as repositories for training data.
Patient confidentiality concerns when sharing patient data between units to train ML platforms	• Robust scrutiny of data governance for existing databases. • Development of technologies in accordance with existing ethical and legal frameworks. • Synthetic multi-parametric MRI image generation.
Slow progress in advancing ML programming	• International collaboration between ML programming teams. • Publishing code for all newly developed ML platforms, making code widely available for further development and scrutiny.
"Black box" conundrum	• Ensure that human users can understand and trace all predictions and decisions made by future ML platforms.
Poor contextualisation of uncertainty by ML programs	• Ensure that ML platforms developed for use in brain tumour management are used in tandem with clinicians, who are better able to contextualise and explain uncertainty.

Brain MR neuro-oncologic imaging

35

Schematic of future artificial intelligence–based neuro-oncologic imaging and clinical management workflow

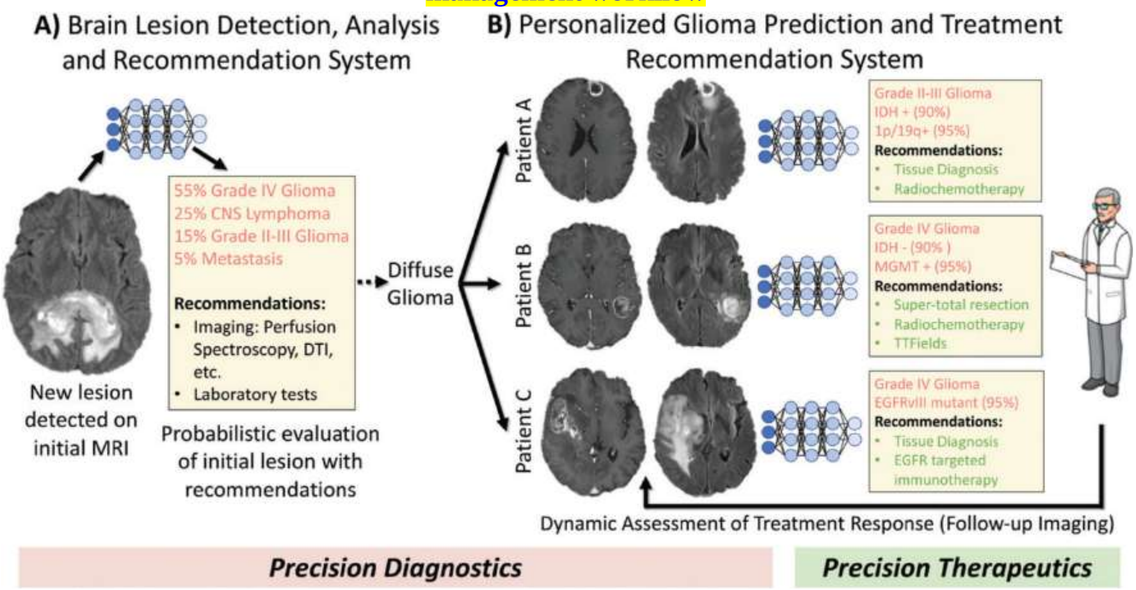

- A, Initial lesion detection and analysis system would generate a probabilistic differential of lesion(s) seen on patient's initial brain MR image (precision diagnostics). It would also recommend additional useful imaging examinations, laboratory tests, or tissue sampling.

- B, Glioma-specific module could make personalized predictions of molecular markers, survival, and treatment responses (precision diagnostics), thereby recommending optimal treatment plan(s), which would be continuously updated on the basis of follow-up imaging (precision therapeutics).
- CNS = central nervous system, DTI = diffusion tensor imaging, EGFR = epidermal growth factor receptor, EGFRvIII = epidermal growth factor receptor variable III, IDH = isocitrate dehydrogenase, MGMT = O6-methylguanine-DNA-methyltransferase, TTFields = tumor-treating fields

AI-Brain

37

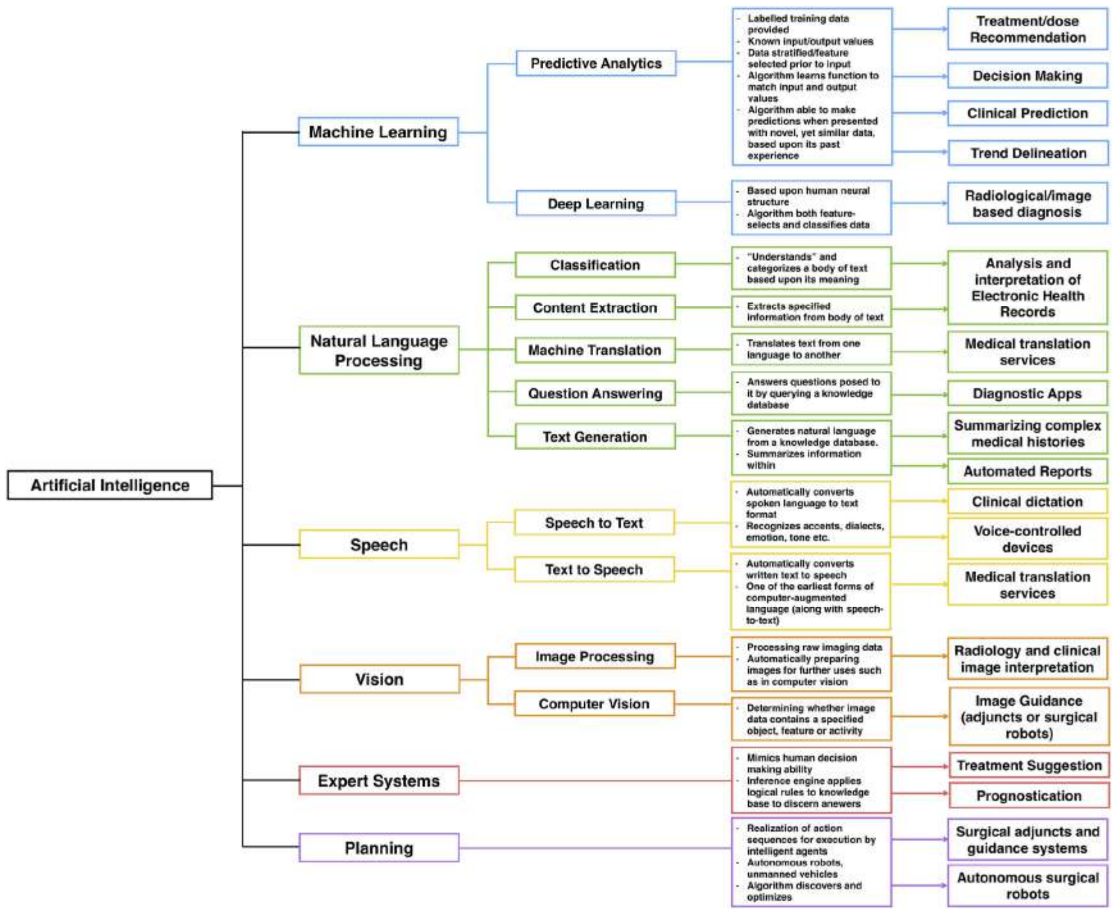

Schematic overview of AI techniques, subdomains, and potential medical applications

- Application examples are not exhaustive

- AI methods have potential applicability to a
  - wide range of clinical tasks,
    - from logistical andsecretarial in nature, to
    - critical diagnostic, decision-making, and interventional tasks

Learning (Machine – AI)

37

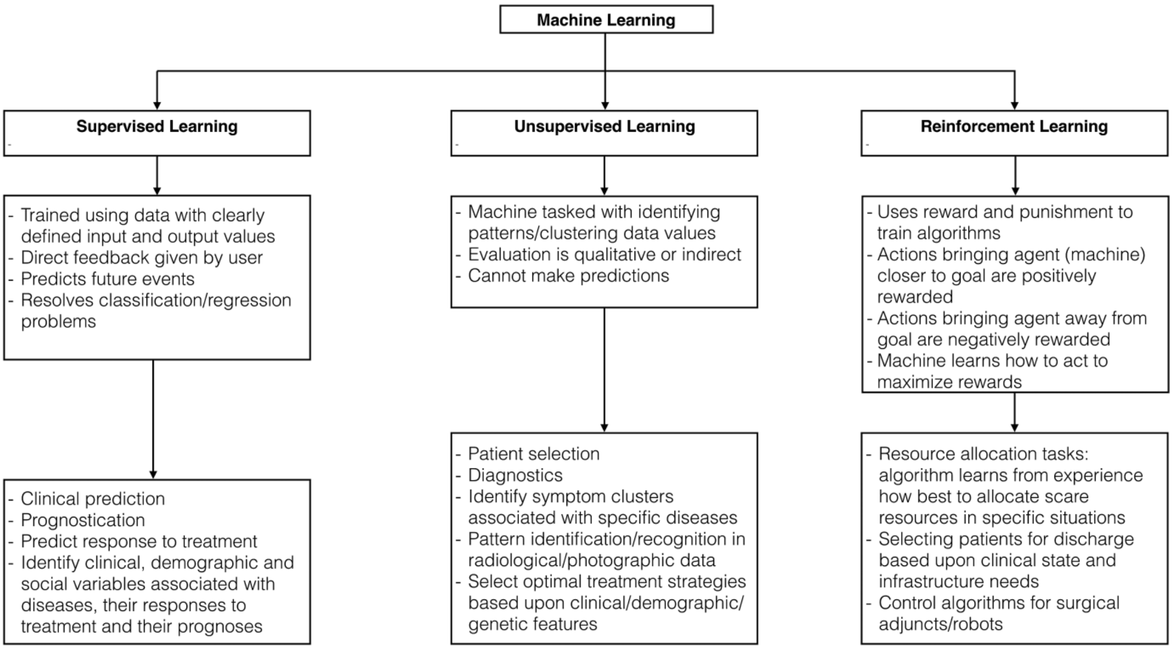

Machine learning &
subdomains of supervised, unsupervised, reinforcement learning
in clinical tasks

- ✓ **Supervised learning**utilizes regression techniques
  - may be utilized for clinical prediction tasks like
    - prognostication and
    - predicting treatment responses

- ✓ **Unsupervised learning** involves clustering data using features in the data, and
  - its most obvious uses are for
    - identifying features in radiological
    - scans or clinical images, or
    - identifying clinically pertinent data clusters
- ✓ Unsupervised learning techniques may be
    - utilized for patient selection, diagnostics, or

- other tasks requiring pattern recognition

✓ **Reinforcement learning**
  - utilizes the concept of an "intelligent agent" assigned a particular goal
  - It navigates its environment on its mission, and
  - is rewarded for every action it takes that brings it closer to its goal, and
  - punished for every action taking it further from its goal
  - Consequently, →the algorithm learns to maximize its reward and complete its task as efficiently aspossible
    - It may be utilized for bureaucratic tasks like resource allocation, or potentially in the control mechanisms of autonomous surgical robots and adjuncts

37

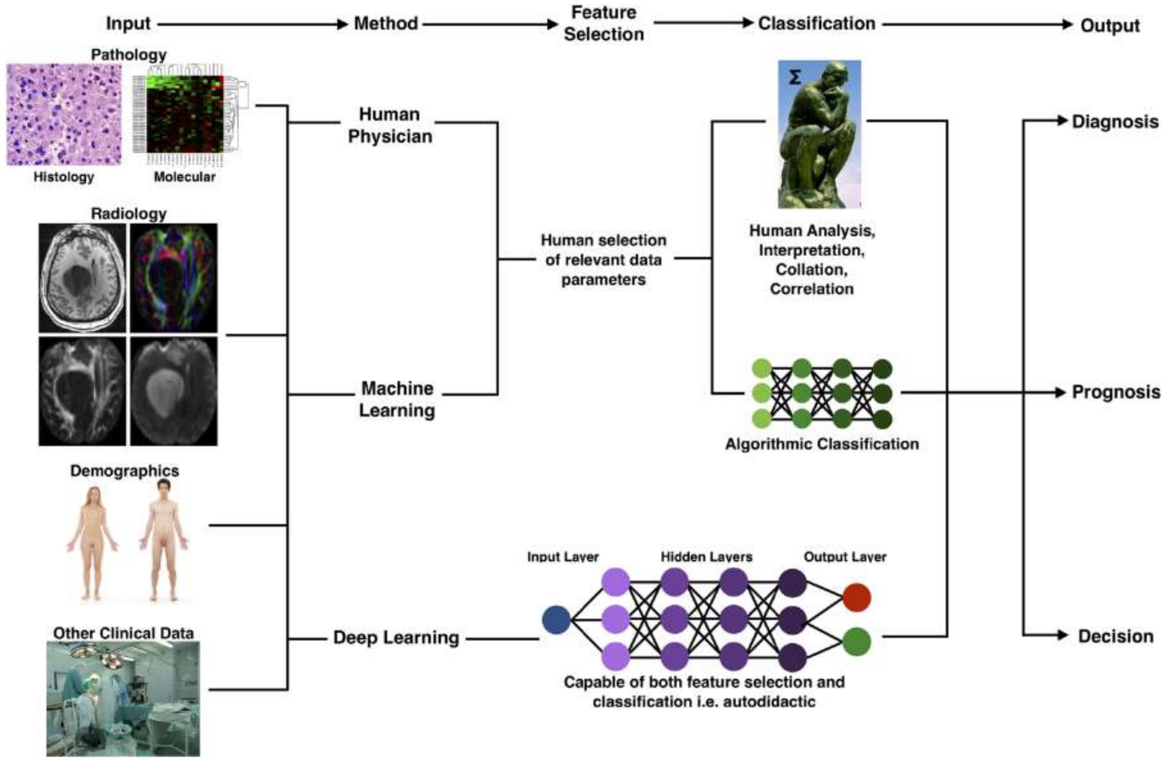

schematic representing noninterventional clinical workflow tasks

- comparing humans, traditional machine learning, deep learning

✓ 1, The data source is comprised of
  - any clinical investigative data that are used to arrive at a diagnosis, prognosis, or clinical decision
  - In neurosurgery, this may involve pathological reports (consisting of histology and molecular information), radiology studies (various sequences e.g., CT and MRI), demographics (eg, age, sex), and
  - any other relevant clinical data (eg, medical comorbidities, blood investigations, etc).

✓ 2, The data are (historically and at present) chosen and interpreted by humans; however, both machine learning and deep learning may see increasing use in the future

- ✓ 3, Feature selection refers to the selection of relevant data characteristics that are considered
  relevant to making an informed decision based upon the data present, and the desired task. For both nonautomated and limited machine learning capabilities, feature selection must be conducted by the human operator. A deep learning algorithm is able to perform both feature selection and classification tasks (4) itself.
- ✓ 4, Classification
  entails the analytical portions of the task, whereby the data are stratified into categories, for example, whether a tumor appears malignant or not. Humans perform these tasks traditionally, based upon their knowledge and experience; this may however entail nonquantitative intuitive cognitive processes. Traditional machine learning algorithms use the data that have already been censored (ie, it is fed only data that the human operators feel are relevant for it to complete its job) to classify the data into
- ✓ the categories relevant to the task at hand. A deep learning algorithm is autodidactic, and can perform feature selection and classification itself. Both feature selection and classification processes may, if subsequently analyzed, be significantly different from how a human would approach data analysis tasks.
- ✓ 5, The output consists of the diagnosis, prognosis, or decision fulfilling the purpose of the clinical workflow

AI + Surgery Neuro-
Pre- / Intra- / Post-Operative

42

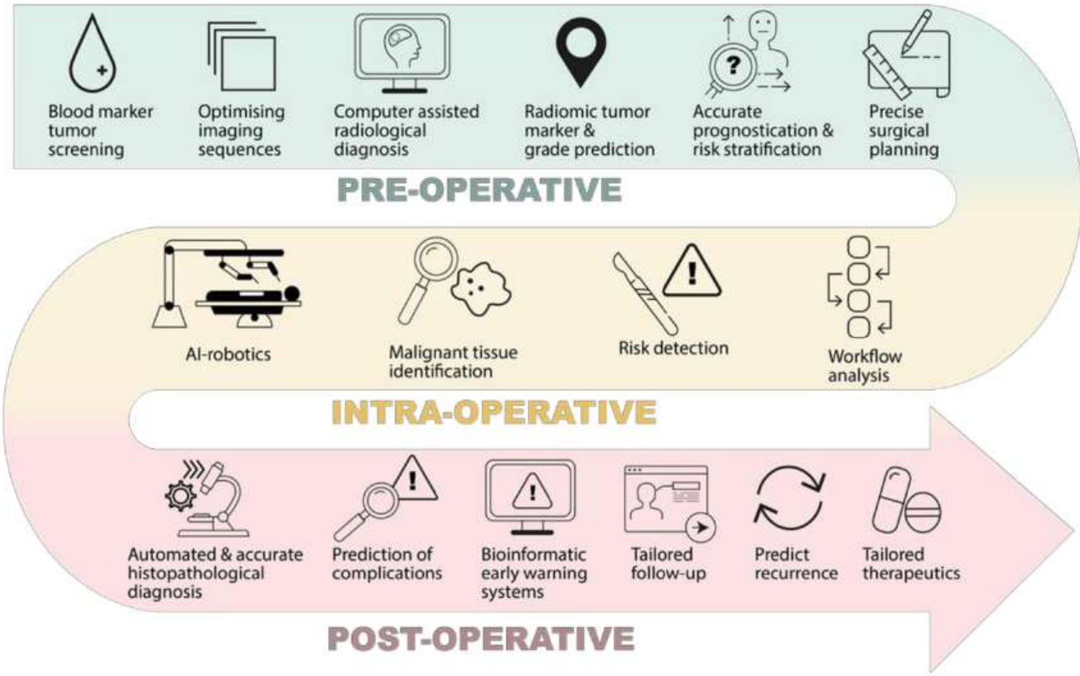

Potential clinical impacts of AI in the neurosurgical management of brain tumours, in the pre-operative, intraoperative, and post-operative phase

43

Literature Search Method

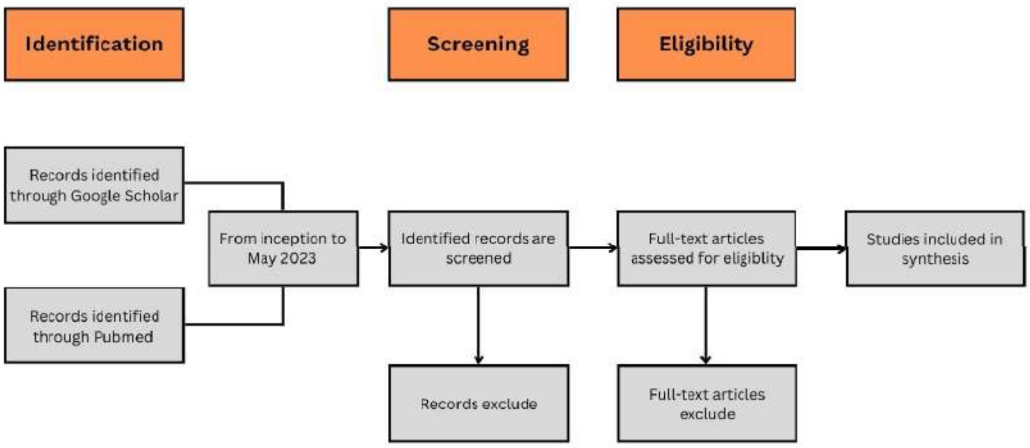

PubMed and Google Scholar were searched

- ✓ AI-related keywords;
- ✓ English literature published from inception to May 2023;
- ✓ Observational studies, case–control studies, cohort studies, clinical trials, meta-analyses, reviews, and guidelines

PRISMA
(Preferred Reporting Items for Systematic Reviews and Meta-Analyses)

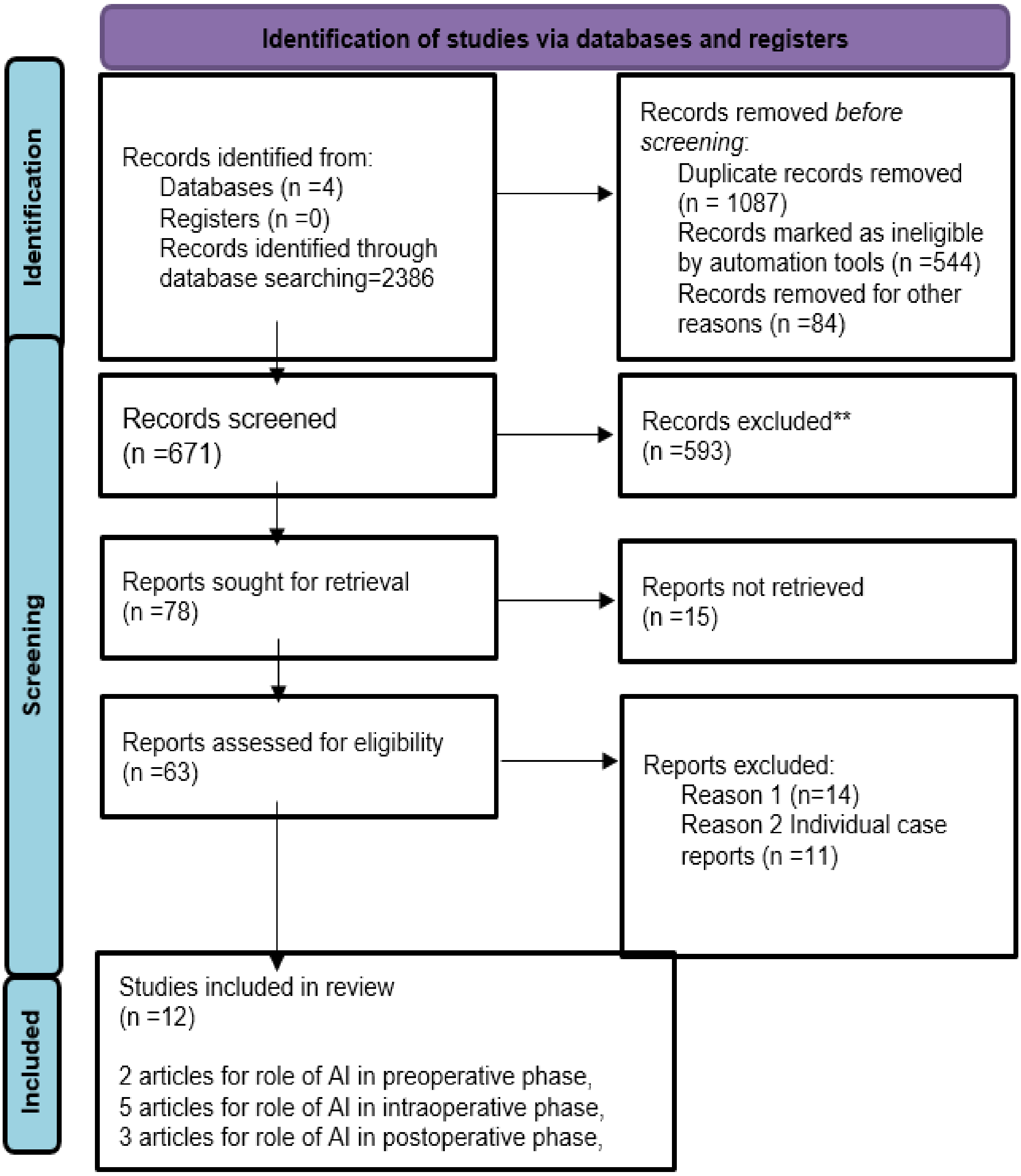

Study selection process according to flowchart.

! Reason 1- Subject not relevant to Neurosurgery.

! Reason 2- Individual case reports

AI +
Neuro [Diseases /surgery]

43

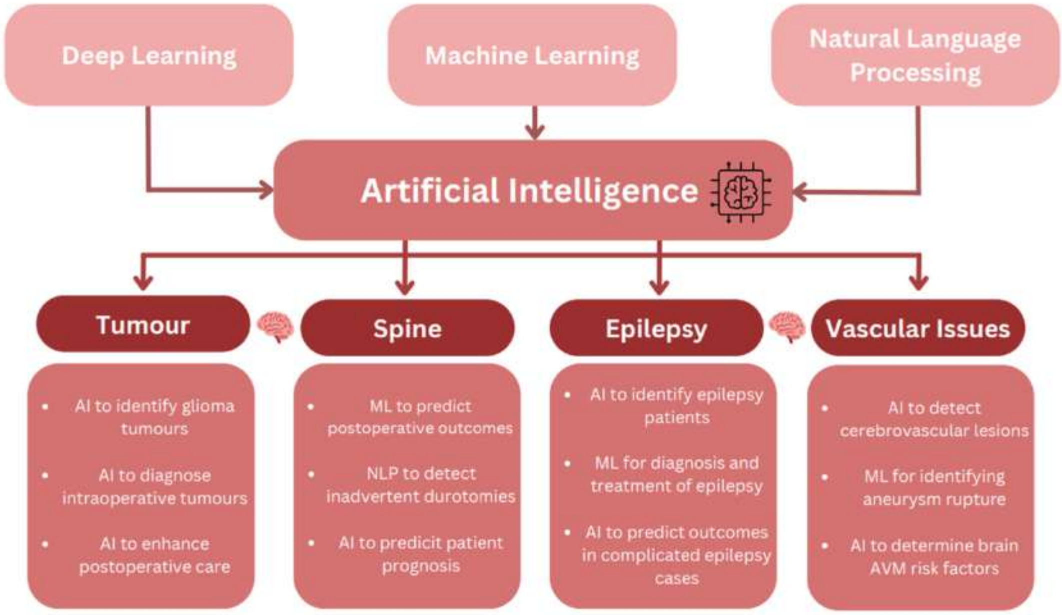

Potentials of AI in neurosurgery

43

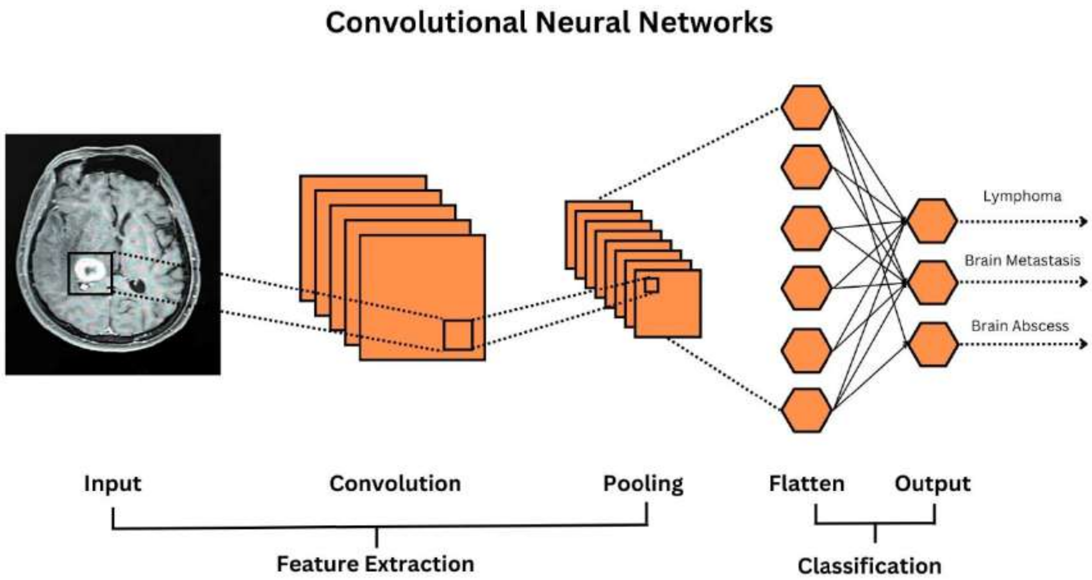

45

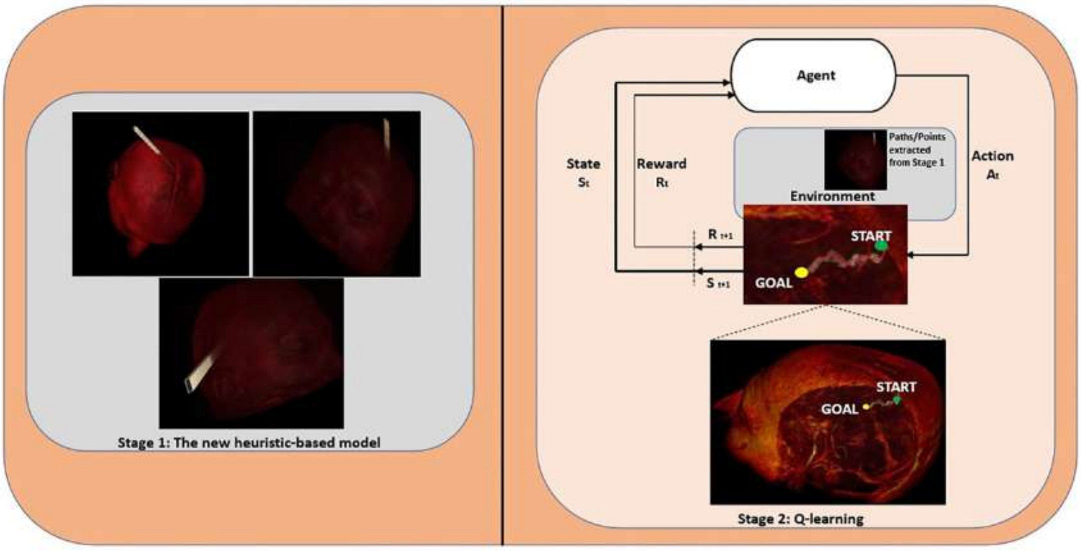

Proposed system architecture
for finding linear and nonlinear access paths
for neurosurgery

45

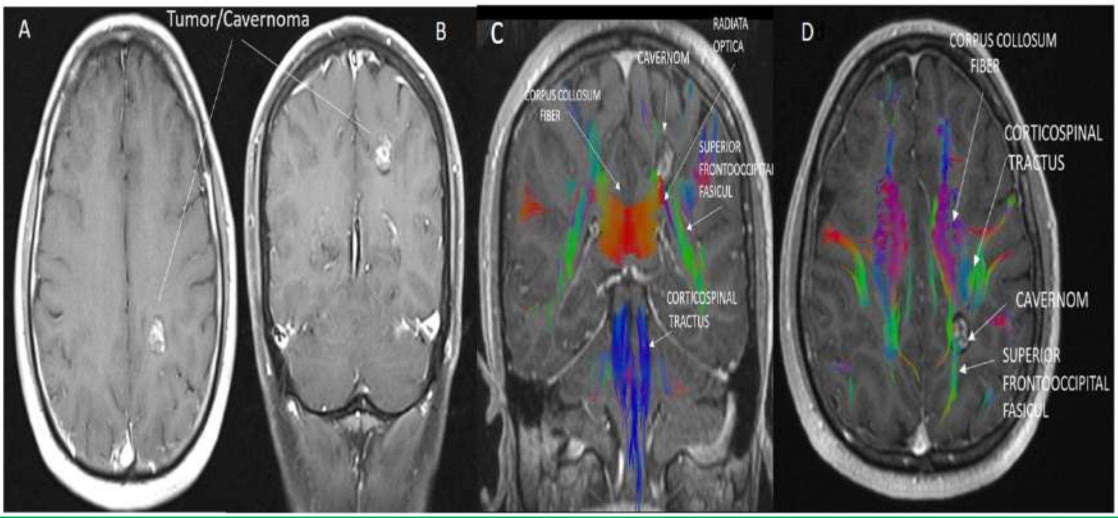

- ✓ (A, B) Cavernoma appearance on axial (A) and coronal (B) contrast-enhanced T1 cranial MRI images.
- ✓ (C,D) The anatomical relationship of the corticospinal tract, superior fronto occipital fasciculus, and corpus callosum transverse fibers with the cavernoma is shown in sagittal and axial MRI tractographyimages. Due to the mass effect of the cavernoma, displacement of the superior fronto occipital fasciculus was observed.

45

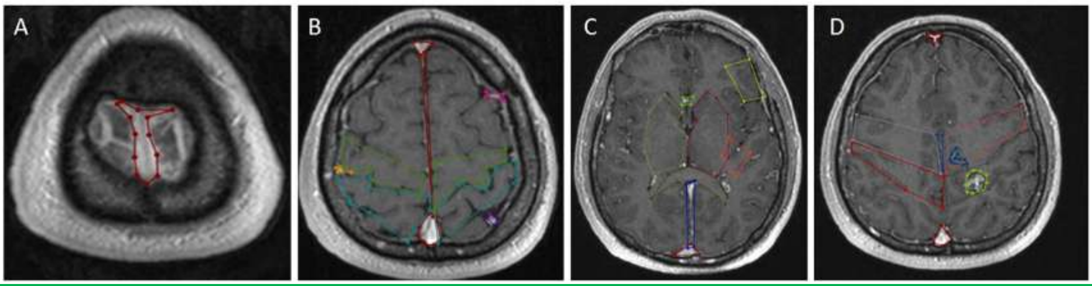

Labeling using contrast-enhanced T1 axial image of cranial MRI.

- ✓ (A) Superior sagittal sinus marked in red at the vertex's midline.
- ✓ (B) Superior sagittal sinus marked with red in the midline in the supraventricular area, precentral gyrus marked with green, postcentral gyrus marked with turquoise, superficial cortical veins marked with pink on the left and dark yellow on the right adjacent to the bilateral frontal lobes.
- ✓ (C) Right basal ganglia and thalamus marked with yellow in the right cerebral hemisphere at the ventricular level; left basal ganglia and thalamus marked with light red in the left cerebral hemisphere at the ventricular level, Broca's area in the left frontal lobe with light yellow, Wernicke's area posterior to Sylvian fissure marked with orange; The anterior cerebral arteries are marked in light green anteriorly in the midline, the corpus callosum splenium in green and the sinus rectus in blue in the midline posteriorly.
- ✓ (D) Right postcentral gyrus marked red, cavernom/tumor marked yellow-green, pericallosal artery marked blue on the midline and posterior inferior frontal artery marked blue

45

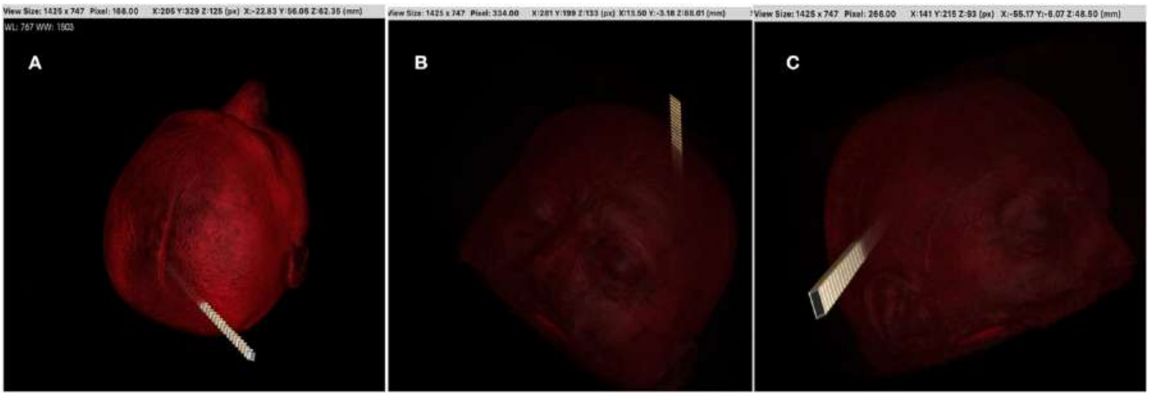

The research algorithm was created for time efficiency compared with the time-consuming RL algorithm.

- ✓ The goal is to find the most ideal cranial entry points.
- ✓ Machine learning was not used in this method.
- ✓ Cranial entry points were scored using the equivalent areas and tumor location in Table 1 and compared with each other.

- + With this algorithm,
  - o it was possible to sort by five most ideal entry points, 10 entry points, or worst entry points.

- In addition, this algorithm provided a linear access path to tumor tissue in the shape of a rectangular prism or cylinder. The entrance area in the images was determined as 1.5 cm2.
- The algorithm has been adjusted to allow this area to be increased or decreased.
- This algorithm can be useful in tubular operative systems or rigid endoscopic systems.
- In this study, we took these points (the most ideal 4,900 points) as the starting points of RL. Image(A,B) are the ideal best rated and image (C) the worst-rated sample entry points

45

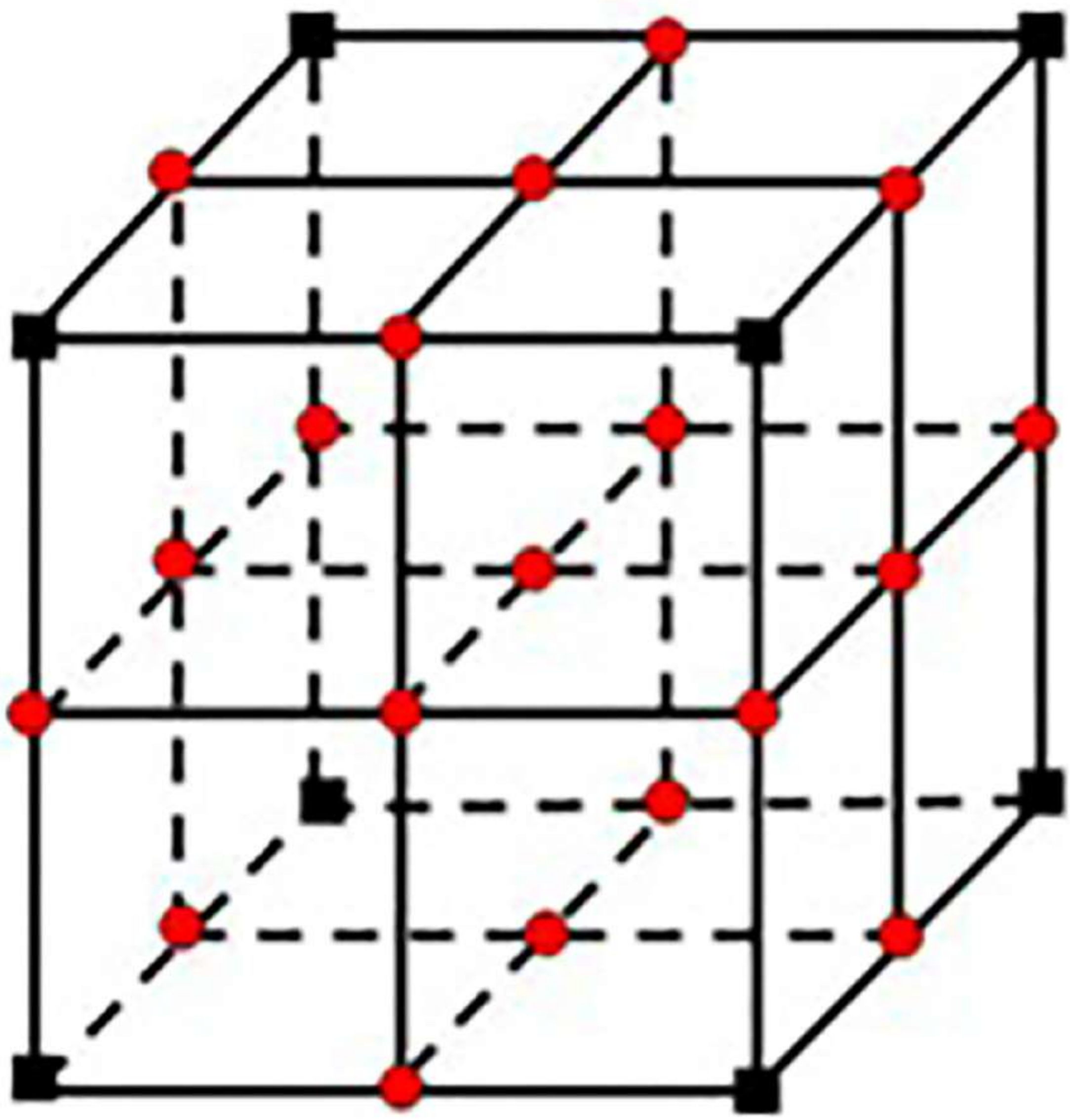

45

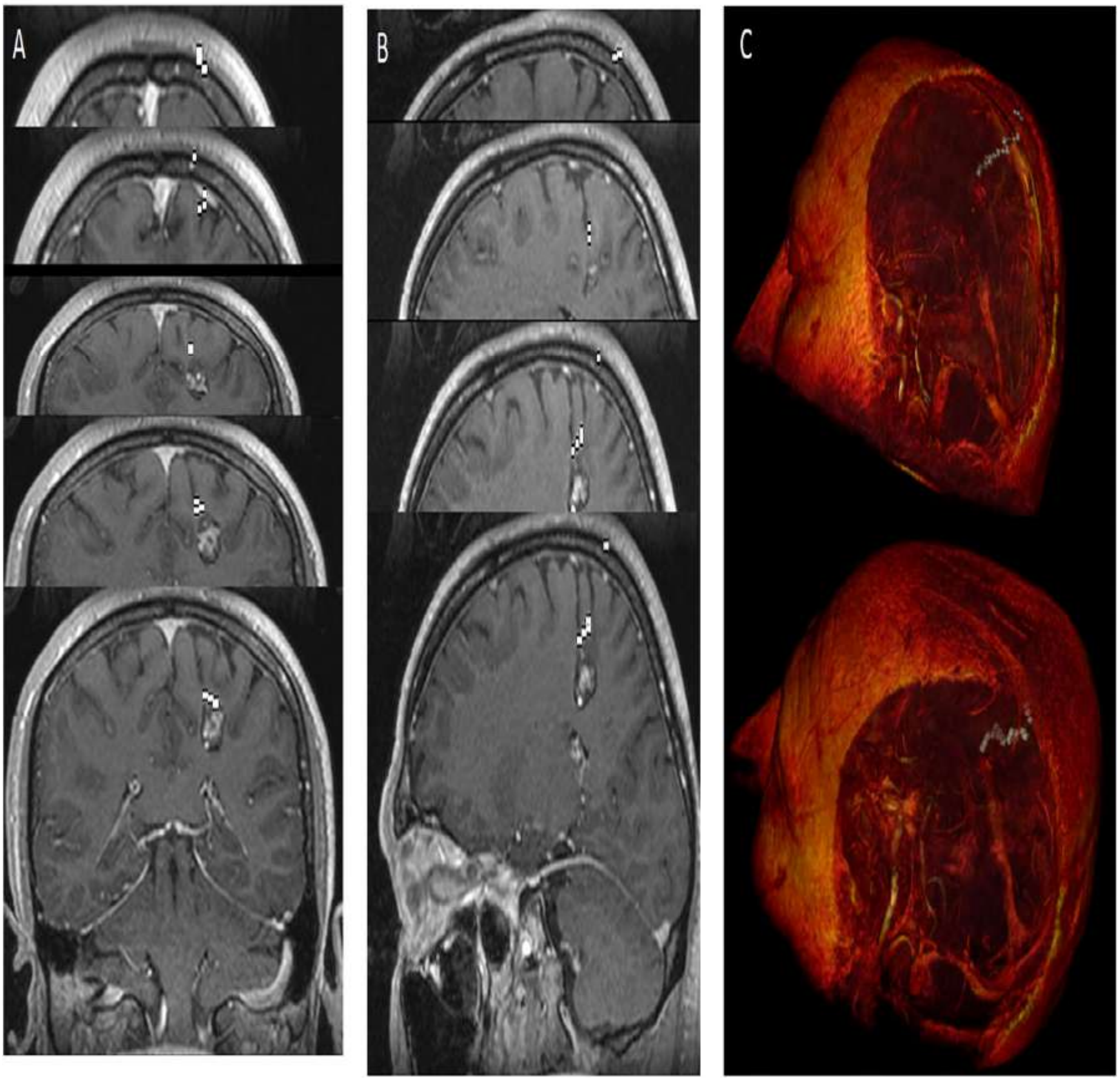

Most ideal cortico-tumoral approach is recommended by RL

- ✓ Images were added one after another to show the nonlinear pathway
  - o RL extracted the most optimal pathway by performing a random-onset point analysis of the entire intracranial area. Demonstration of the approach reaching the tumor from the base of the postcentral sulcus

- (A) showing the pathway in coronal sections
- (B) Showing the pathway in sagittal sections
- (C) Showing the 3-dimensional pathway with image processing

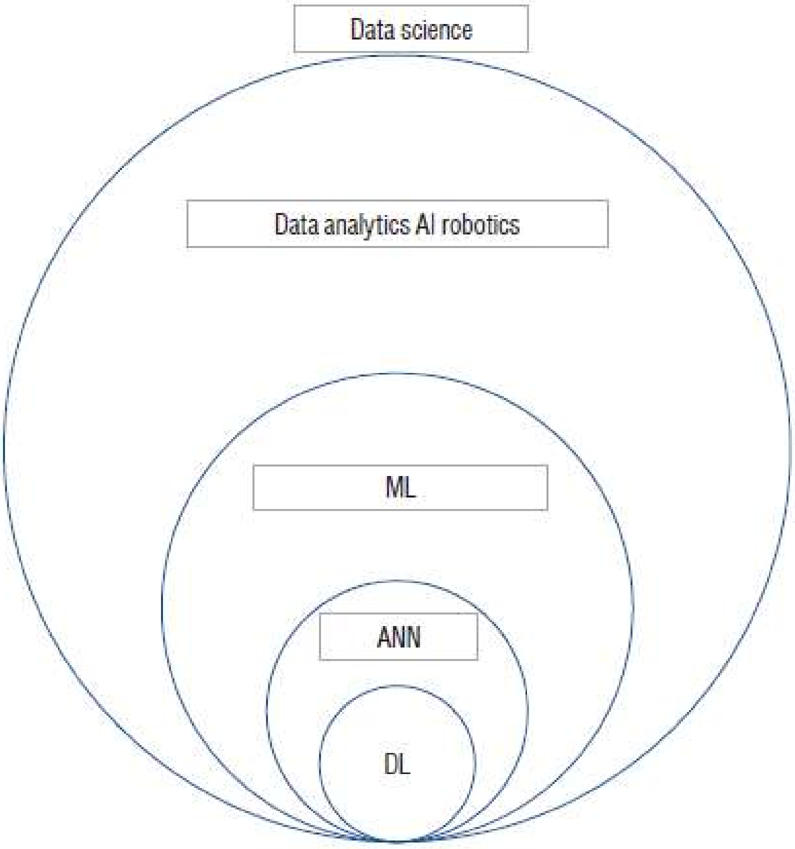

AI : artificial intelligence, ML : machine learning, ANN : artificial neural network, DL : deep learning

47

Recent research in the eld of neurosurgery by analyzing images with artificial intelligence

Study	Journal	Article title	Algorithms used in the study
Scherer et al.[32] (2016)	Stroke	Development and validation of an automatic segmentation algorithm for quantification of intracerebral hemorrhage	RF
Urbizu et al.[42] (2018)	J Neurosurgery	Machine learning applied to neuroimaging for diagnosis of adult classic Chiari malformation: role of the basion as a key morphometric indicator	7 machine learning algorithms trained : NB, DT, K-NN, LR, SVM, LDA
Paliwal et al.[27] (2018)	Neurosurg Focus	Outcome prediction of intracranial aneurysm treatment by flow diverters using machine learning	SVM, LR, K-NN, ANN
Hale et al.[14] (2018)	Neurosurg Focus	Machine learning analyses can differentiate meningioma grade by features on magnetic resonance imaging	K-NN, SVM, NB, ANN
Huang et al.[18] (2019)	J Neurosurgery Spine	A computer vision approach to identifying the manufacturer and model of anterior cervical spinal hardware	KAZE feature extractor, K-means clustering, SVM
Burström et al.[7] (2019)	J Neurosurgery Spine	Machine learning for automated 3-dimensional segmentation of the spine and suggested placement of pedicle screws based on intraoperative cone-beam computer tomography	Multiple segmentation algorithms trained (not mentioned)
Staartjes et al.[37] (2020)	J Neurosurgery	Neural network–based identification of patients at high risk for intraoperative cerebrospinal fluid leaks in endoscopic pituitary surgery	DL

RF : random forest, NB : boosted DT, DT : decision tree, K-NN : K-nearest neighbors, LR : logistic regression, SVM : support vector machine, LDA : linear discriminant assay, ANN : artificial neural network, DL : deep learning

47

Recent research in the eld of neurosurgery by predicting with artificial intelligence

Study	Journal	Article title	Algorithms used in the study
Kalagara et al.[19] (2018)	J Neurosurgery Spine	Machine learning modeling for predicting hospital readmission following lumbar laminectomy	DT
Staartjes et al.[36] (2018)	Neurosurg Focus	Utility of deep neural networks in predicting gross-total resection after transsphenoidal surgery for pituitary adenoma: a pilot study	DL
Muhlestein et al.[26] (2019)	Neurosurgery	Predicting inpatient length of stay after brain tumor surgery: developing machine learning ensembles to improve predictive performance	29 machine learning algorithms trained
Hernandes Rocha et al.[15] (2019)	J Neurosurgery	A traumatic brain injury prognostic model to support in-hospital triage in a low-income country: a machine learning-based approach	9 machine learning algorithms trained : K-NN, Bayesian GLM, etc.
Goyal et al.[11] (2019)	J Neurosurgery Spine	Can machine learning algorithms accurately predict discharge to nonhome facility and early unplanned readmissions following spinal fusion? Analysis of a national surgical registry	7 machine learning algorithms trained : predictive hierarchical clustering, classification algorithm
Siccoli et al.[35] (2019)	Neurosurg Focus	Machine learning-based preoperative predictive analytics for lumbar spinal stenosis	7 machine learning algorithms trained : RF, XGBoost, GLMs, BDT, K-NN, GLMs, ANN
Tunthanathip et al.[40] (2019)	Neurosurg Focus	Machine learning applications for the prediction of surgical site infection in neurological operations	DT, NB with Laplace correction, K-NN, ANN
Lee et al.[21] (2019)	World Neurosurgery	Prediction of IDH1 mutation status in glioblastoma using machine learning technique based on quantitative radiomic data	Classification algorithms : K-NN, SVM, DT, RF, NB, LDA, GBM
Senders et al.[34] (2020)	Neurosurgery	An online calculator for the prediction of survival in glioblastoma patients using classical statistics and machine learning	15 machine learning algorithms trained
Staartjes et al.[37] (2020)	J Neurosurgery	Neural network-based identification of patients at high risk for intraoperative cerebrospinal fluid leaks in endoscopic pituitary surgery	DL
Hopkins et al.[17] (2020)	J Neurosurgery Spine	Using machine learning to predict 30-day readmissions after posterior lumbar fusion: an NSQIP study involving 23,264 patients	DL

DT : decision tree, DL : deep learnin, K-NN : K-nearest neighbors, GLM : generalized linear model, RF : random forest, BDT : boosted decision tree, ANN : artificial neural network, NB : boosted DT, IDH1 : isocitrate dehydrogenase 1, SVM : support vector machine, LDA : linear discriminant assay, GBM : gradient boosting model, NSQIP : National Surgical Quality Improvement Program

Robots +
[Surgery + Neuro-]

TABLE 1. Milestones Along the Path From Robots to AI in Medicine

Pre-1946	Automatic machines and calculating device but not AI. Wondrous ancient automata described
1920s	The word "robot" replaces the word "automaton"
1928	Eric, a battery-powered, aluminum-skinned robot with 11 electromagnets and a motor that could move its hands and head and be controlled remotely or by voice presented at the Model Engineer's Society in London
1930s	Industrial robots introduced in the United States
1939	Elektro, a 7-foot tall, walking, talking, voice-controlled, humanoid robot weighing 120 kg presented at the World's Fair. It could smoke, speak 700 words and move its head and arms
1949	Manchester Mark 1, first stored program computer, installed. Named "The Electronic Brain"
1950	Alan Turing writes "*Can Machines Think?*"
1955	Logic Theorist – first AI program presented and funded by the RAND Corporation
1956	Dartmouth Summer Research Project on Artificial Intelligence
1963	DARPA funds AI at Massachusetts Institute of Technology
1965	Edward Feigenbaum introduces expert systems at Stanford (The Heuristic Programming Project)
1968	The famed science fiction writer, Arthur C. Clarke, predicts that by 2001, machines will be smarter than humans
1970s	Automated, computer-assisted EKG readings
1973	Image analysis of digitized retinal angiography
1973	Expert system assistance for renal disease
1978	Mirsky and others predict no more than 3 to 8 years before human intelligence is surpassed by computers
1978	CASNET introduced for expert system computer-assisted diagnosis of glaucoma
1981	The PC is introduced with the PC DOS operating system
1980s	Early investigation of machine vision adaptations to medical image analysis
1983	Two expert medical systems, the "Internist-I" and "Cadeuceus" introduced
1988	Computer-assisted resection of subcortical lesions
1988	Automated computer-assisted detection of peripheral lung lesions
1990	Human Genome Project begins
1997	An IBM computer defeats Gary Kasparove in chess
1997	Dragon Software introduces first public speech recognition system
1998	Image Checker computer-assisted diagnostic system for mammography introduced
2000	Proliferation of cheap storage and increasing computer power
2000	Introduction of DL for medical applications
2004	Early reports of computer-assisted diagnosis of retinal disease
2007	IBM Watson introduced
2010	Passage of the Patient Protection and Affordable Care Act. EMRss proliferate
2010	Computer-assisted diagnosis in endoscopy
2011	Digital assistant introduced commercially
2012	Computer-assisted segmentation of sectional brain images
2012	Computer-assisted brain tumor grading
2017	Chatbots introduced for patient intake
2018	AI trials for gastroenterology diagnosis begin
2018	FDA approves Viz.AI, AI-assisted clinical decision support system for stroke triage
2020	Stacked neural networks applied to EKG interpretation

EKG, electrocardiogram; EMRs, electronic medical record.

Clinical applications	Practice management
Automated cytology	Trend analysis
Frozen section screening	Clinical trials management
Computer-assisted radiological review	Preoperative communication
Image fusion applications	Postoperative follow-up
Radiosurgical planning	FQR system
Robotics	Informed consent
Allergy screening	Human resource management
Medication allergy screening	Revenue cycle management
Electronic medical records analysis	Quality management systems
Personalized implants	Chatbots for websites
Electrophysiological monitoring	Patient communications
Neuro-intensive care decision support	Scheduling
Tight glycemic control systems	Workflow optimization
Surgical modeling	Selected writing tasks

FQR, Frequently Asked Questions.

48

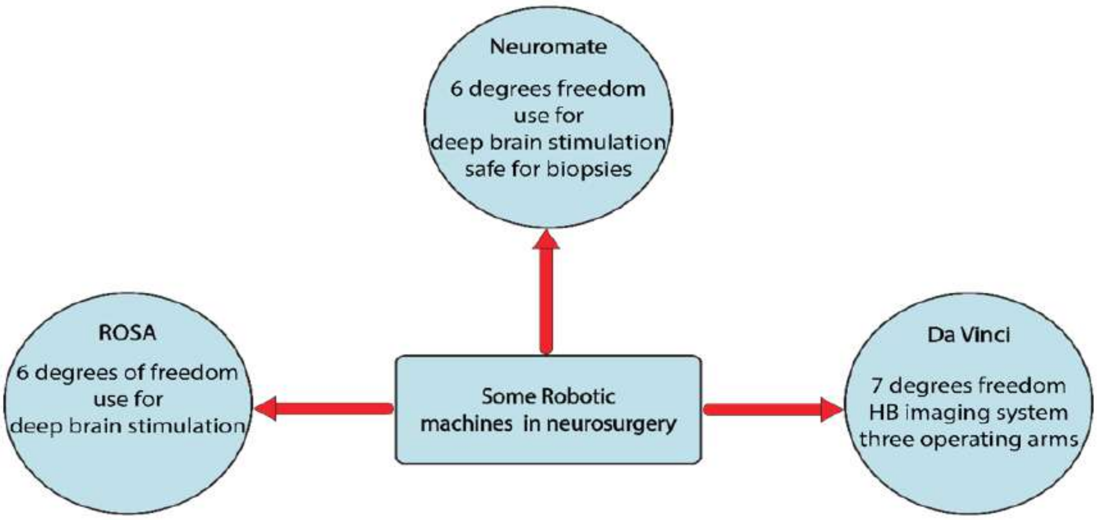

Major classifications of Robotic Machines in Neurosurgery

- ✓ degrees of freedom.
  - i) ROSA

- ii)Neuromate
- iii) Da Vinci

Unanswered research questions That may pave the way For future research

48

1. Can AI fully replace neurosurgeons and what would be its consequences?
2. It has shown that neurosurgery benefits from AI, but what are the cons?
3. How effective is AI in neurosurgery compared with other fields of medicine?
4. How long will it take until the full implementation of AI in neurosurgery?
5. Can the practice of AI use in other fields of science be considered in neurosurgical procedures, what are some of the ways?
6. Can AI be used equally in all types of neurosurgical procedures?
7. If the human factor is absent, will patients trust AI?
8. Will AI be as accurate in complex cases as in simple tasks?
9. Why the higher accuracy of AI compared to specialists in specific cases doesn't lead to their total replacement?
10. The role of IQ in neurosurgery. Does the lower IQ of AI-powered robotics limit their use in Neurosurgery??

50

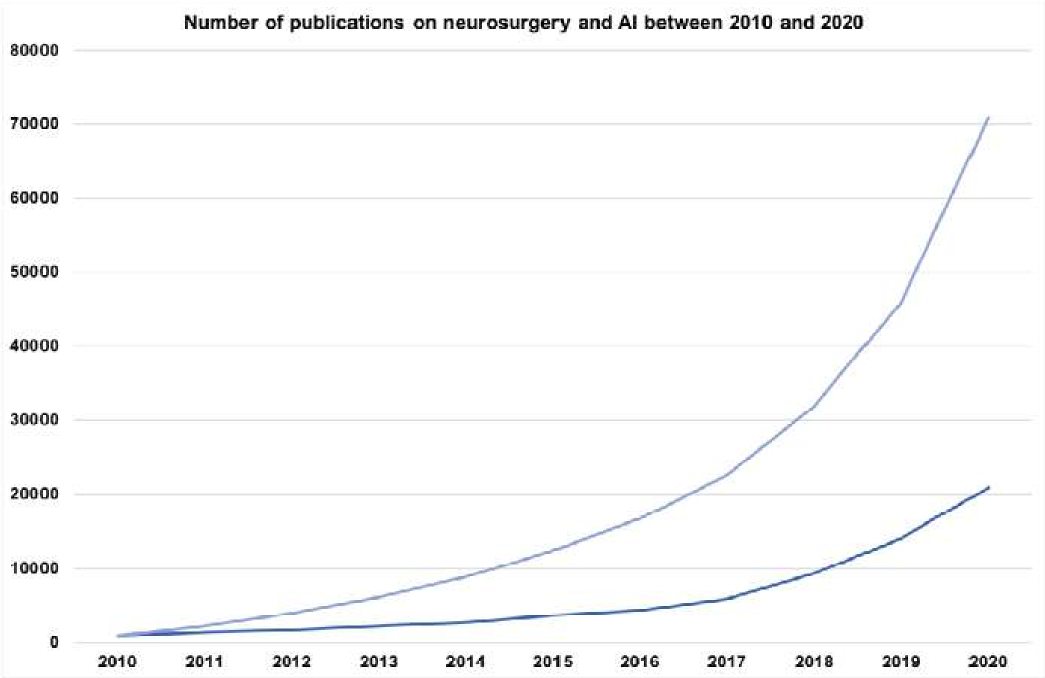

Absolute and the cumulative number of publications involved neurosurgery and artificial intelligence in their title or abstract over the past decade.

- Database PubMed
  - Search Words: Neurosurgery OR neurological surgery OR brain surgery
  - AND artificial intelligence OR machine learning OR deep learning
- title or abstract
- from 2010–2020.

Relationship between artificial intelligence, machine learning and deep learning.

50

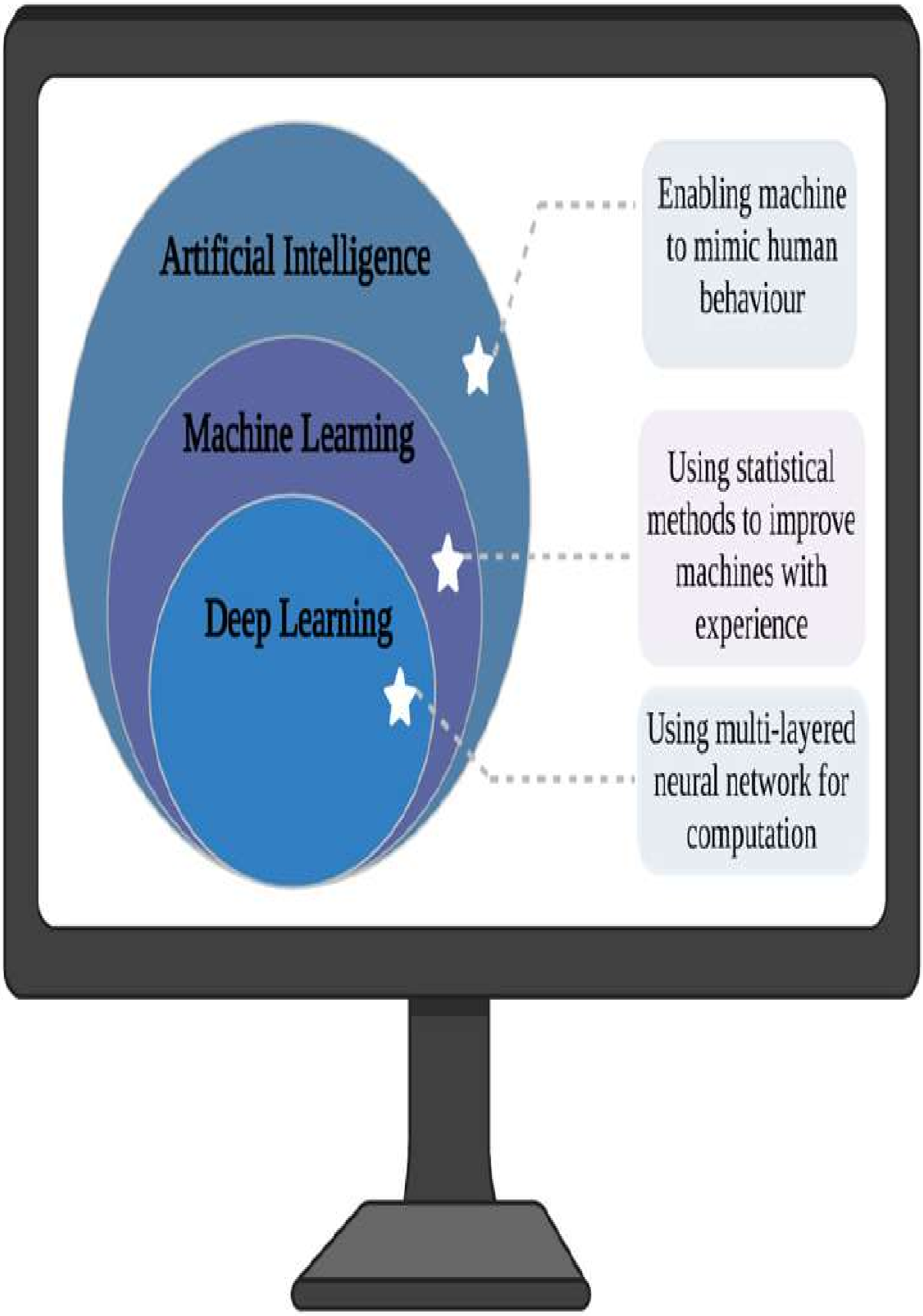

- ✓ AI aims to mimic the intelligent behaviour of humans
- ✓ ML as a branch of AI
    - uses statistics and computer sciences to improve the performance of machines as experience accumulates.
- ✓ DL uses multi-layered neural networks to learn computation

Figure was made using Biorender

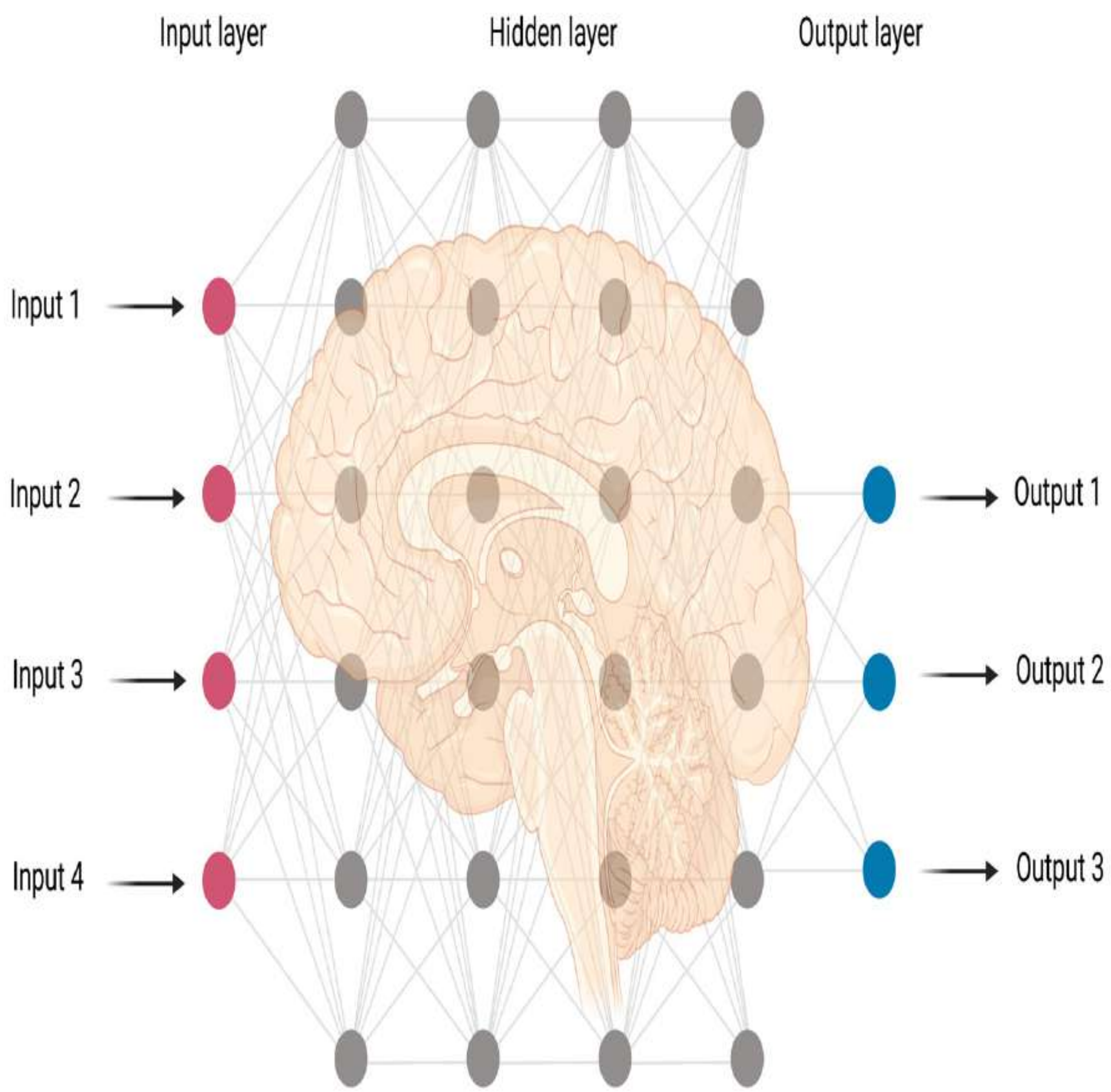

An overview of multilayer perception

- ! in the context of the artificial neural network
- ! of deep learning model
- ! with multiple interconnected layers.

o The figure was made using Biorender

50

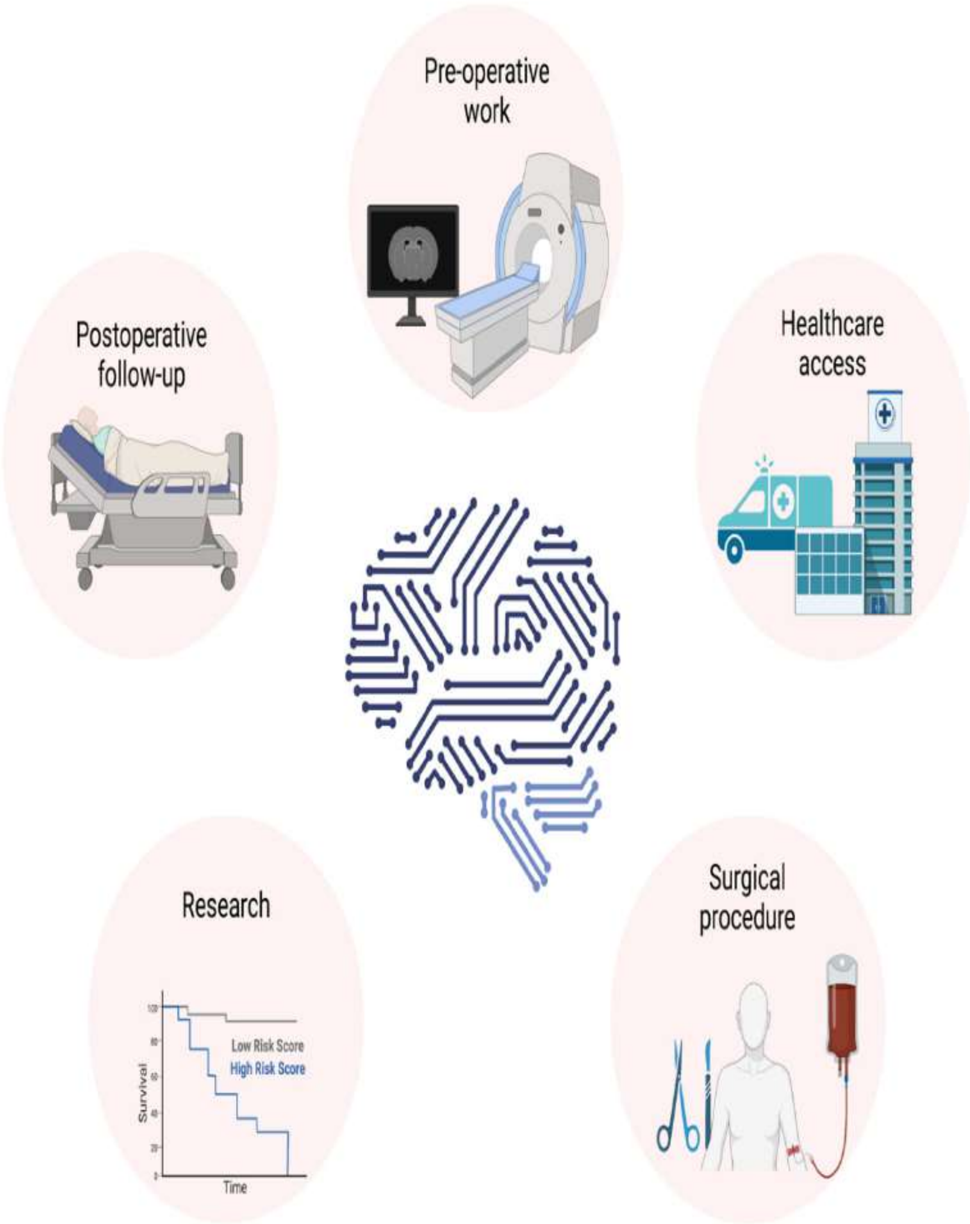

Role of AI in neurosurgery.

- ✓ AI helps neurosurgery in
  - Pre-operative work,
  - Intra-operative surgical procedures,
  - Postoperative follow-up,
- Improving clinical research and
- Expanding access to healthcare.

Figure was made using Biorender

Brain-computer interface (BCI) Overview

50

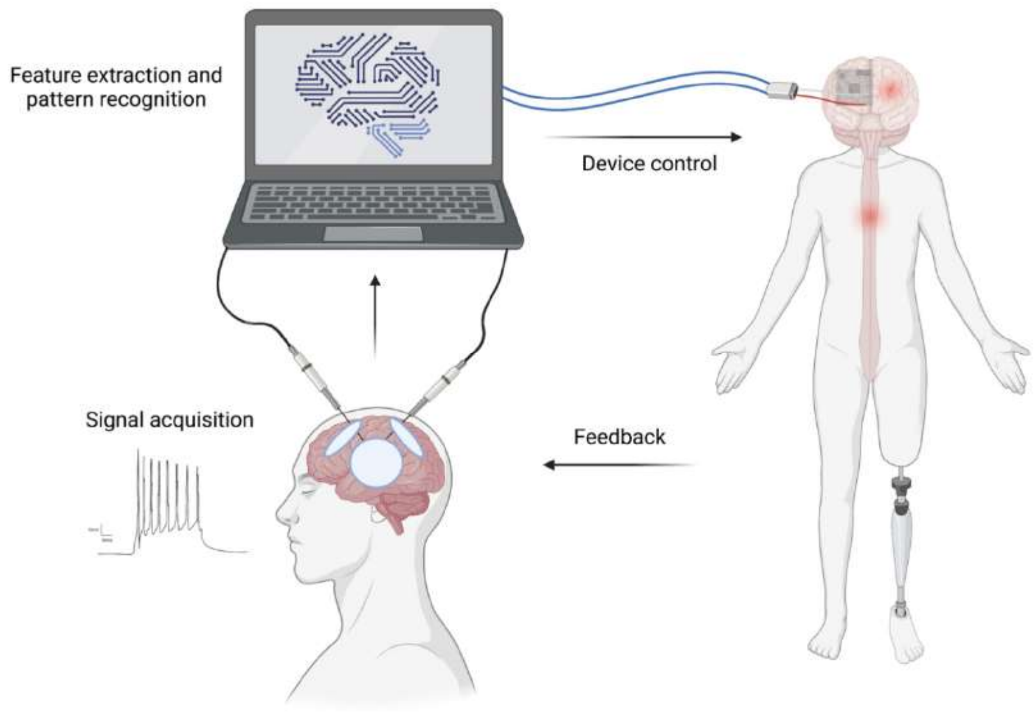

- ✓ AI working together with BCI restores and enhances the sensory and motor functions of the central and peripheral nervous systems.
- ✓ AI can improve BCI by facilitating audio sensation, somatic sensation, visual sensation, and etc.
- o Microelectrodes can pick up the signal from the brain and transfer them to AI for processing.
- o AI can process the signal and extract meaningful features from them,
  - o for example, remove the background noise from the readings,
  - o identify the logic in the data and
  - o produce a coherent outcome [98,100].
- o Feedback from the outcome can then be sent to the cortex to adjust the function, thereby providing a real-time adjustment of the behaviour.

The figure was made using Biorender

51

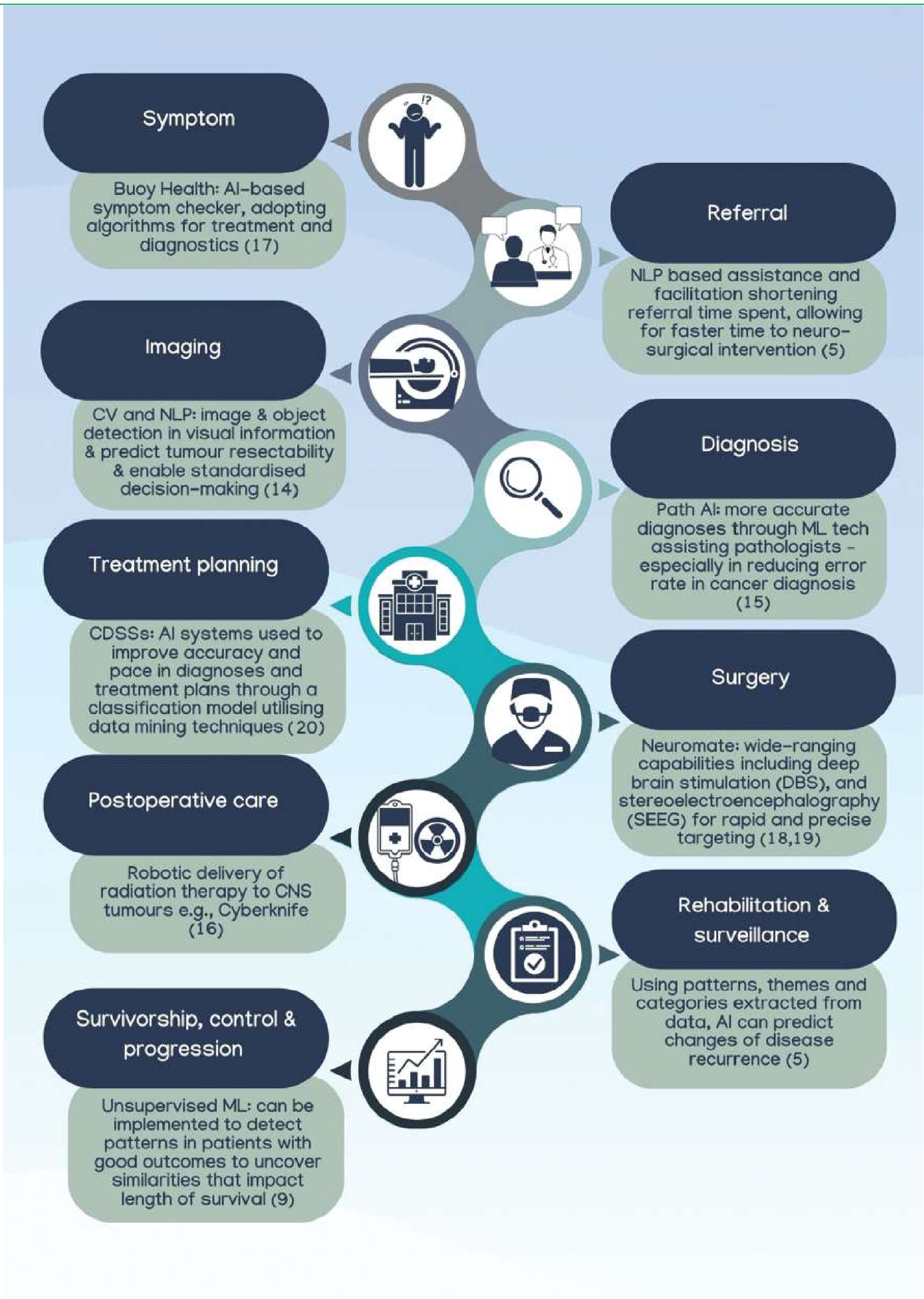

The neurosurgical patient pathway and examples of AI's roles at each stage

Virtual reality& Medicine related timeline

52

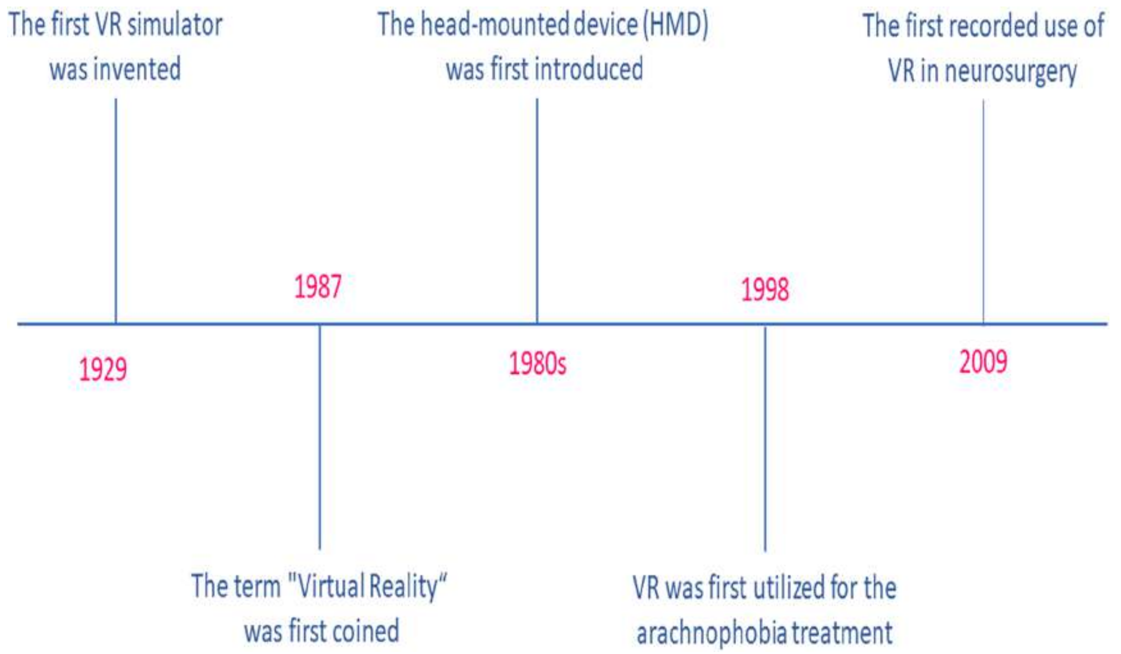

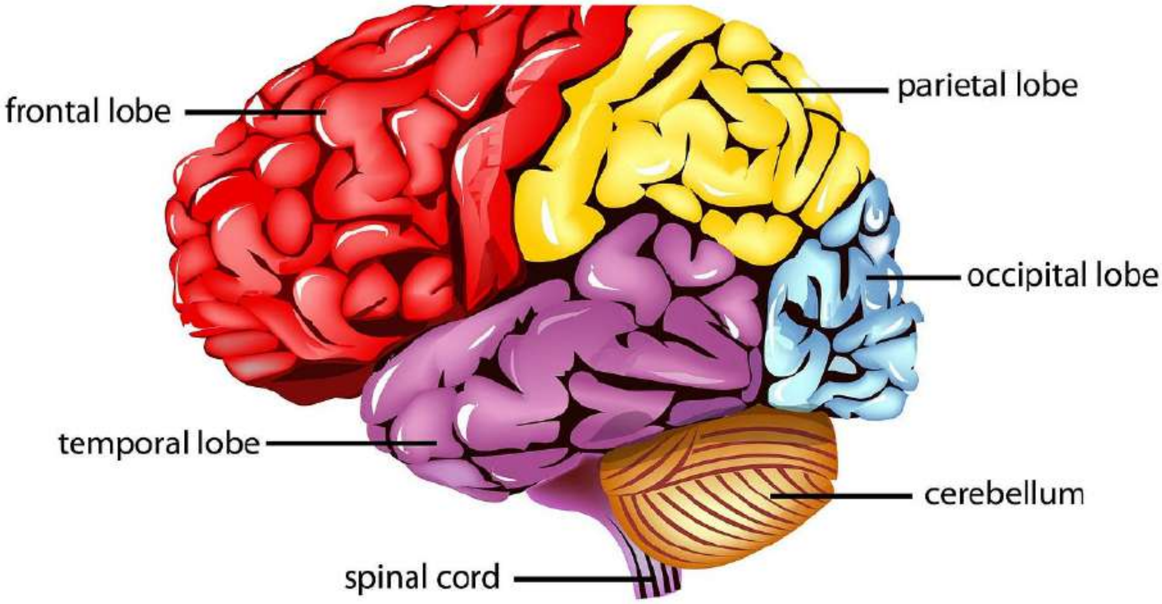
frontal lobe
parietal lobe
occipital lobe
temporal lobe
cerebellum
spinal cord

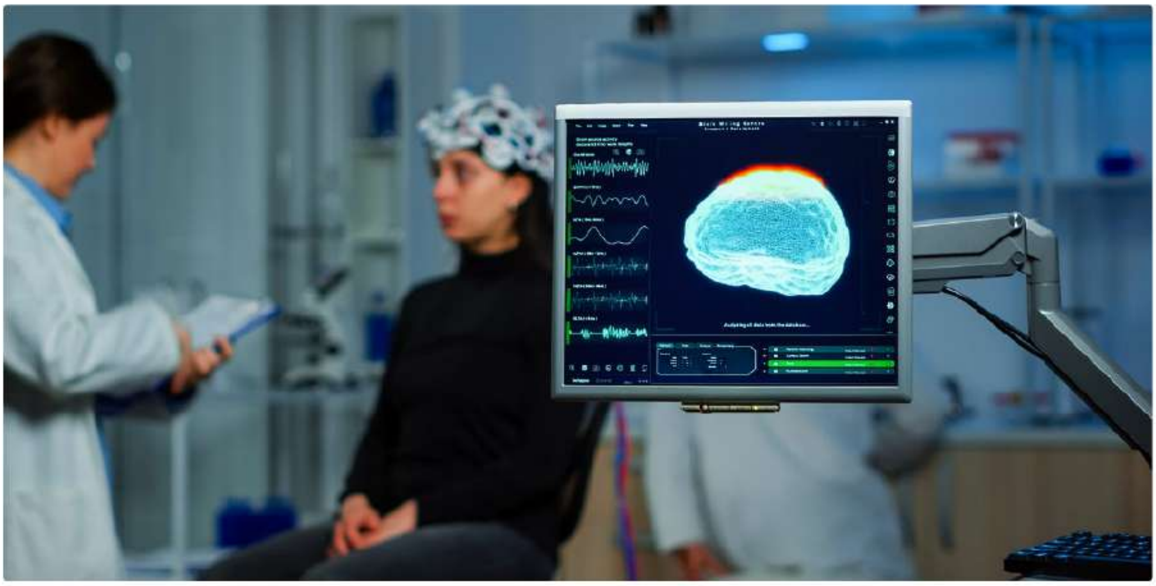

Bridging Neuroscience and Data Science: Simulating the Human Brain’sDecision-Making Mechanism

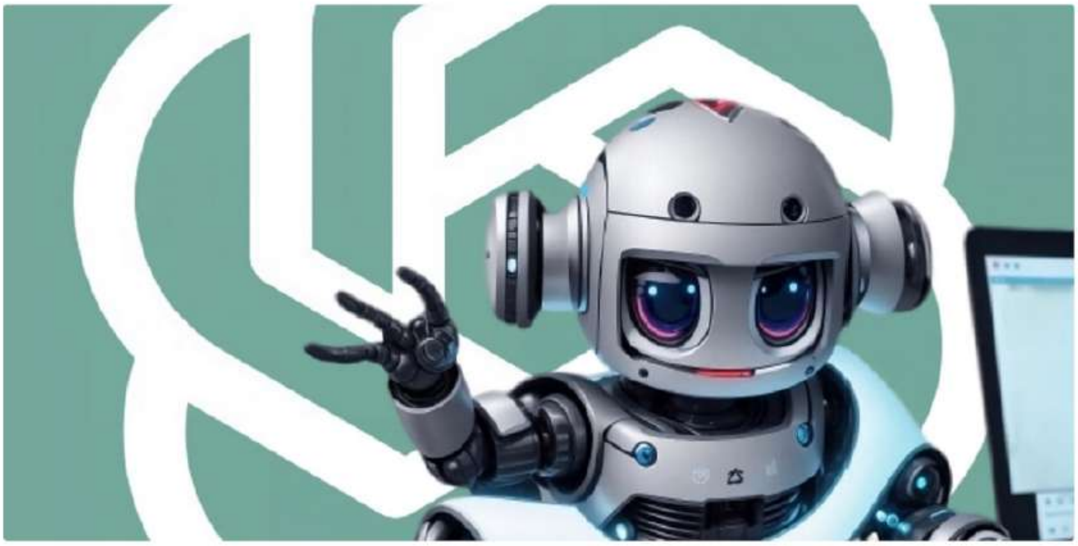

ChatGPT Uses


STORZ

"[With virtual reality] we can plan out how we can approach a tumor and avoid critical areas like the motor cortex or the sensory areas. Before, we didn't have the ability to reconstruct it in three dimensions; we'd have to do it in our minds."

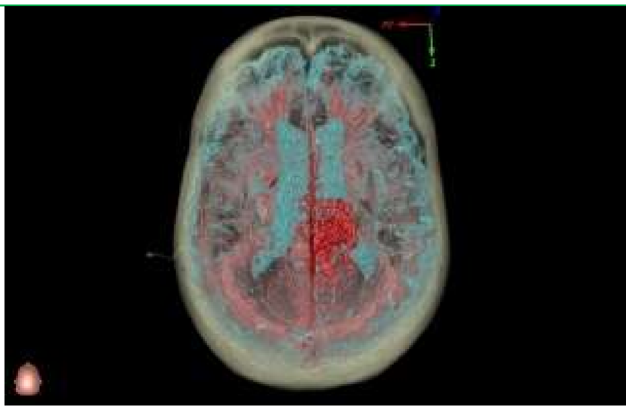

Novel application of virtual reality in patient engagement for deep brain-stimulation: A pilot study

A surgeon using the AI trainer on a dummy "patient

35

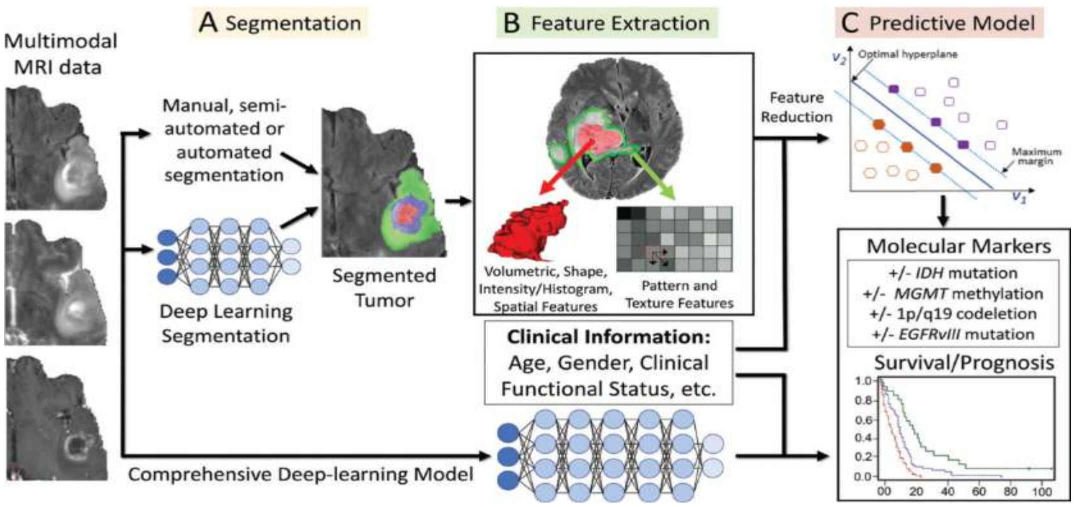

Workflow of radiomics in neuro-oncology.

- A, After preprocessing steps, multimodal MR images are segmented by using automated or manual methods.
- B, This is followed by feature extraction with use of a variety of different techniques.
- C, Machine learning methods are then trained on the features to generate models of underlying molecular markers and predict survival. Deep learning models can be used for performing each of the described steps individually or in a more comprehensive fashion (bottom pathway of figure).
- ✓ EGFRvIII = epidermal growth factor receptor variable III,
- ✓ IDH = isocitrate dehydrogenase,
- ✓ MGMT = O6-methylguanine-DNA-methyltransferase